# Appendix E: Power Analysis Results for the Combined Model

Caption for figures:
Power curves (top panel) show the estimated power to detect a hotspot/coldspot of various effect sizes for each sample size (number of transect segments) from 1 to 200. Red solid, dashed, and dotted lines represent the estimated power to detect a hotspot of 3, 10, and 20 times the reference mean, respectively. Blue solid, dashed, and dotted lines represent the estimated power to detect a coldspot of ⅓, 1/10, and 1/20 times the reference mean, respectively. Blue lines that are absent indicate that the estimated power to detect a coldspot was undefined because the effect size times the reference mean was less than or equal to one. Boxplots (bottom panel) show the distribution of estimated power to detect a hotspot/coldspot of various effect sizes based on the number of transect segments surveyed within each grid cell for each spatial resolution. The number of grid cells with survey effort and the percentage of grid cells that achieve 80% power to detect a hotspot/coldspot are shown below the horizontal axis.

Citation for main document:
Leirness JB, Kinlan BP. 2018. Additional statistical analyses to support guidelines for marine avian sampling. Sterling (VA): US Department of the Interior, Bureau of Ocean Energy Management. OCS Study BOEM 2018-063. iii+43 p.

## List of Figures

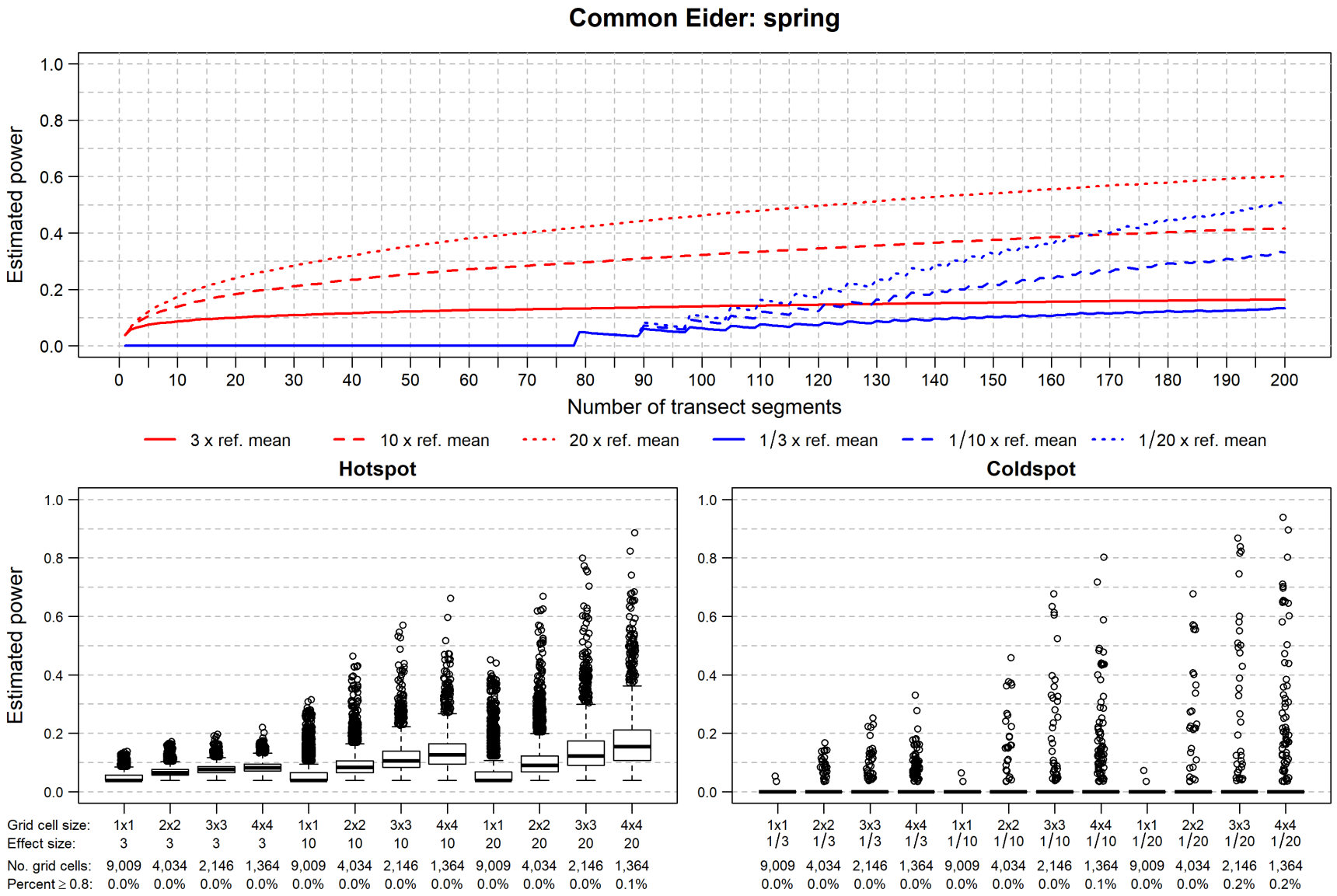


**Figure E1. Power analysis results for Common Eider during spring based on the combined model (type I error rate = 0.05)**

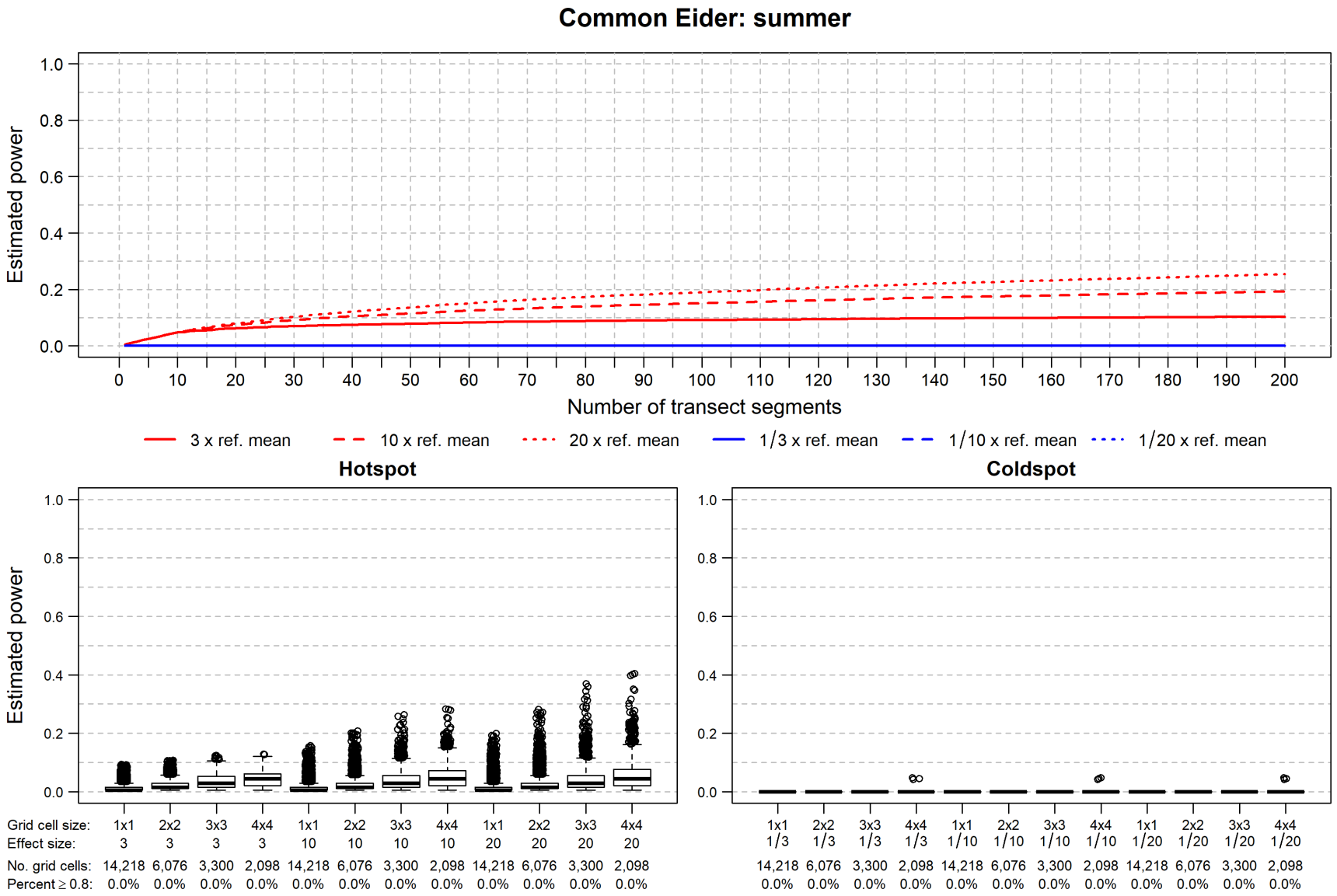


**Figure E2. Power analysis results for Common Eider during summer based on the combined model (type I error rate = 0.05)**

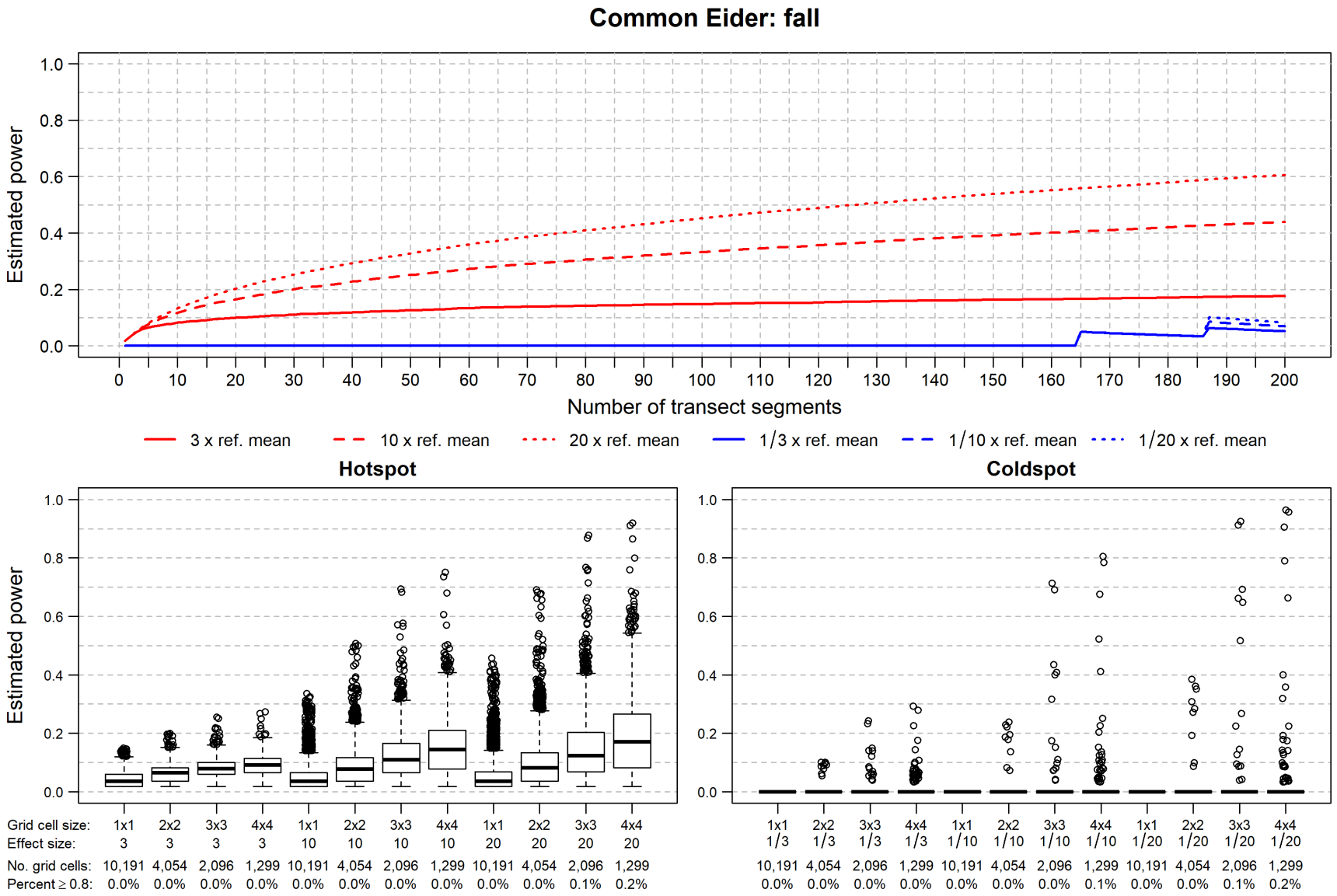


**Figure E3. Power analysis results for Common Eider during fall based on the combined model (type I error rate = 0.05)**

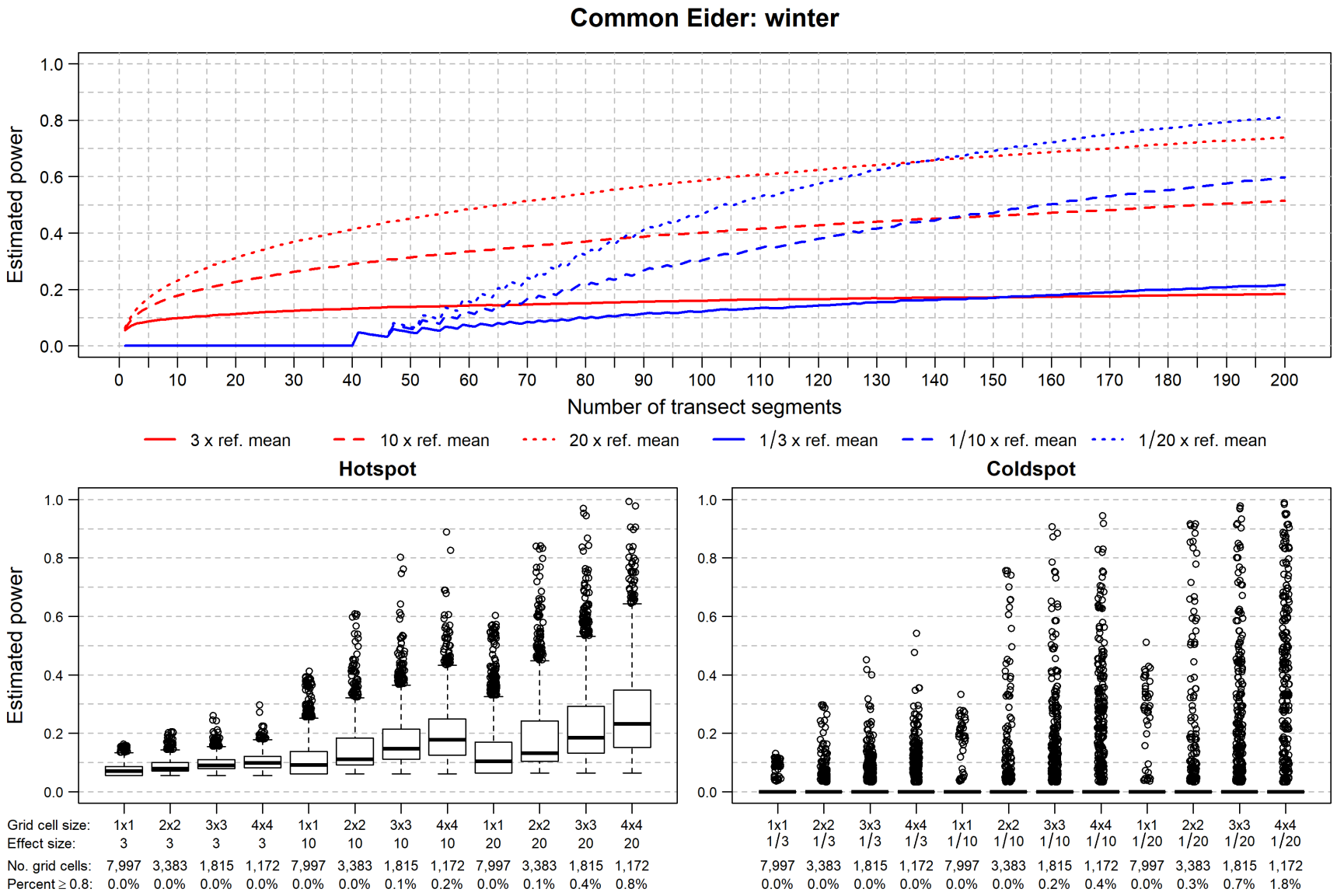


**Figure E4. Power analysis results for Common Eider during winter based on the combined model (type I error rate = 0.05)**

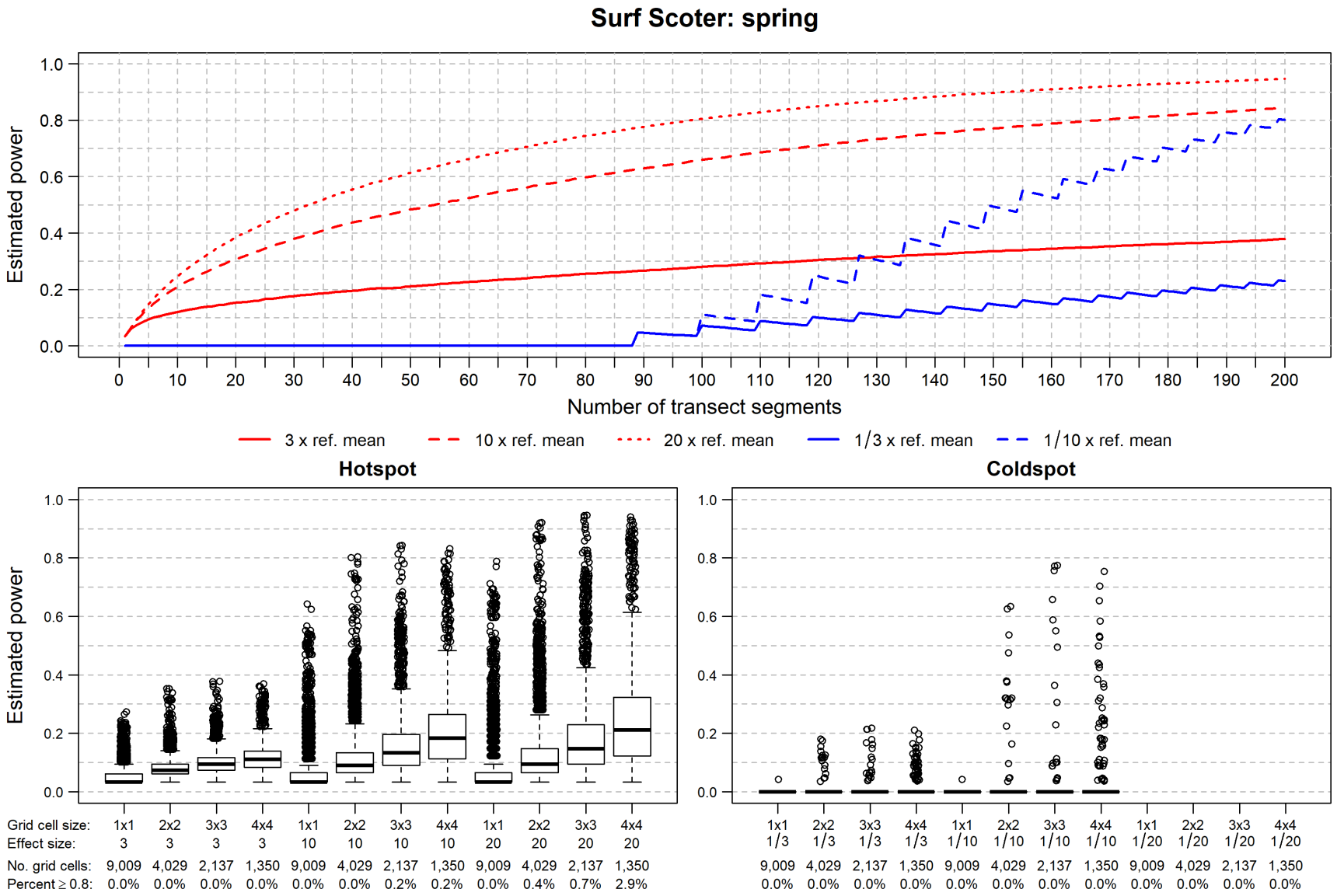


**Figure E5. Power analysis results for Surf Scoter during spring based on the combined model (type I error rate = 0.05)**

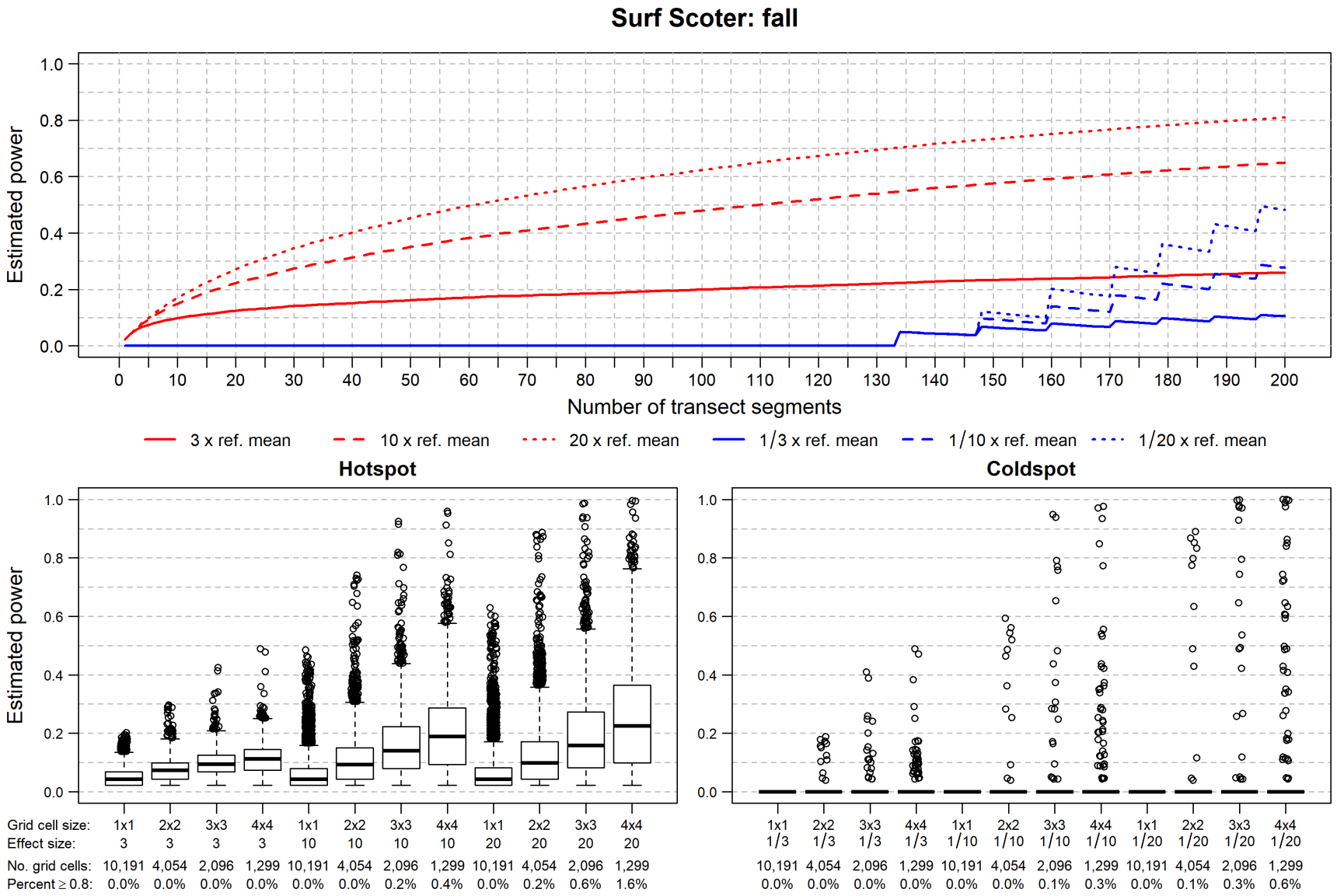


**Figure E6. Power analysis results for Surf Scoter during fall based on the combined model (type I error rate = 0.05)**

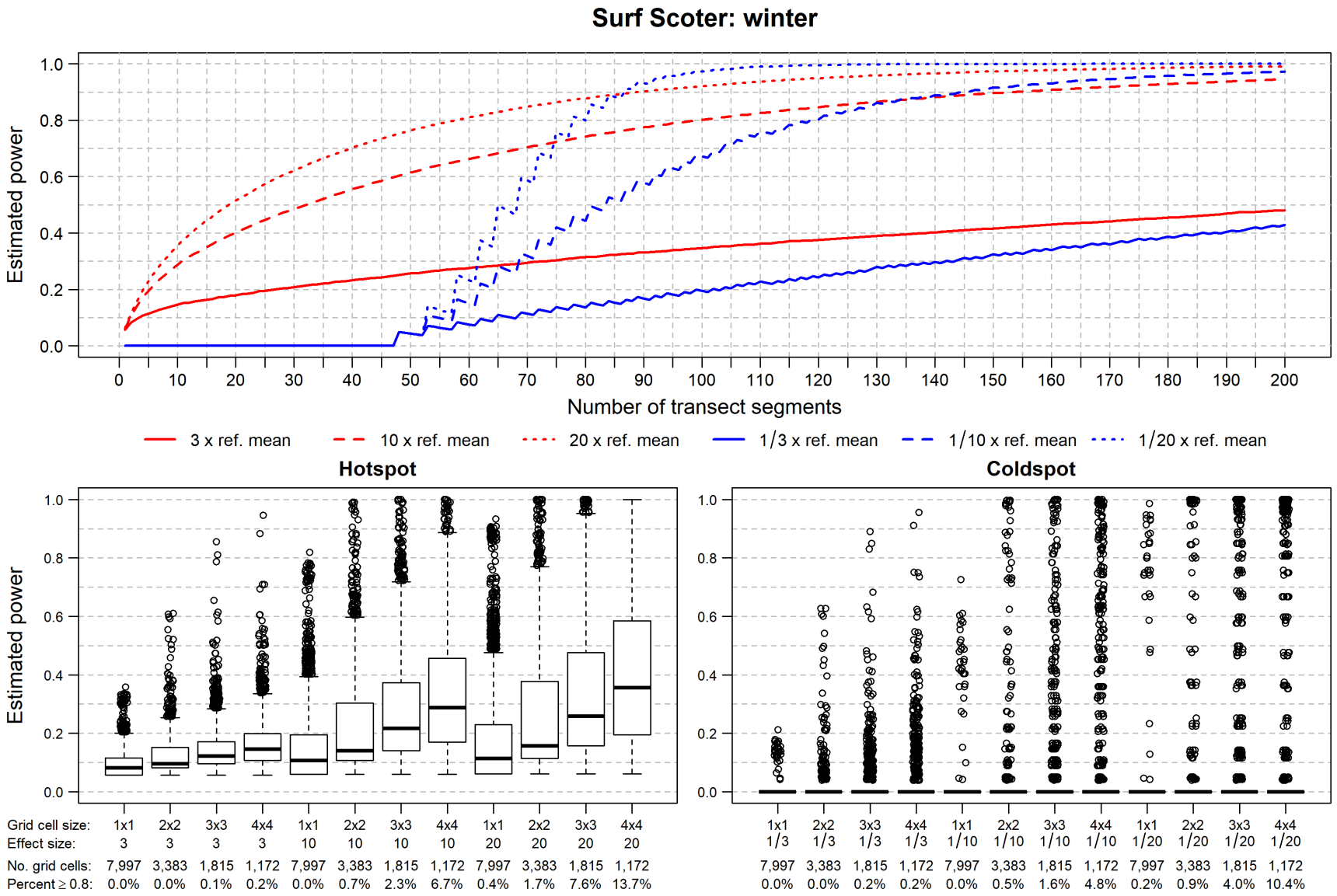


**Figure E7. Power analysis results for Surf Scoter during winter based on the combined model (type I error rate = 0.05)**

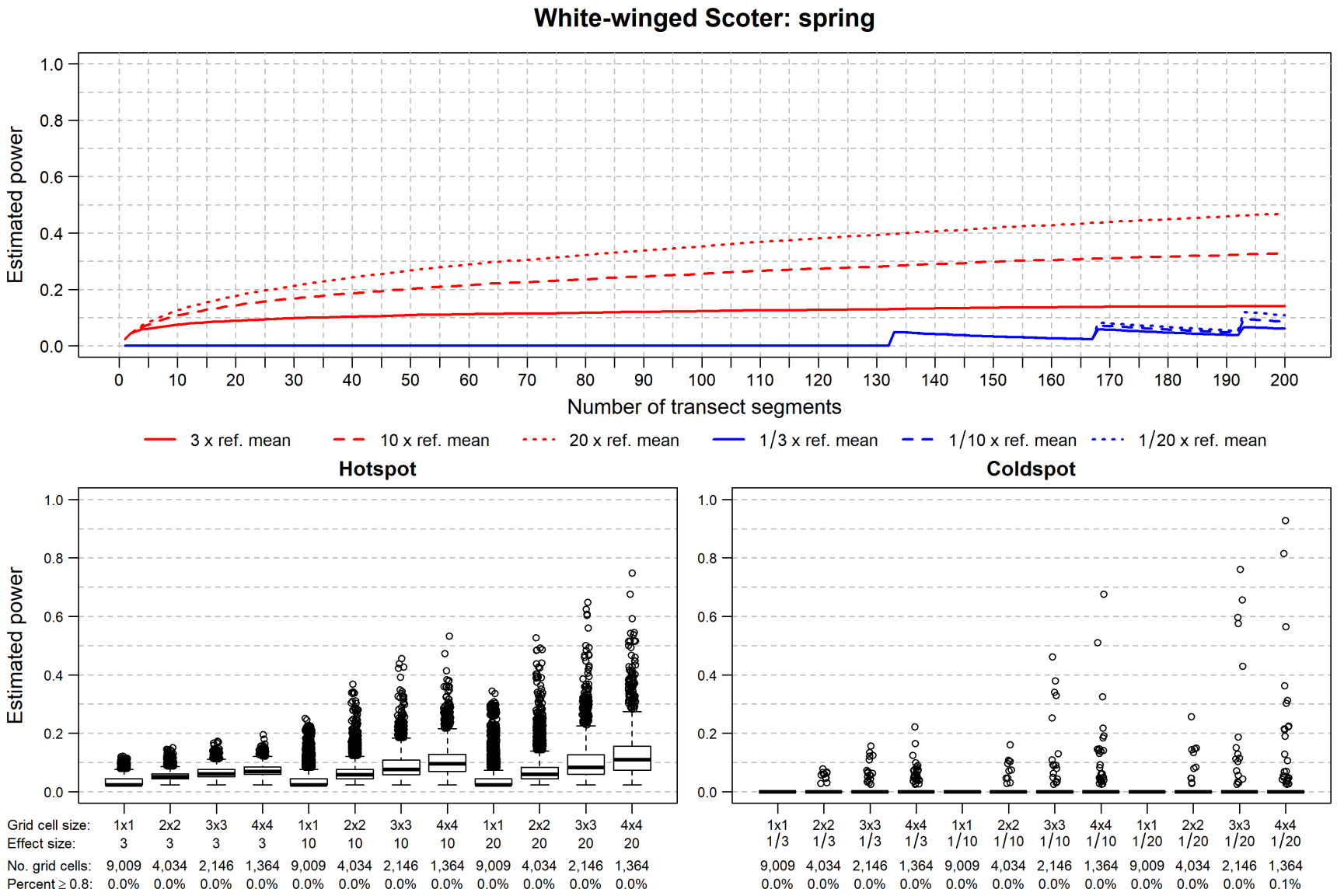


**Figure E8. Power analysis results for White-winged Scoter during spring based on the combined model (type I error rate = 0.05)**

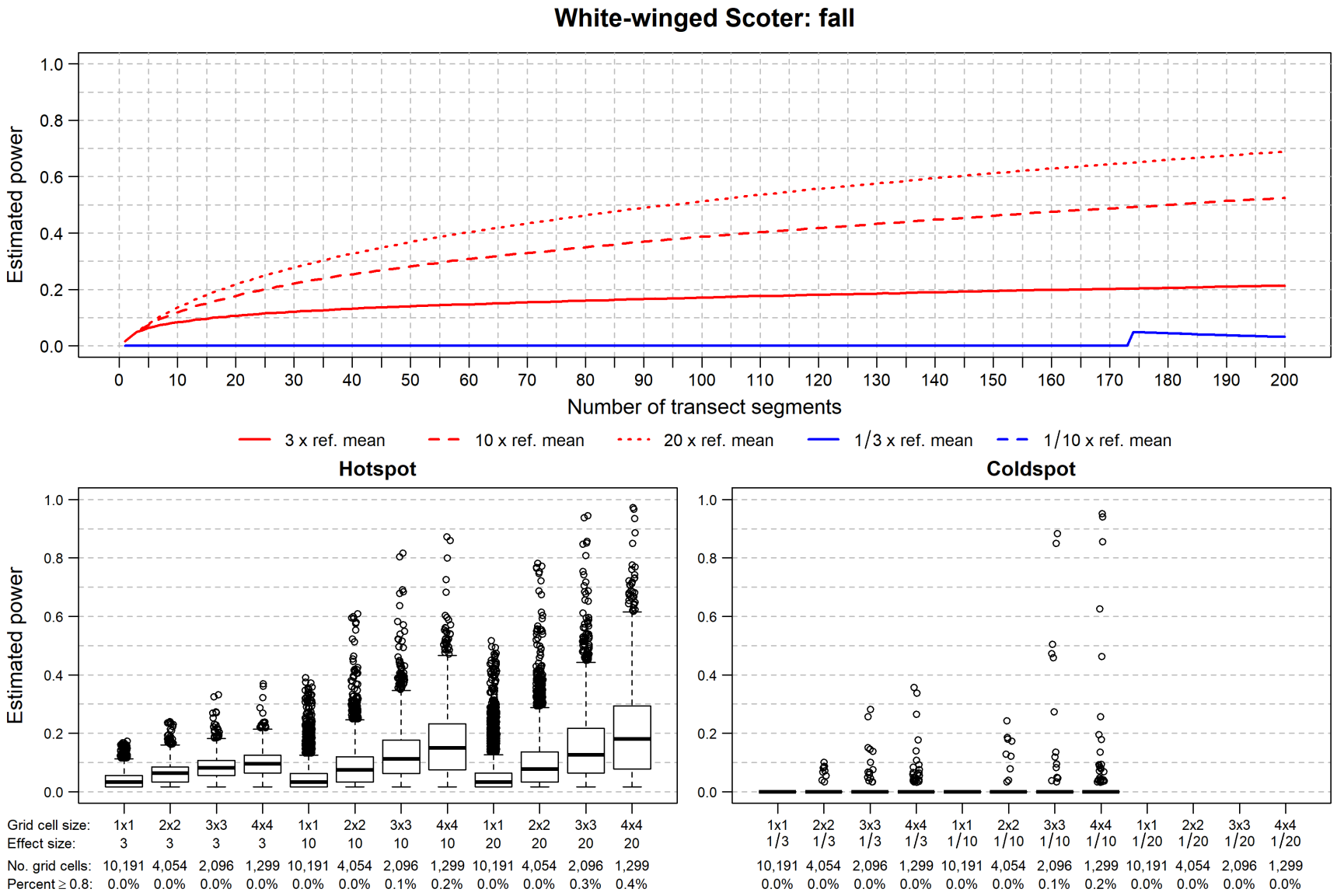


**Figure E9. Power analysis results for White-winged Scoter during fall based on the combined model (type I error rate = 0.05)**

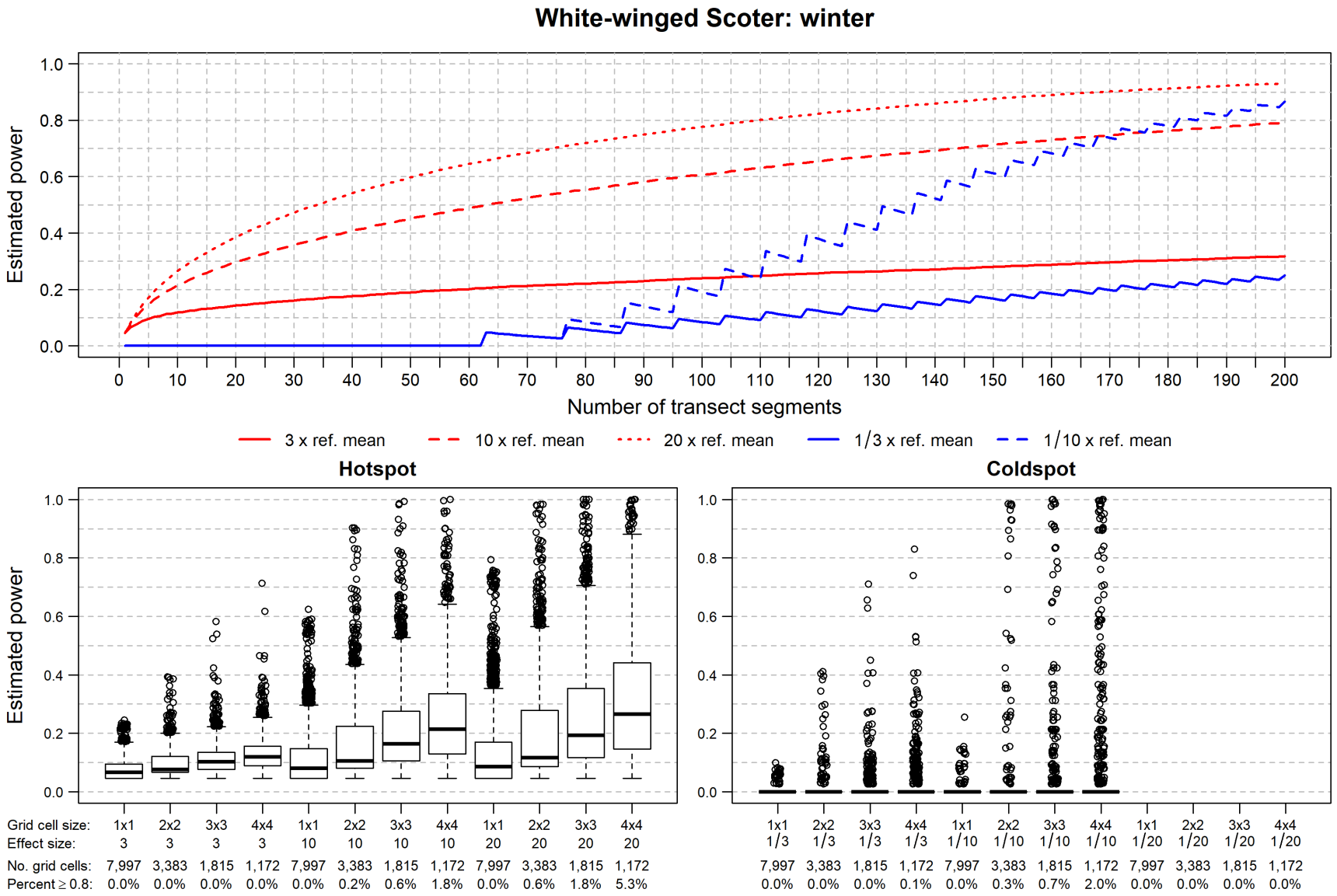


**Figure E10. Power analysis results for White-winged Scoter during winter based on the combined model (type I error rate = 0.05)**

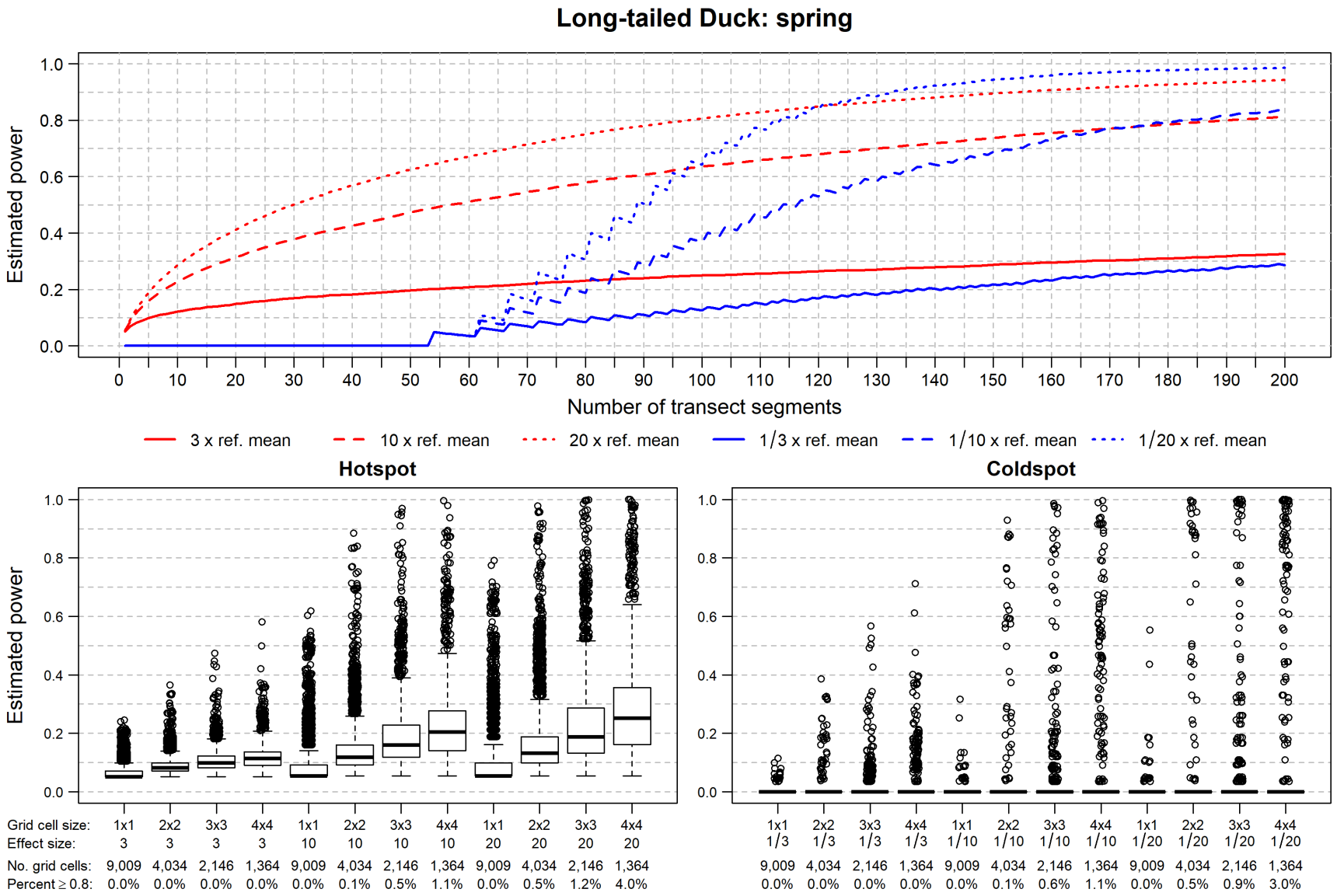


**Figure E11. Power analysis results for Long-tailed Duck during spring based on the combined model (type I error rate = 0.05)**

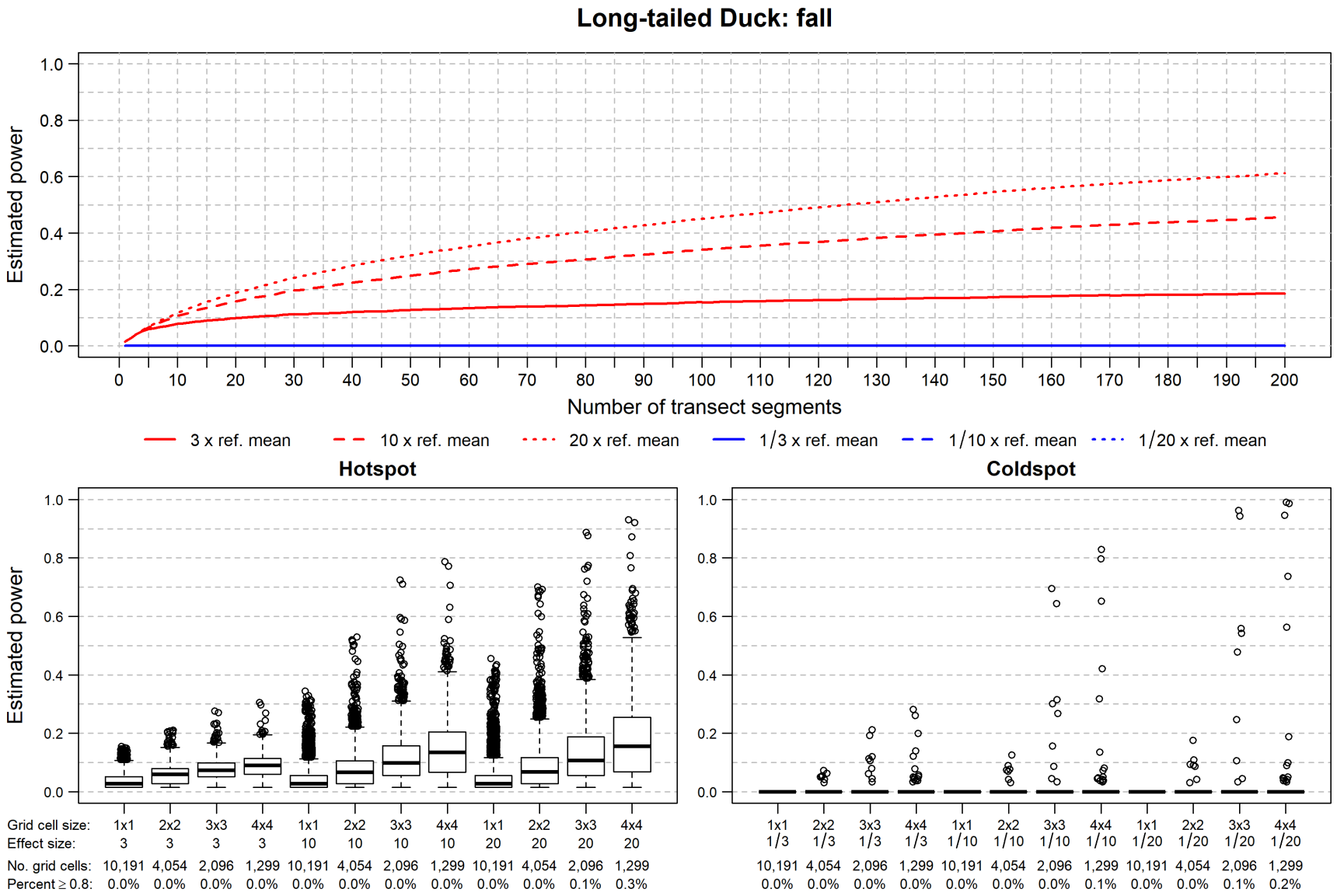


**Figure E12. Power analysis results for Long-tailed Duck during fall based on the combined model (type I error rate = 0.05)**

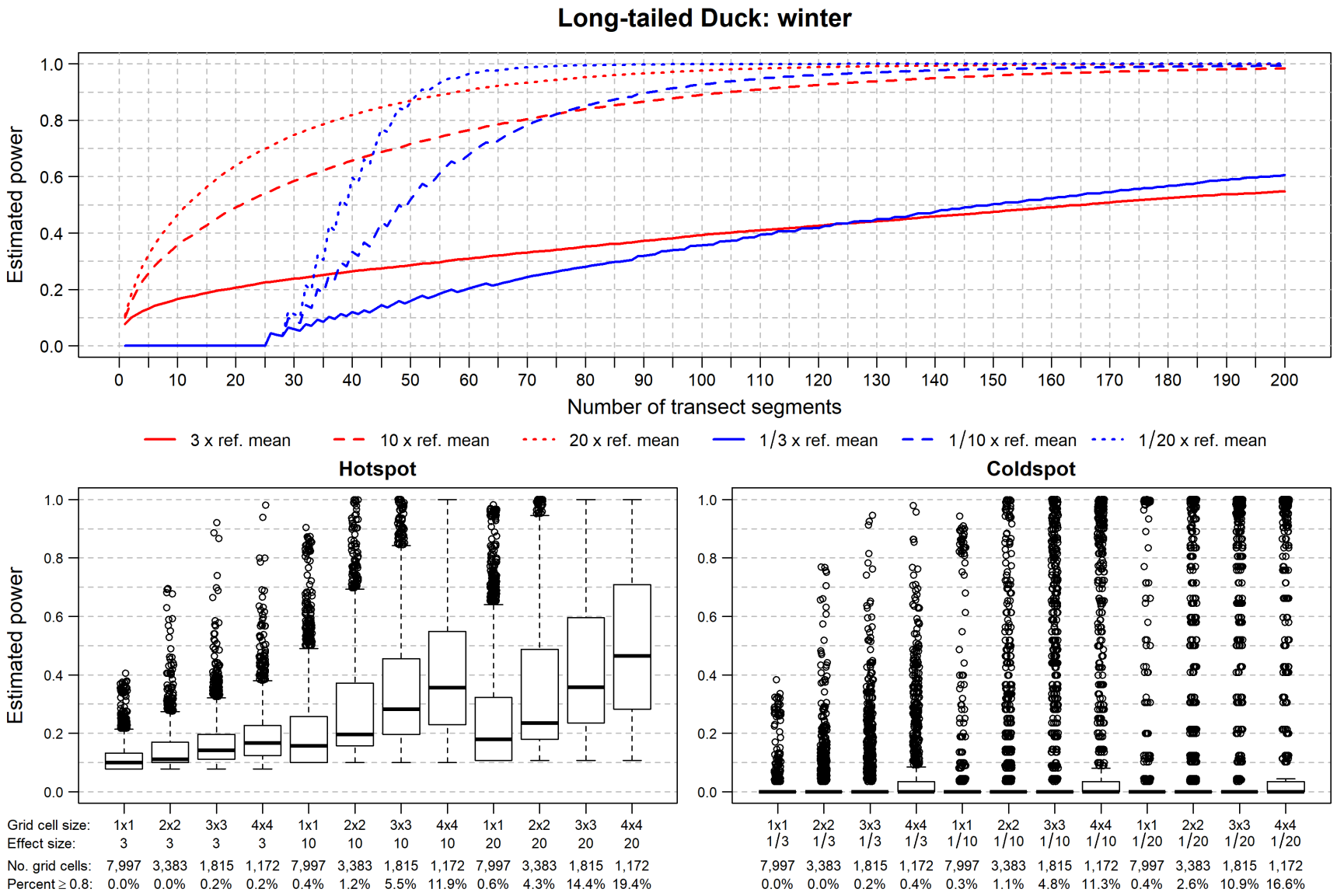


**Figure E13. Power analysis results for Long-tailed Duck during winter based on the combined model (type I error rate = 0.05)**

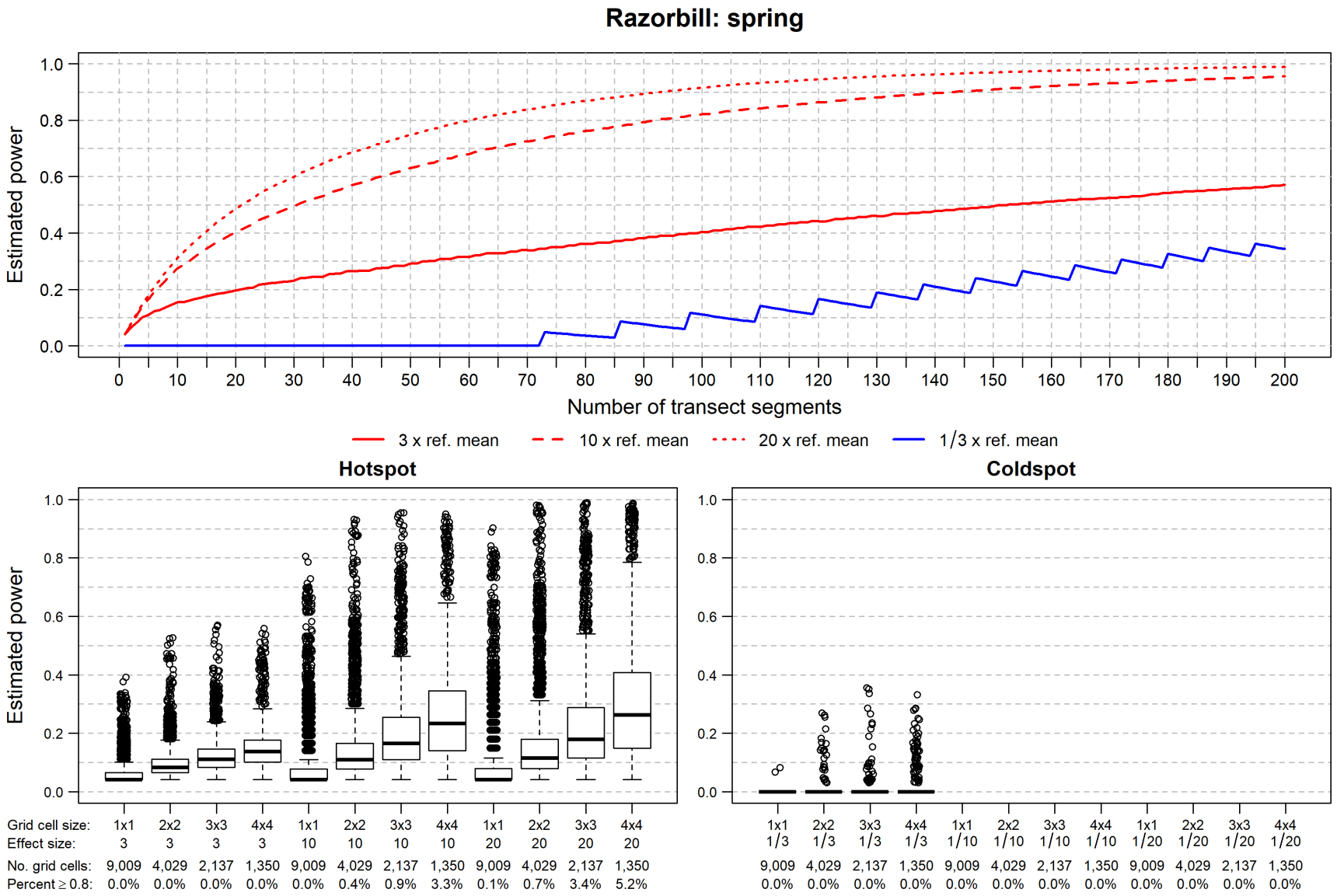


**Figure E14. Power analysis results for Razorbill during spring based on the combined model (type I error rate = 0.05)**

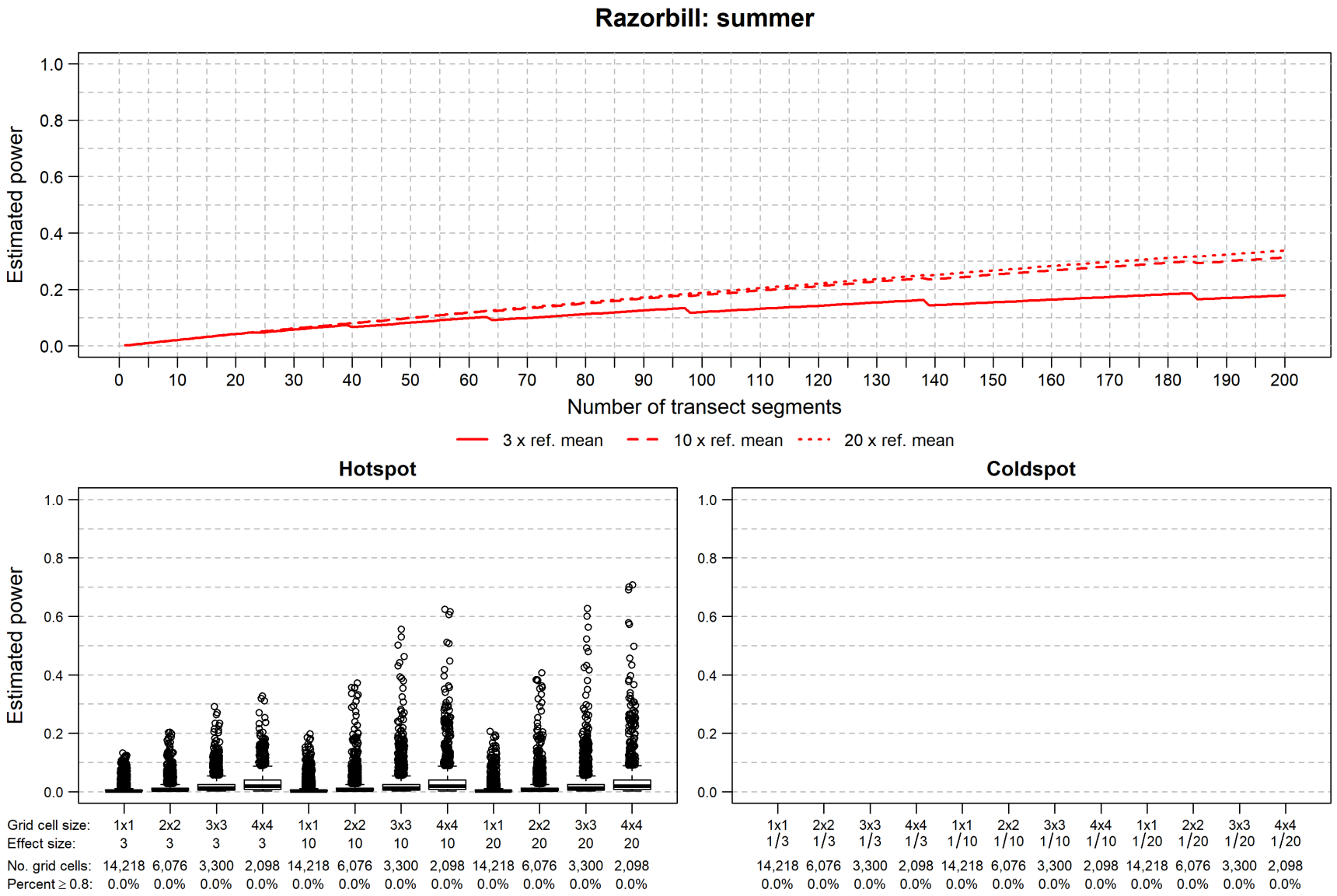


**Figure E15. Power analysis results for Razorbill during summer based on the combined model (type I error rate = 0.05)**

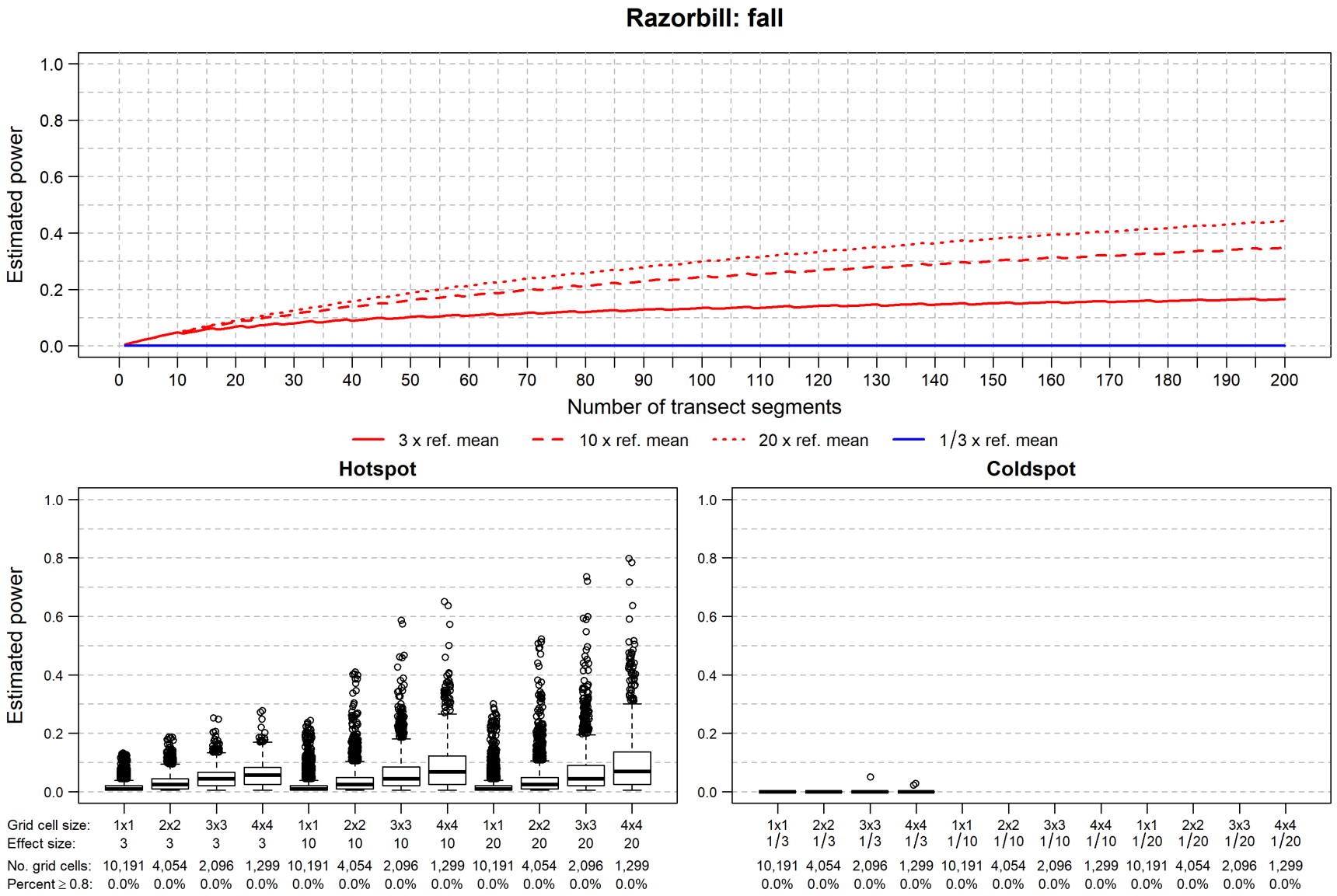


**Figure E16. Power analysis results for Razorbill during fall based on the combined model (type I error rate = 0.05)**

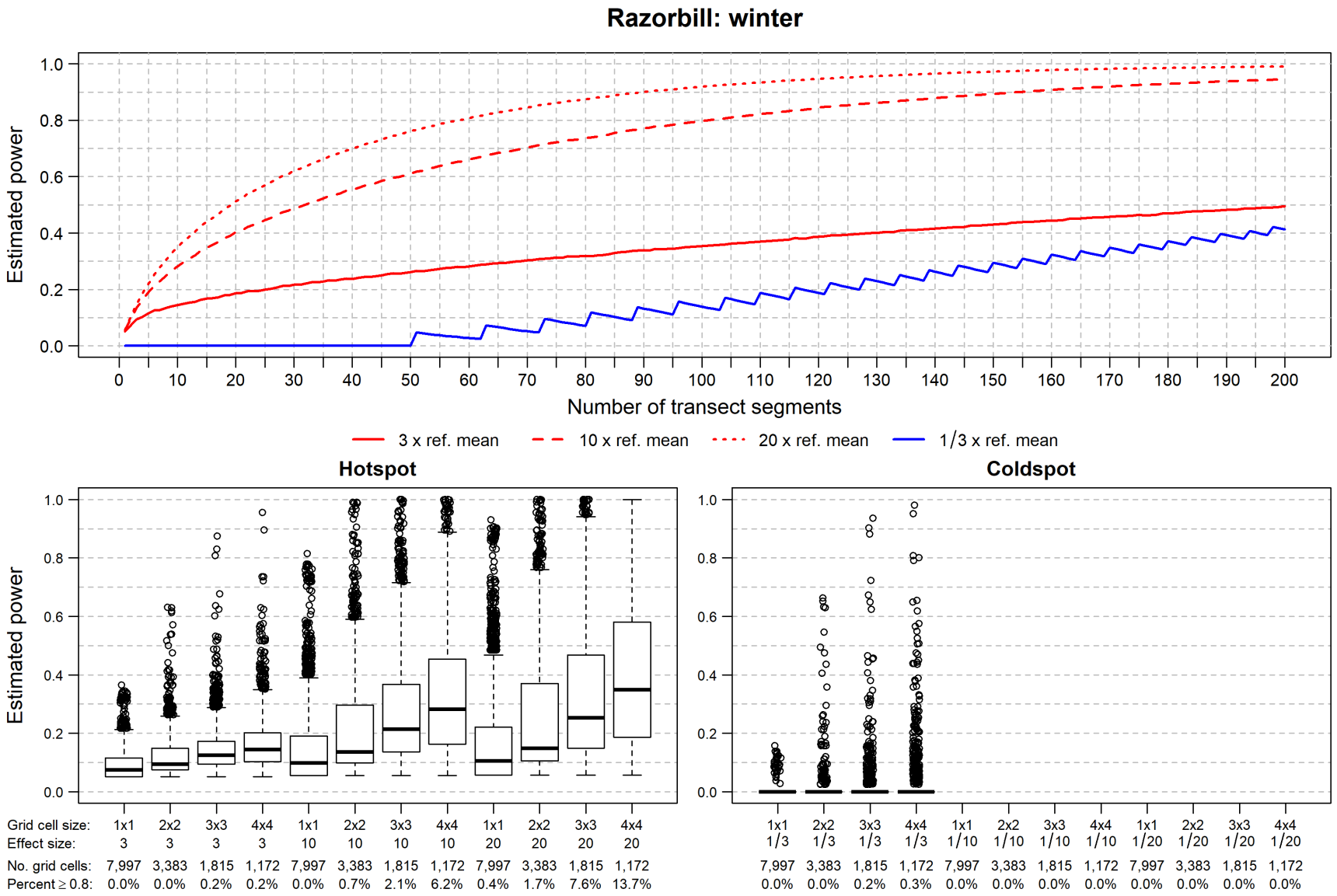


**Figure E17. Power analysis results for Razorbill during winter based on the combined model (type I error rate = 0.05)**

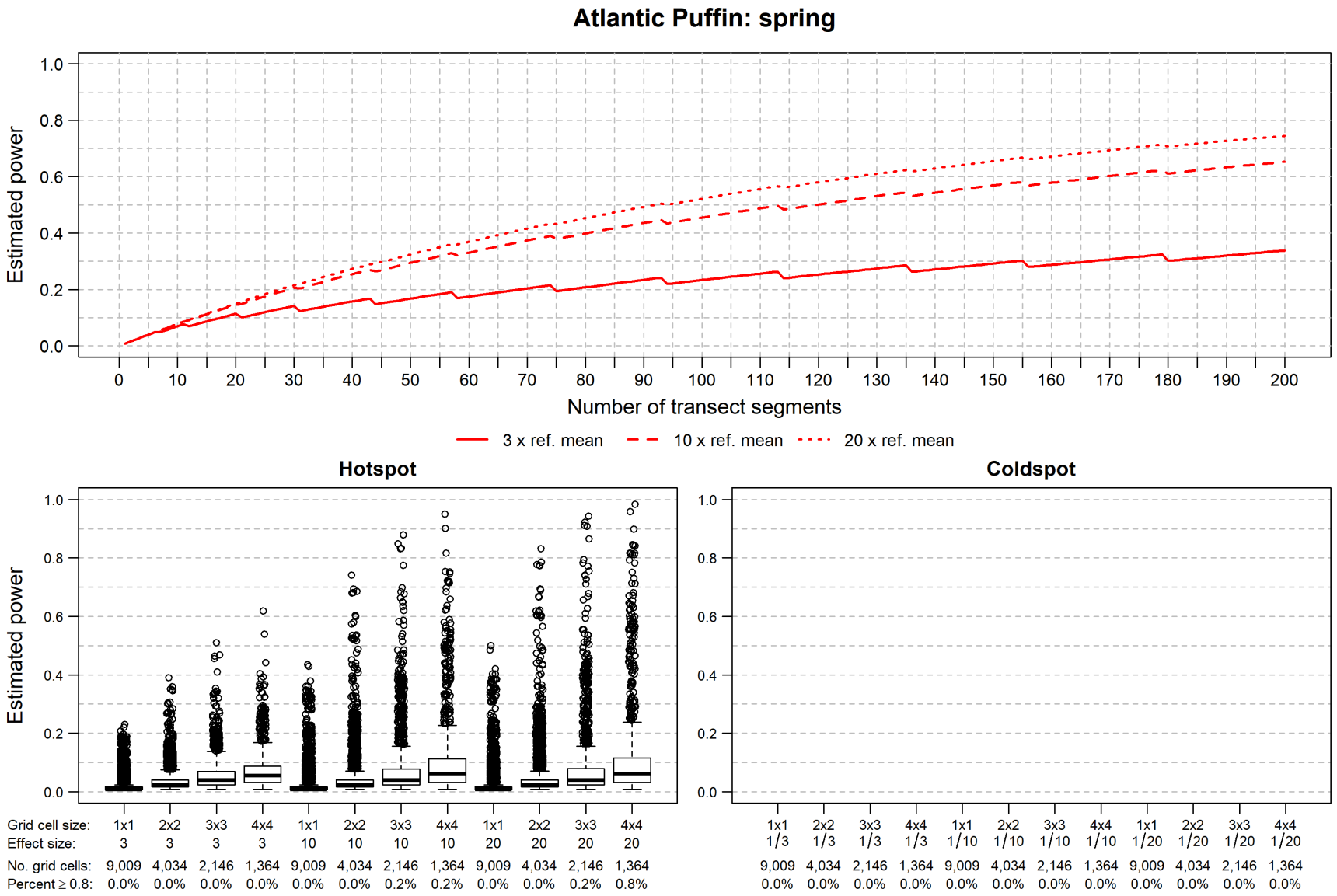


**Figure E18. Power analysis results for Atlantic Puffin during spring based on the combined model (type I error rate = 0.05)**

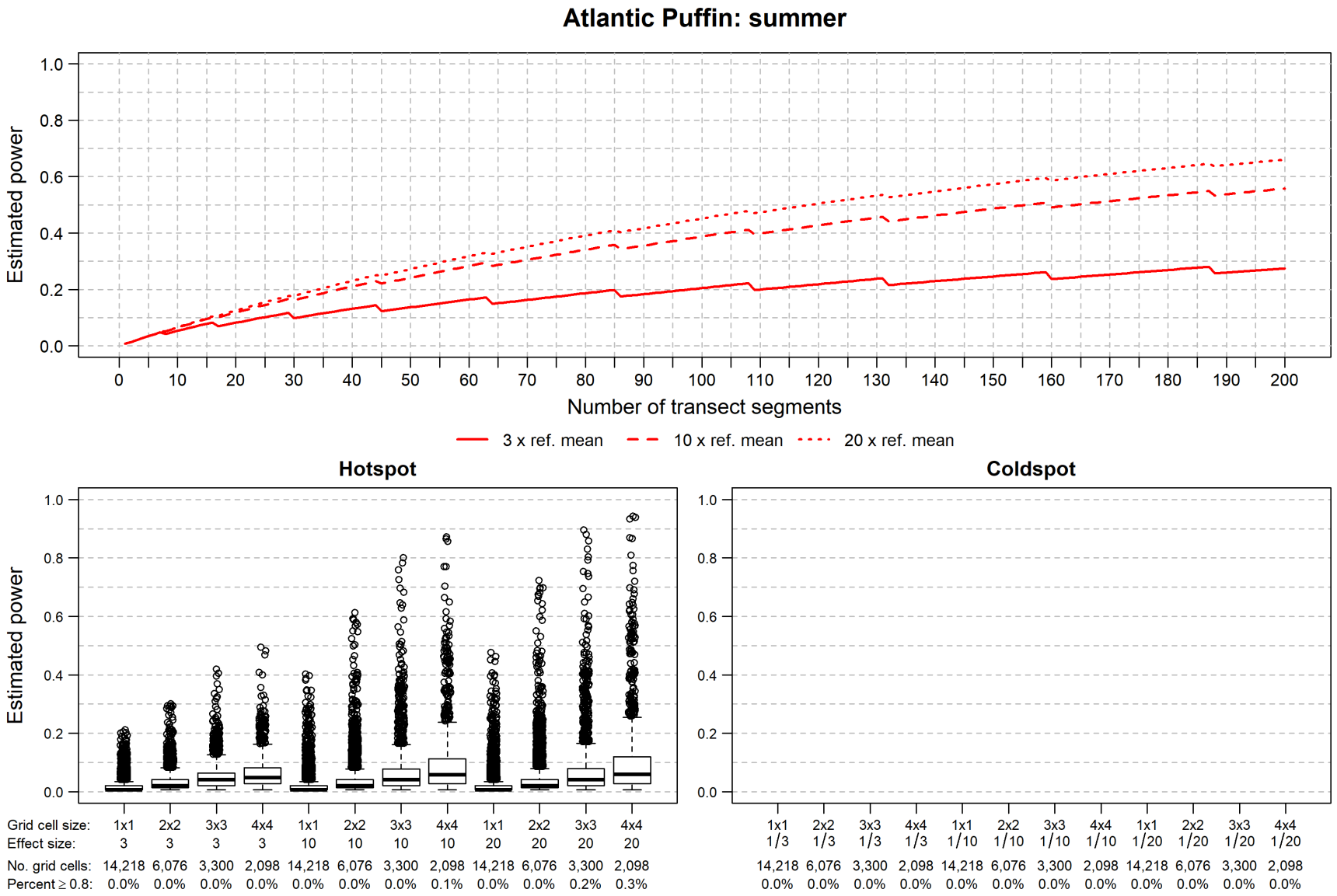


**Figure E19. Power analysis results for Atlantic Puffin during summer based on the combined model (type I error rate = 0.05)**

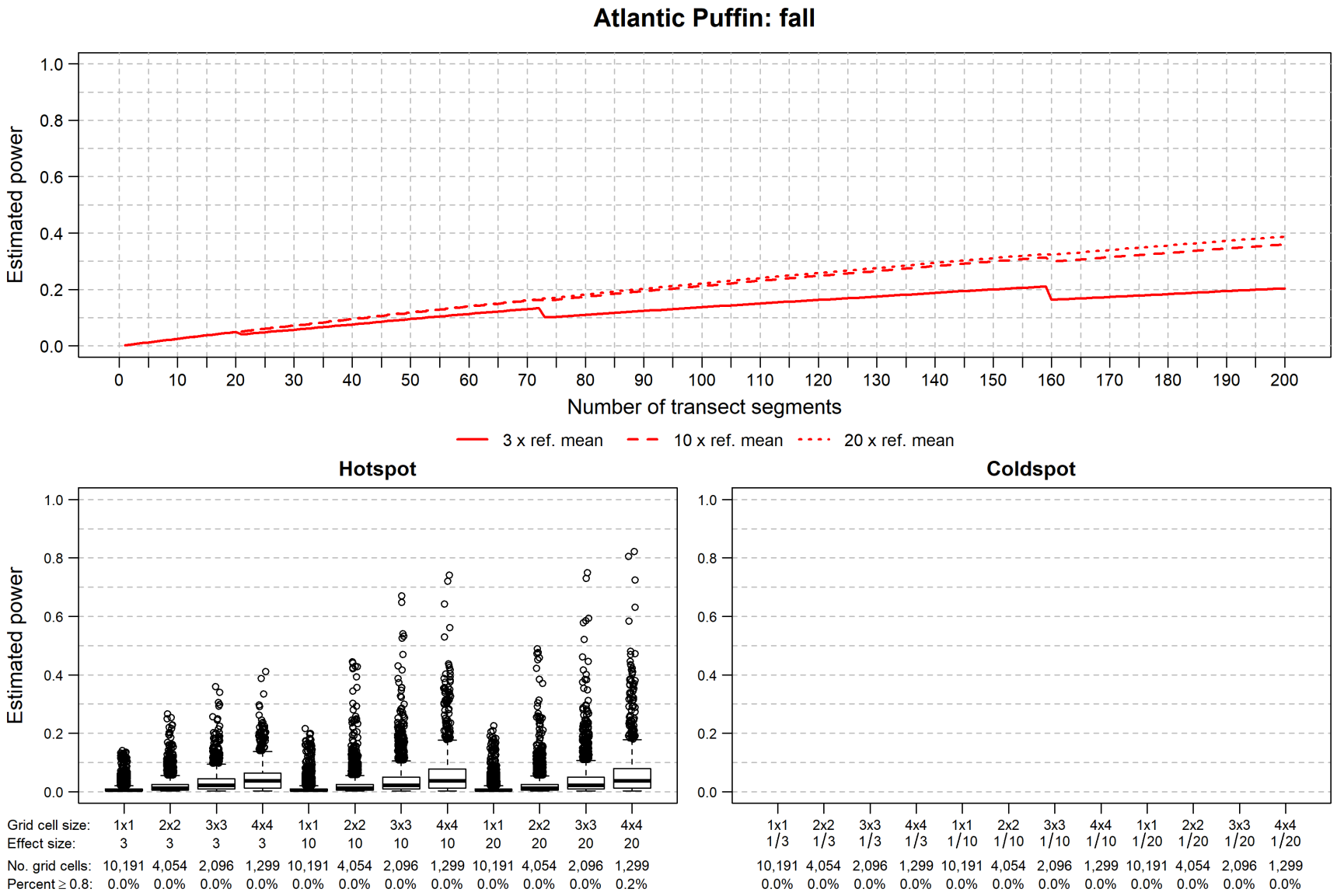


**Figure E20. Power analysis results for Atlantic Puffin during fall based on the combined model (type I error rate = 0.05)**

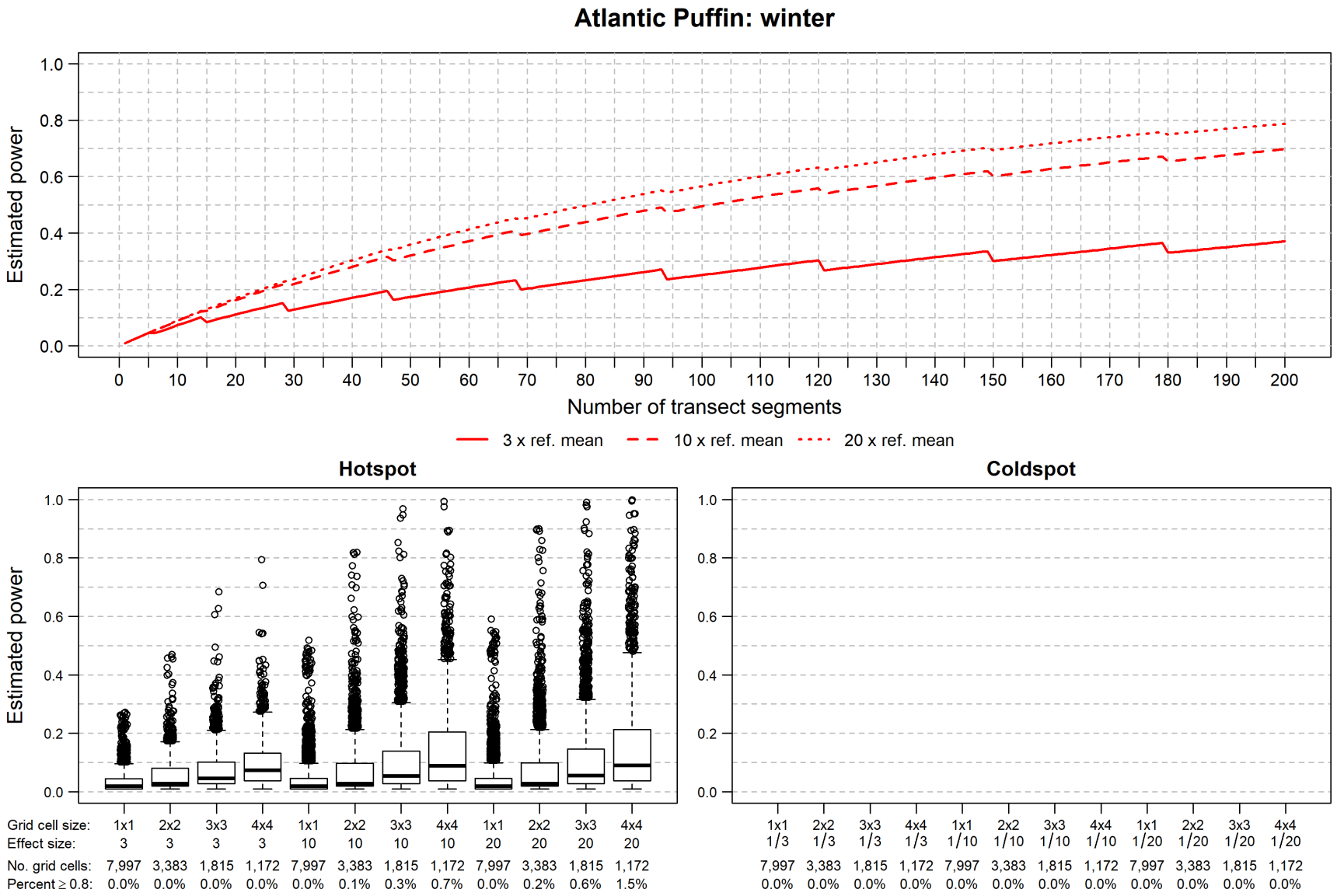


**Figure E21. Power analysis results for Atlantic Puffin during winter based on the combined model (type I error rate = 0.05)**

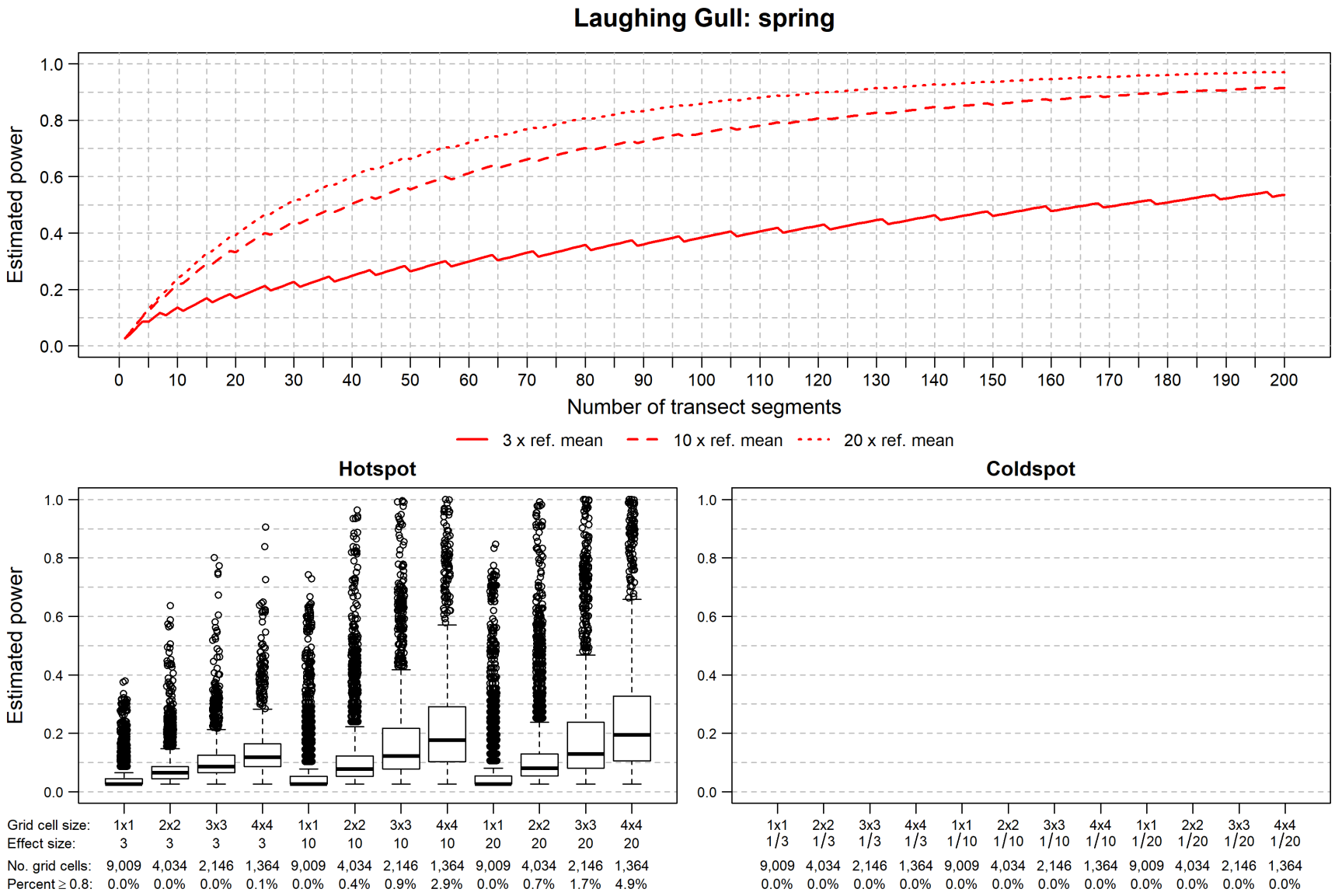


**Figure E22. Power analysis results for Laughing Gull during spring based on the combined model (type I error rate = 0.05)**

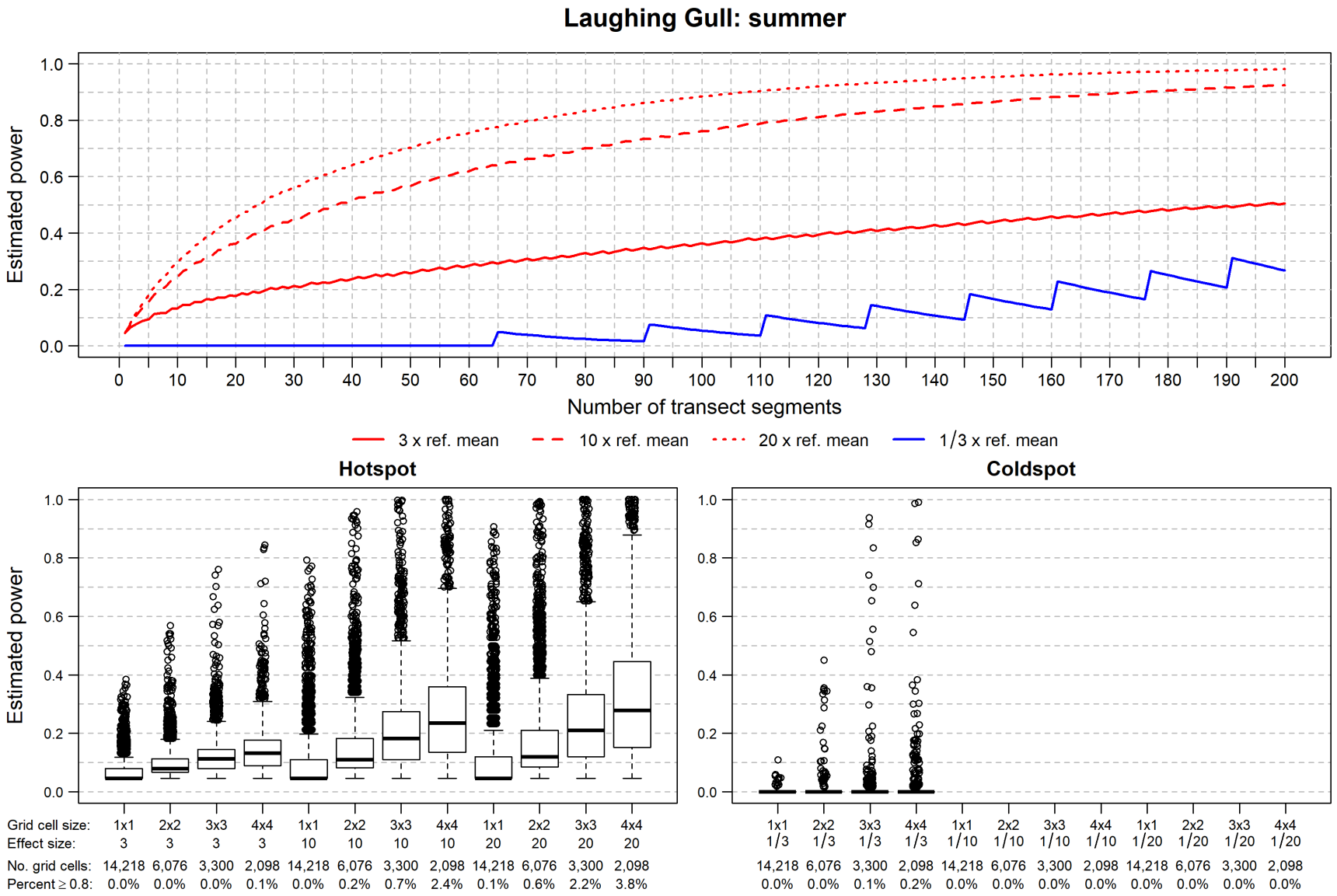


**Figure E23. Power analysis results for Laughing Gull during summer based on the combined model (type I error rate = 0.05)**

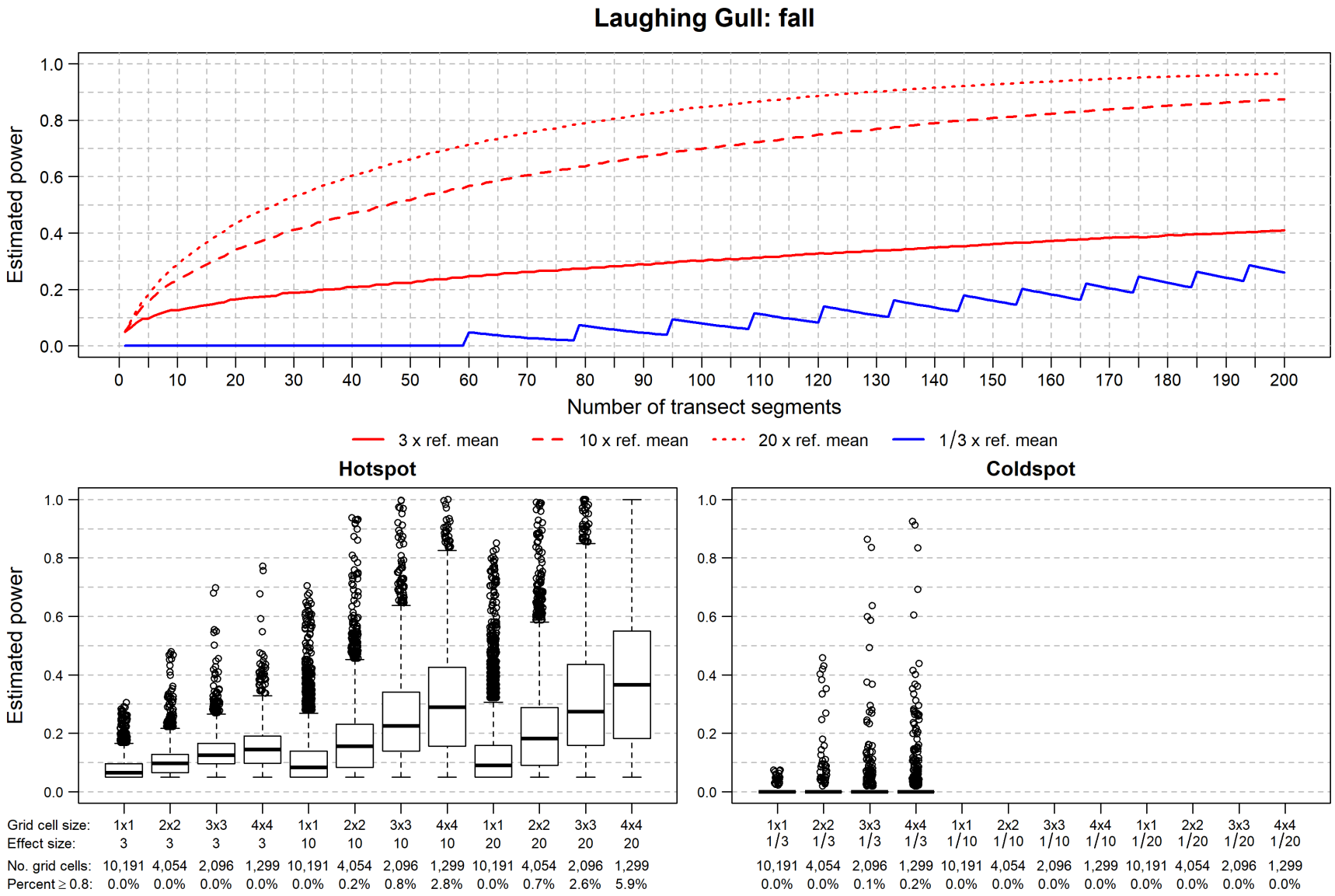


**Figure E24. Power analysis results for Laughing Gull during fall based on the combined model (type I error rate = 0.05)**

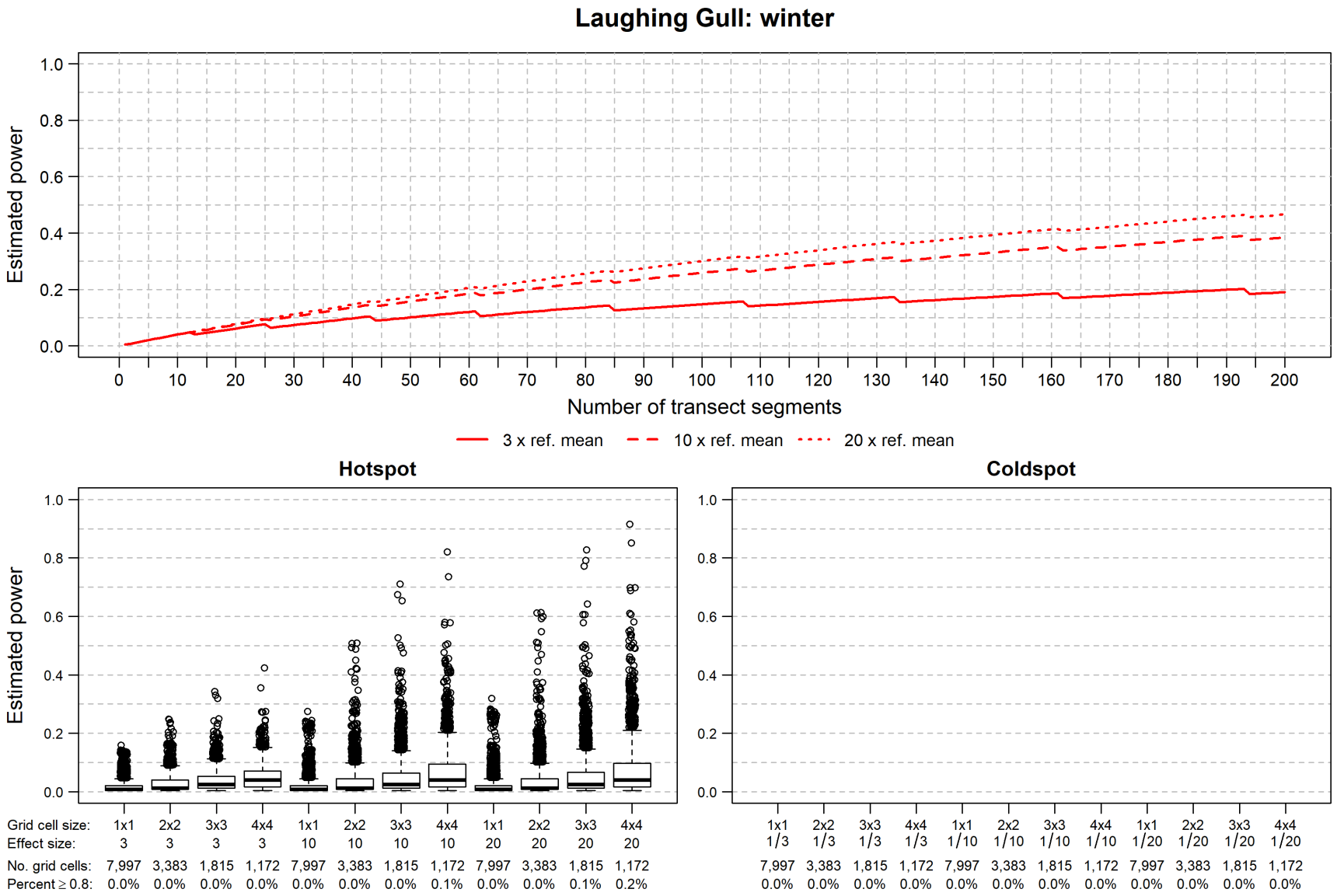


**Figure E25. Power analysis results for Laughing Gull during winter based on the combined model (type I error rate = 0.05)**

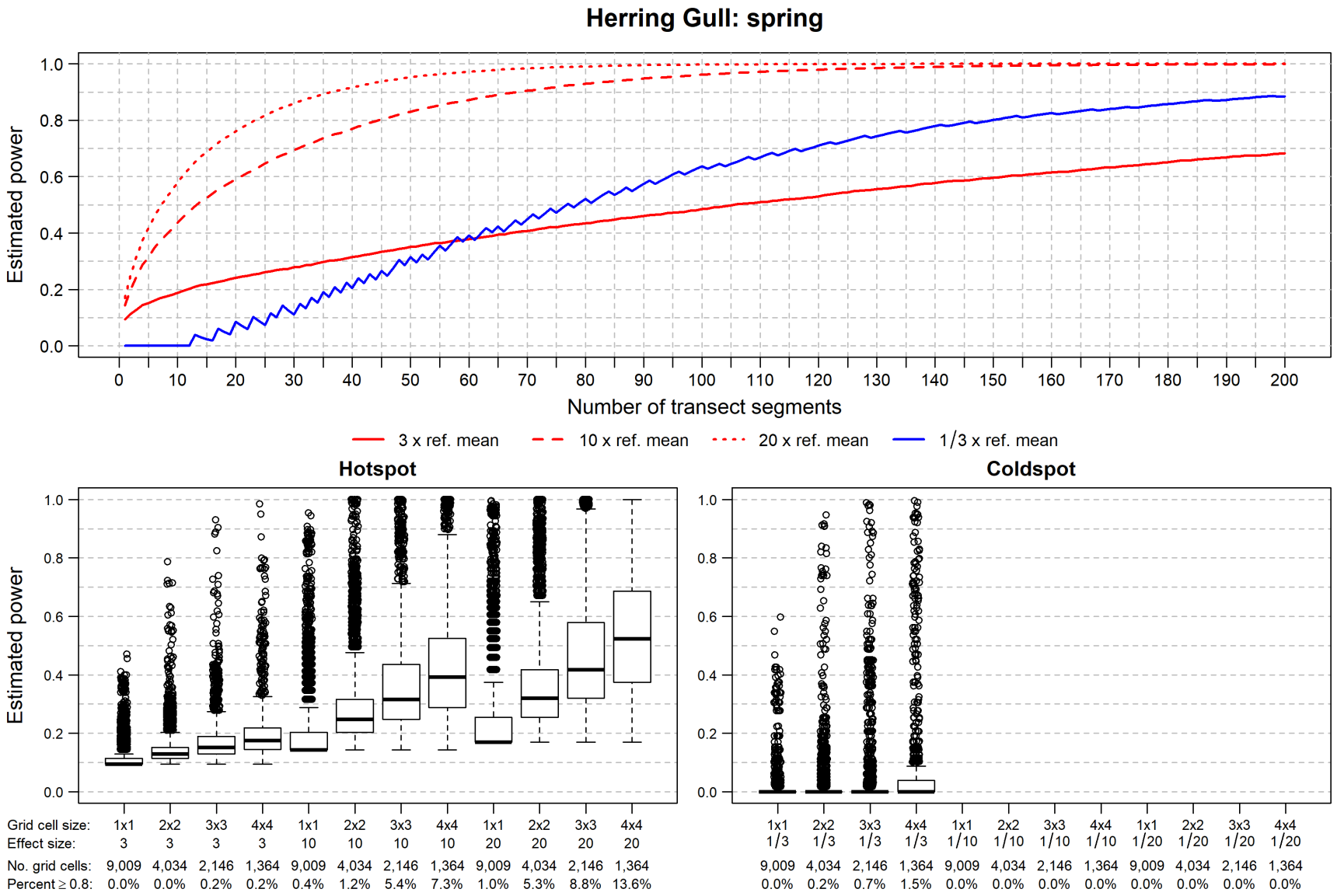


**Figure E26. Power analysis results for Herring Gull during spring based on the combined model (type I error rate = 0.05)**

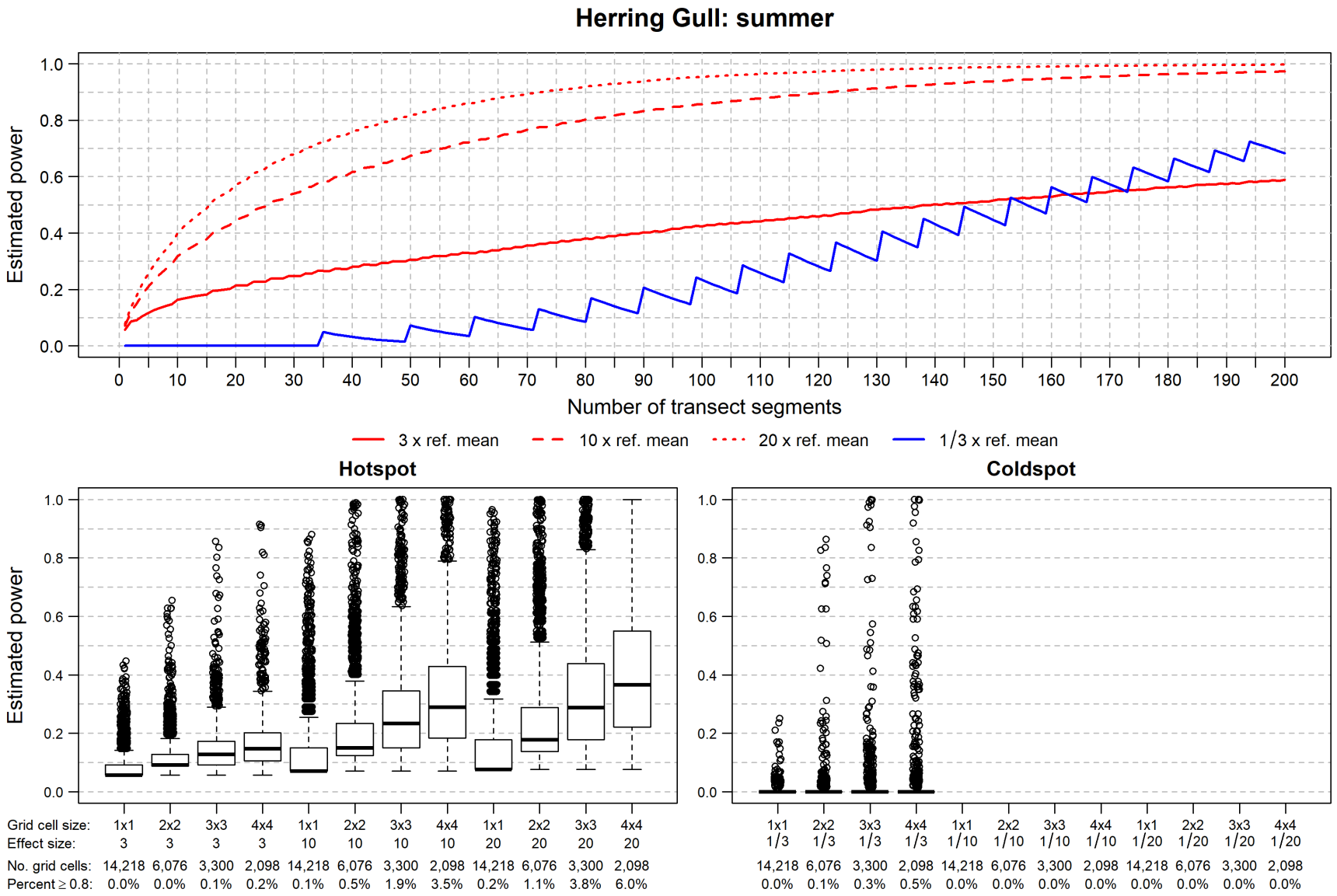


**Figure E27. Power analysis results for Herring Gull during summer based on the combined model (type I error rate = 0.05)**

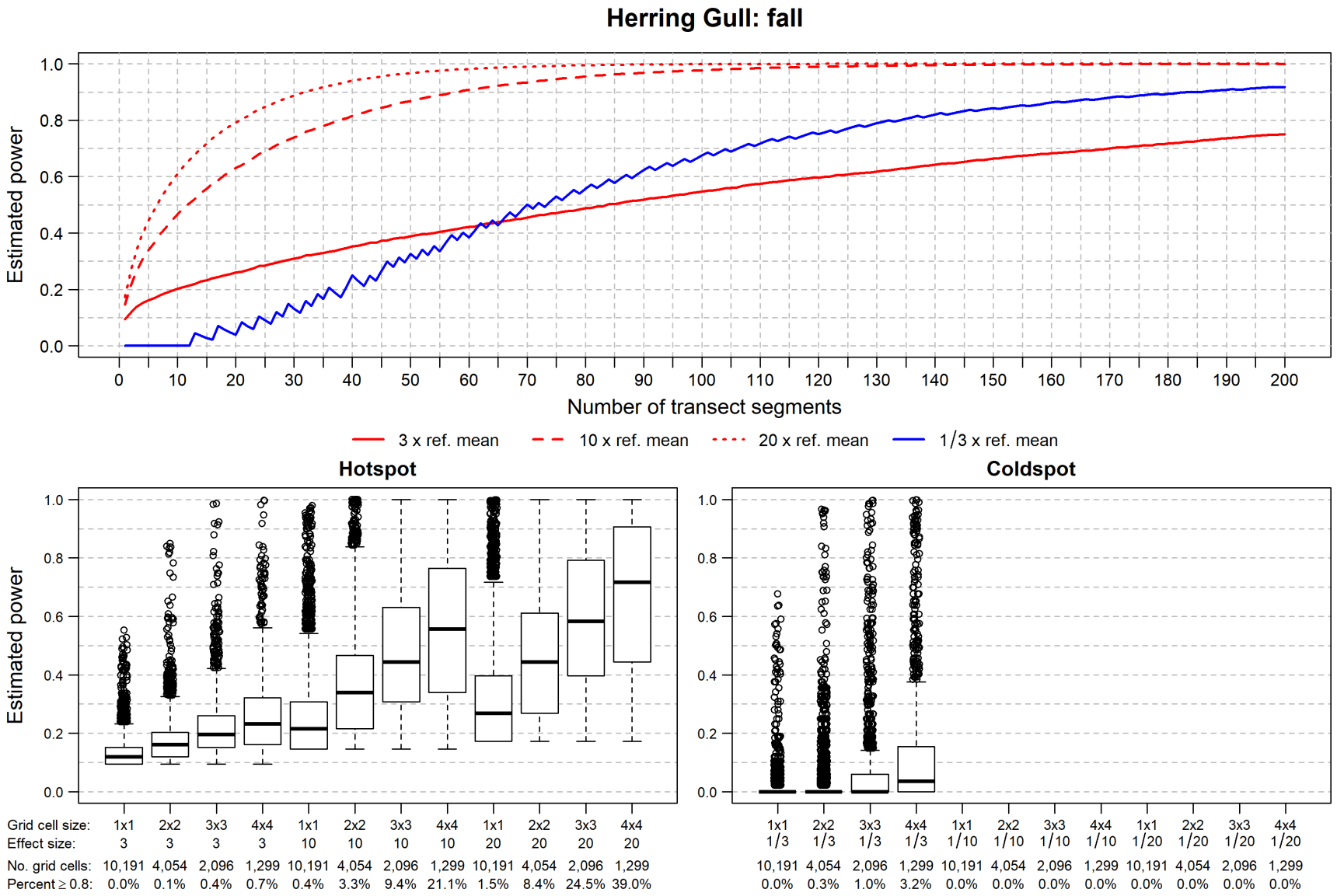


**Figure E28. Power analysis results for Herring Gull during fall based on the combined model (type I error rate = 0.05)**

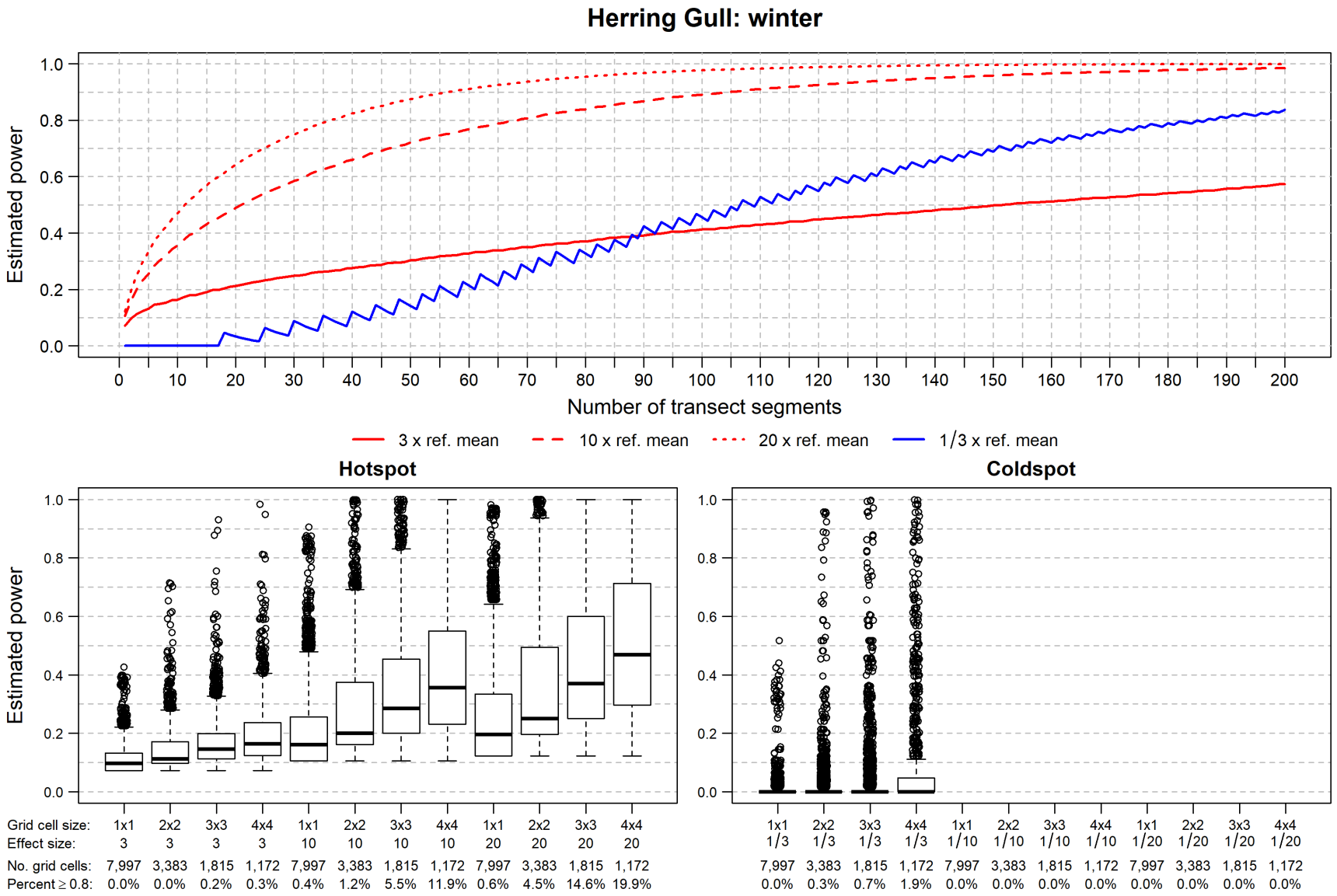


**Figure E29. Power analysis results for Herring Gull during winter based on the combined model (type I error rate = 0.05)**

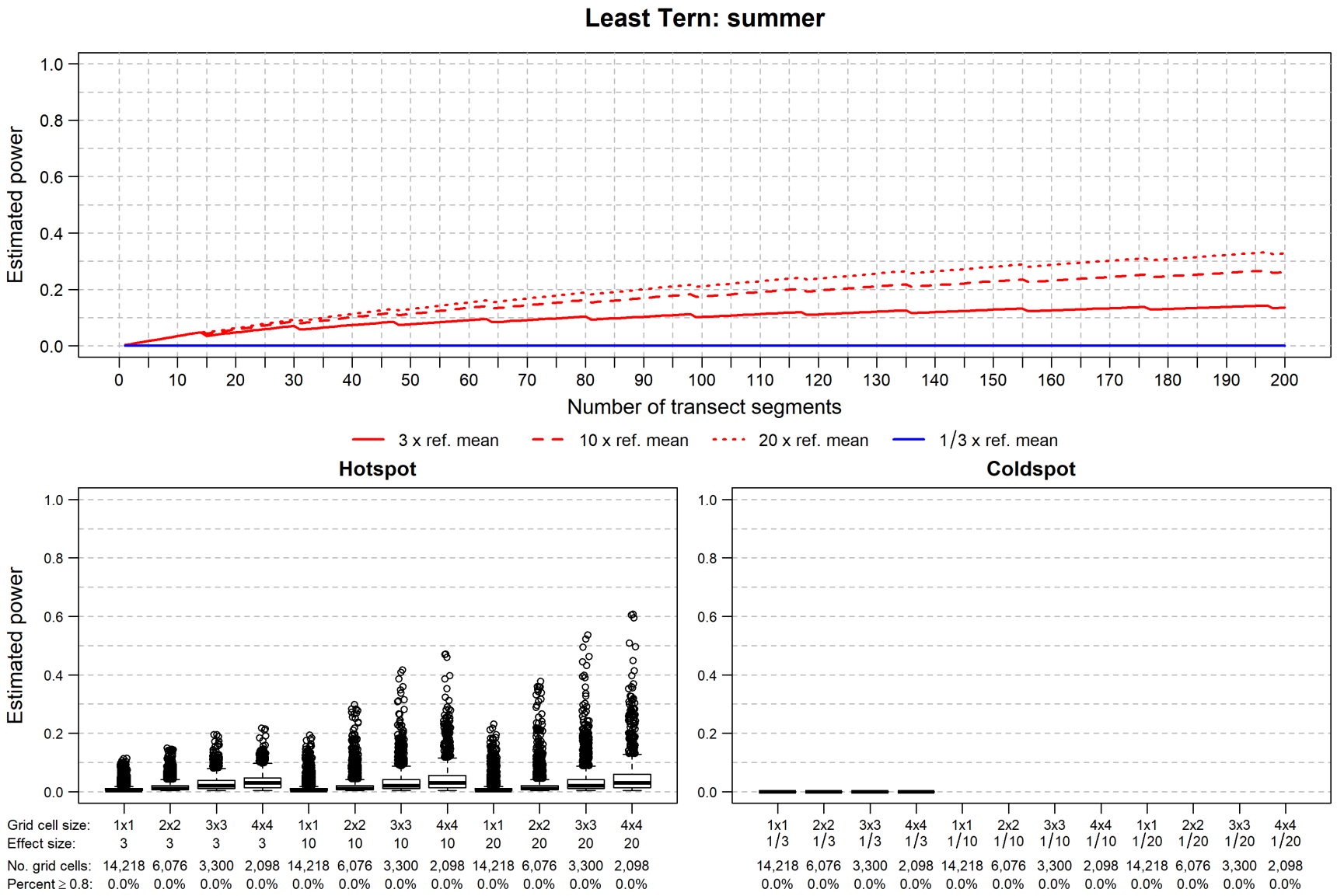


**Figure E30. Power analysis results for Least Tern during summer based on the combined model (type I error rate = 0.05)**

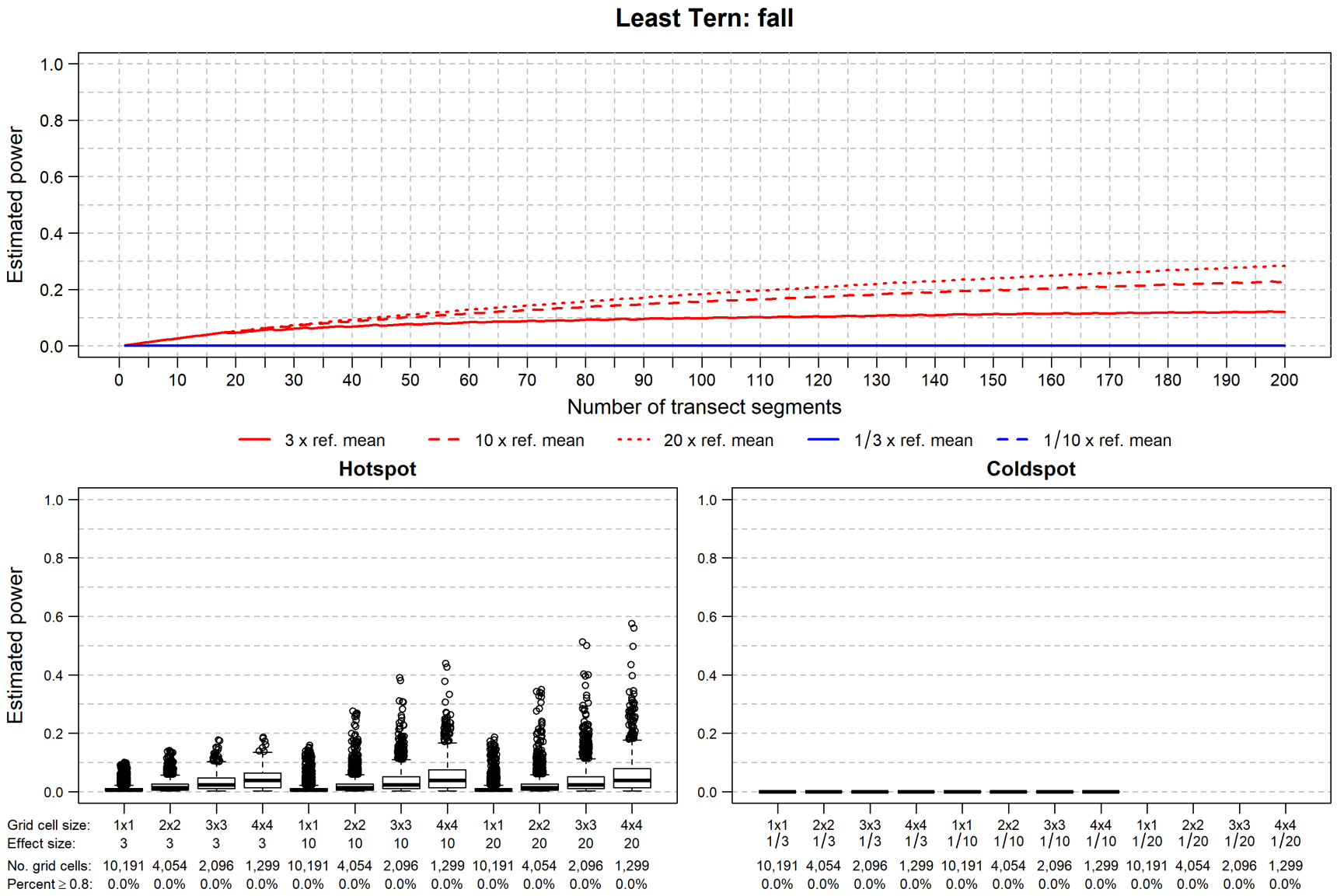


**Figure E31. Power analysis results for Least Tern during fall based on the combined model (type I error rate = 0.05)**

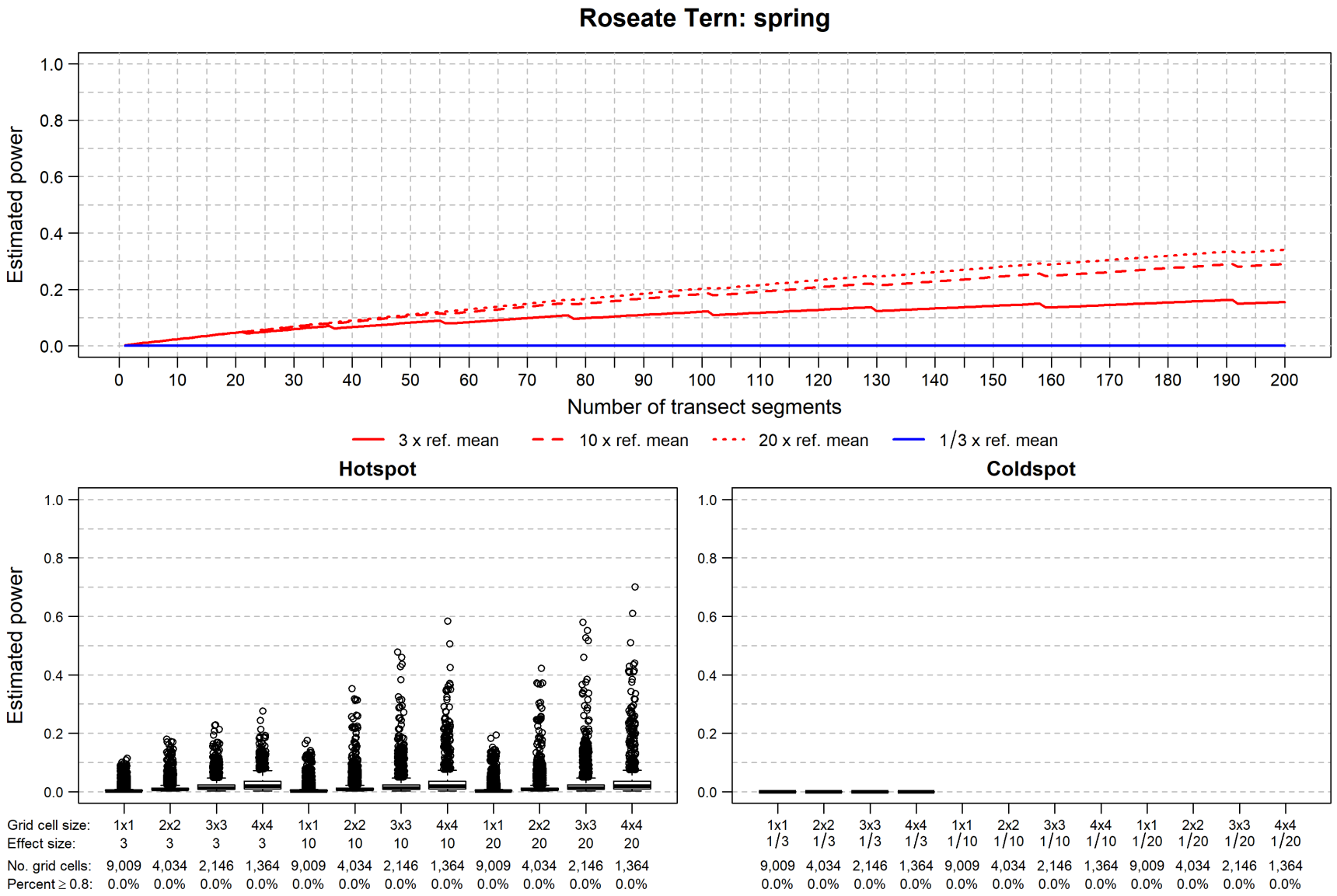


**Figure E32. Power analysis results for Roseate Tern during spring based on the combined model (type I error rate = 0.05)**

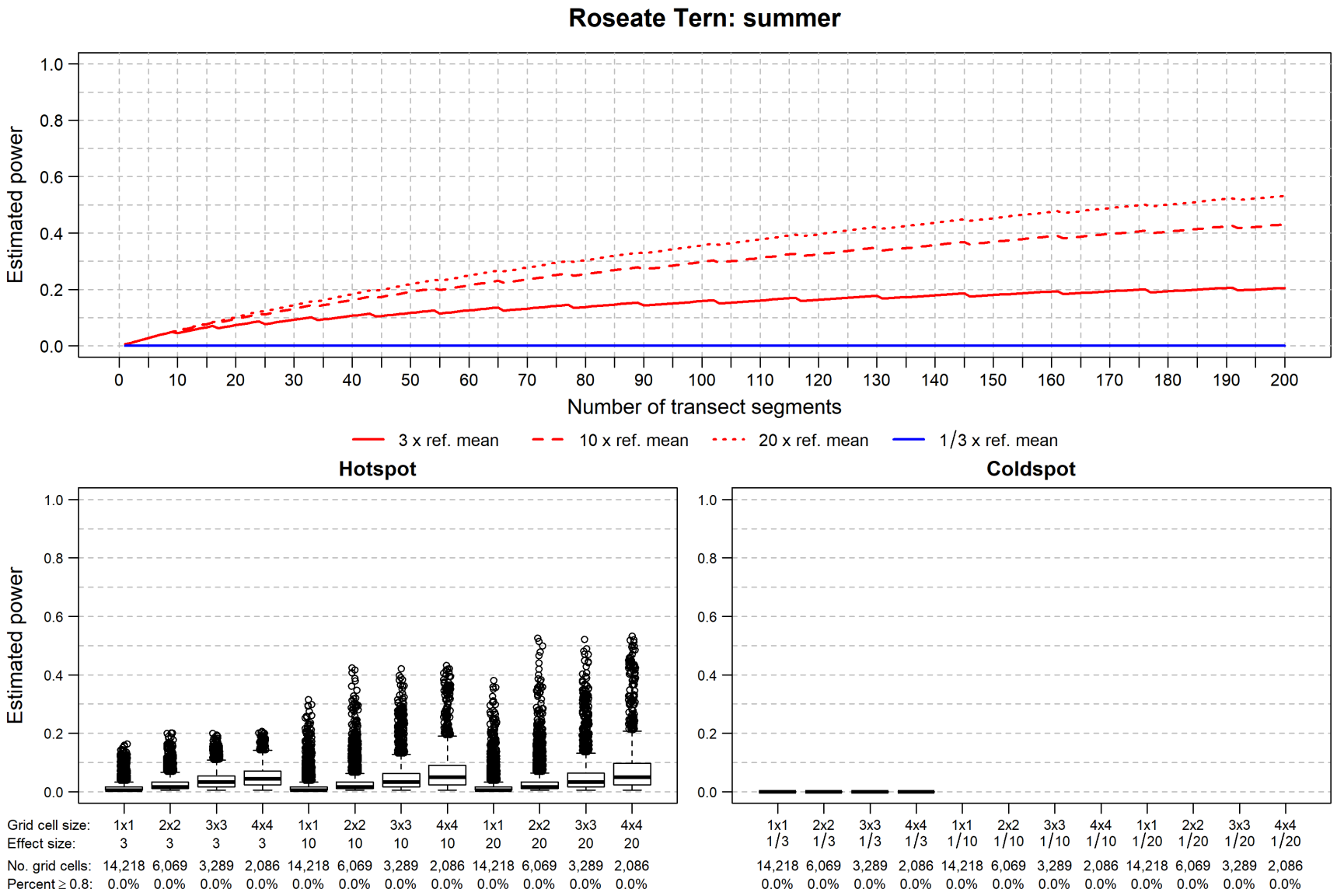


**Figure E33. Power analysis results for Roseate Tern during summer based on the combined model (type I error rate = 0.05)**

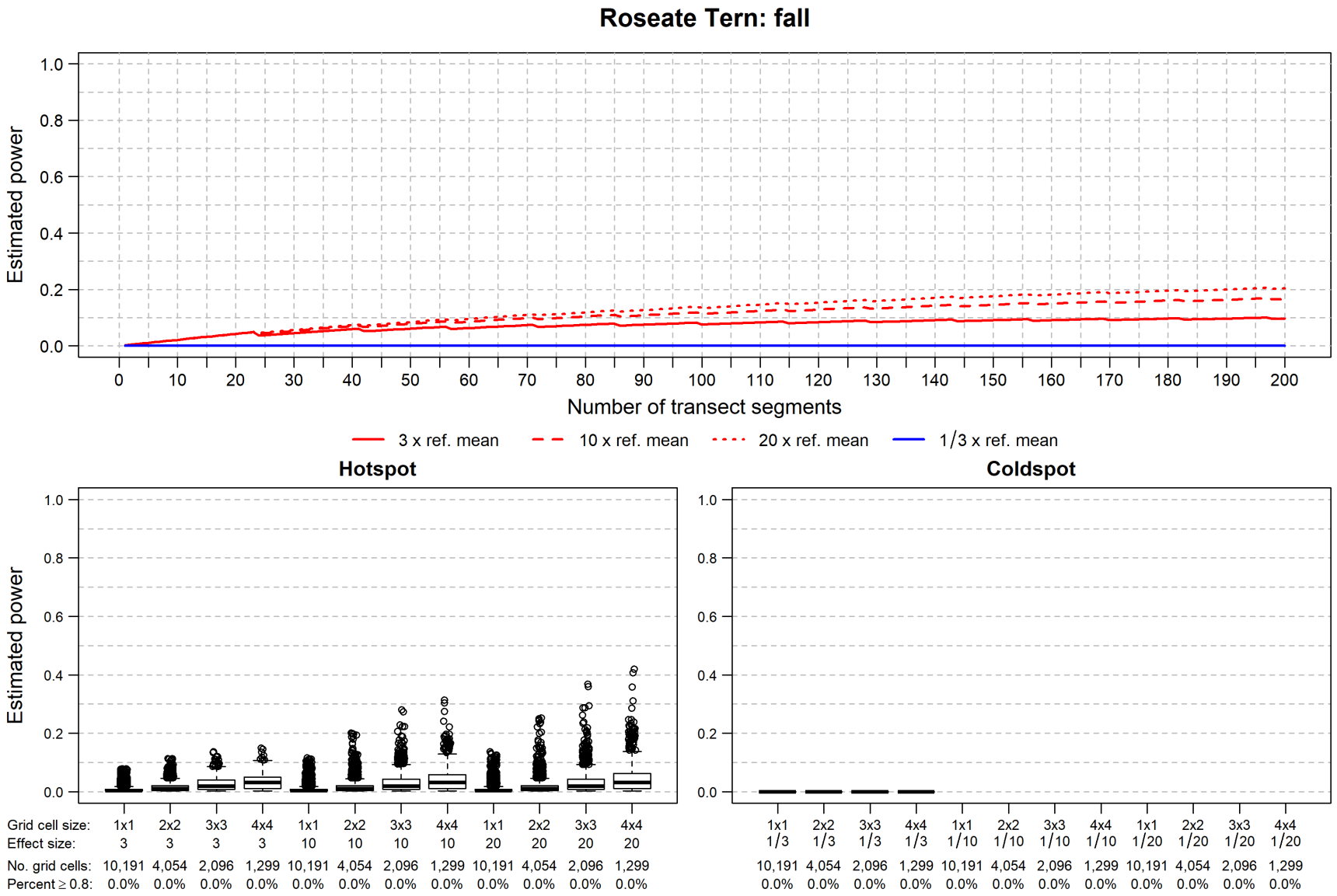


**Figure E34. Power analysis results for Roseate Tern during fall based on the combined model (type I error rate = 0.05)**

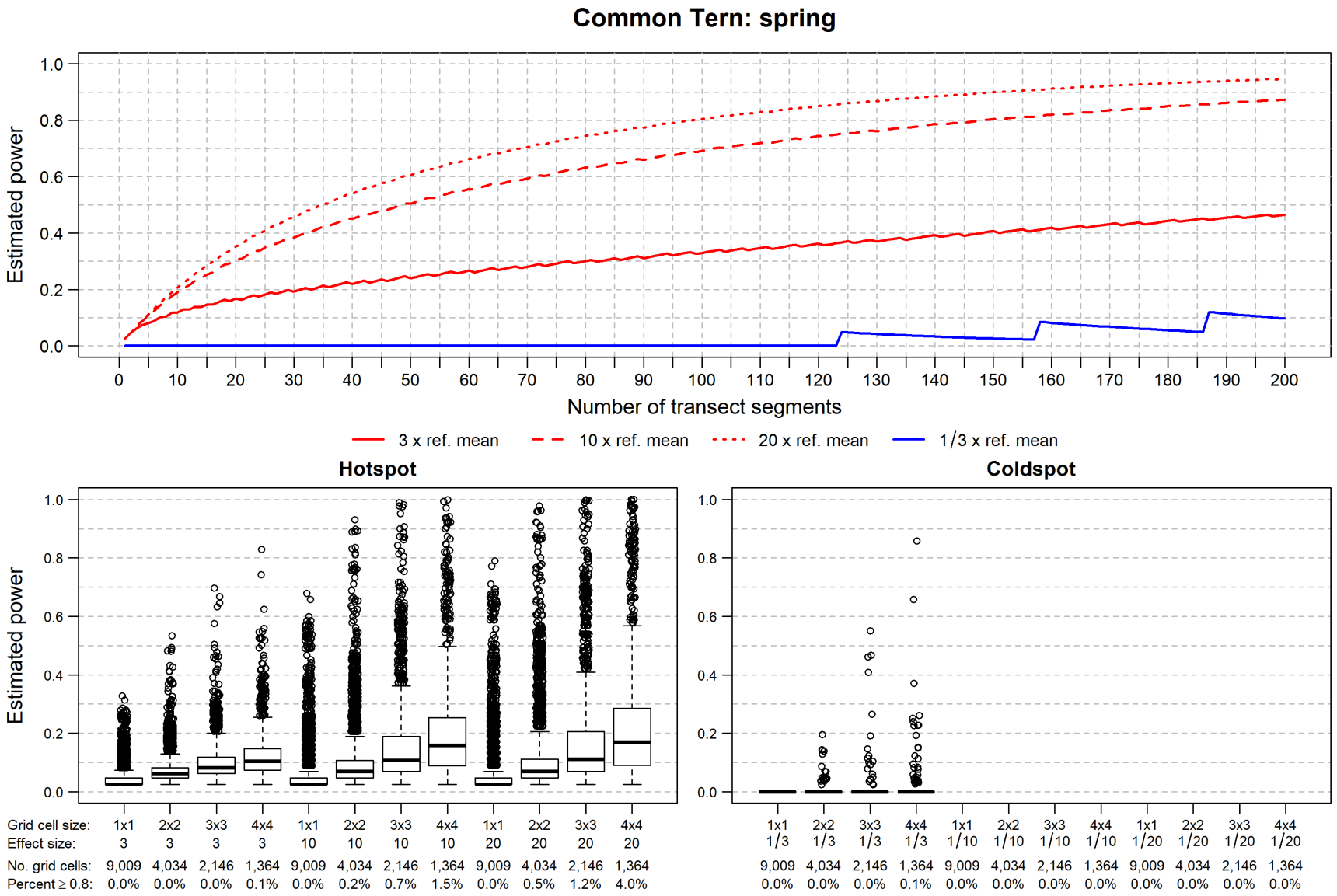


**Figure E35. Power analysis results for Common Tern during spring based on the combined model (type I error rate = 0.05)**

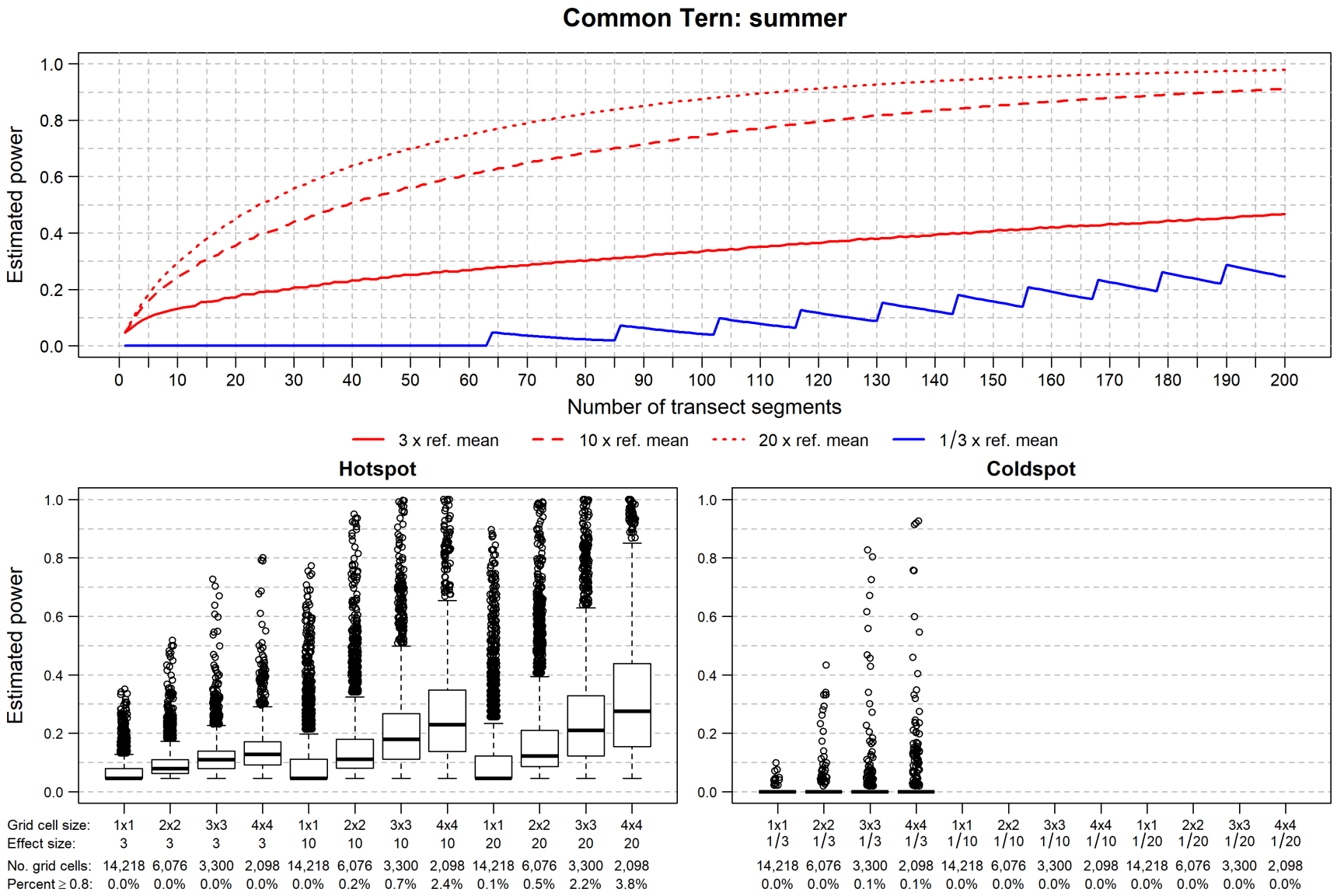


**Figure E36. Power analysis results for Common Tern during summer based on the combined model (type I error rate = 0.05)**

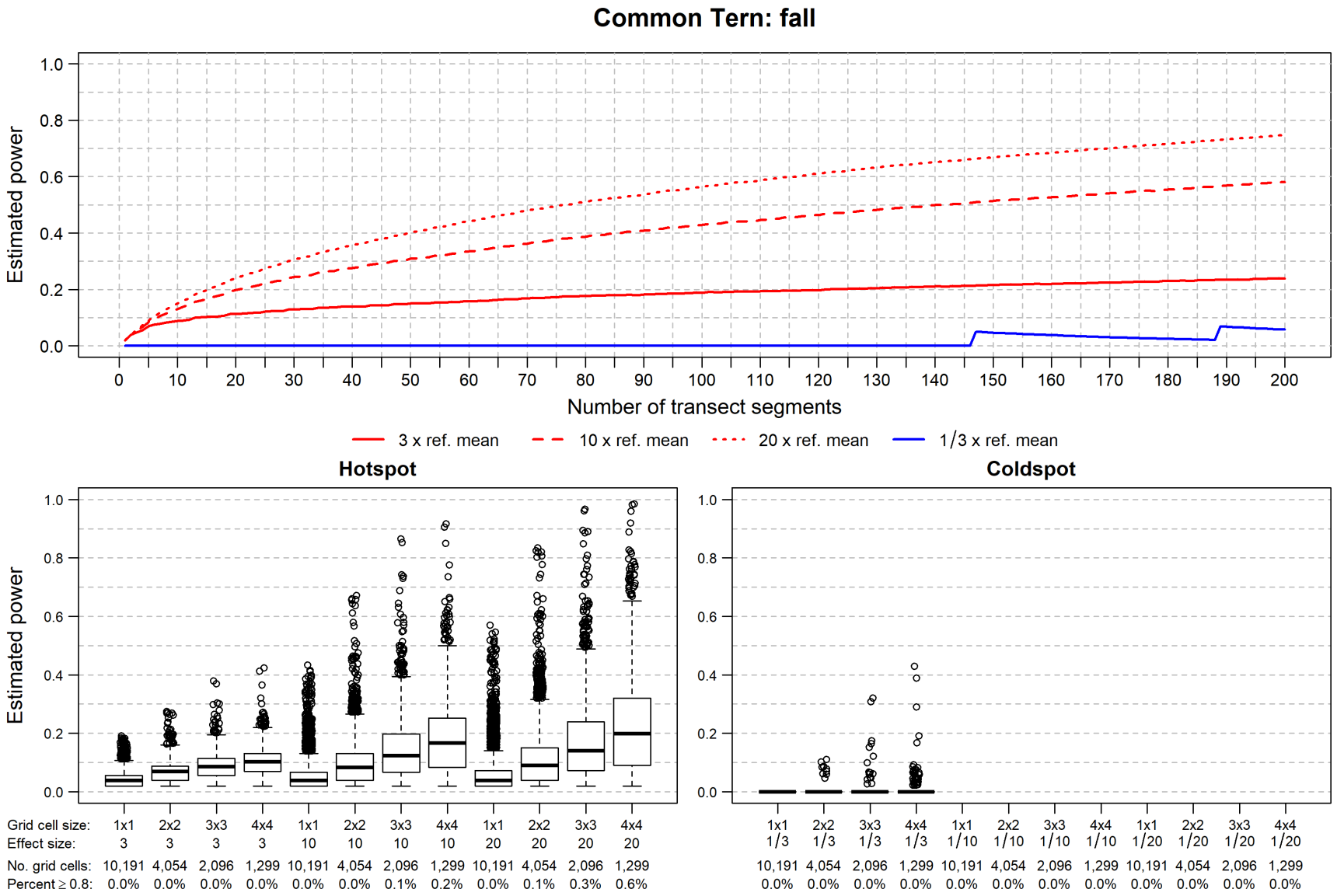


**Figure E37. Power analysis results for Common Tern during fall based on the combined model (type I error rate = 0.05)**

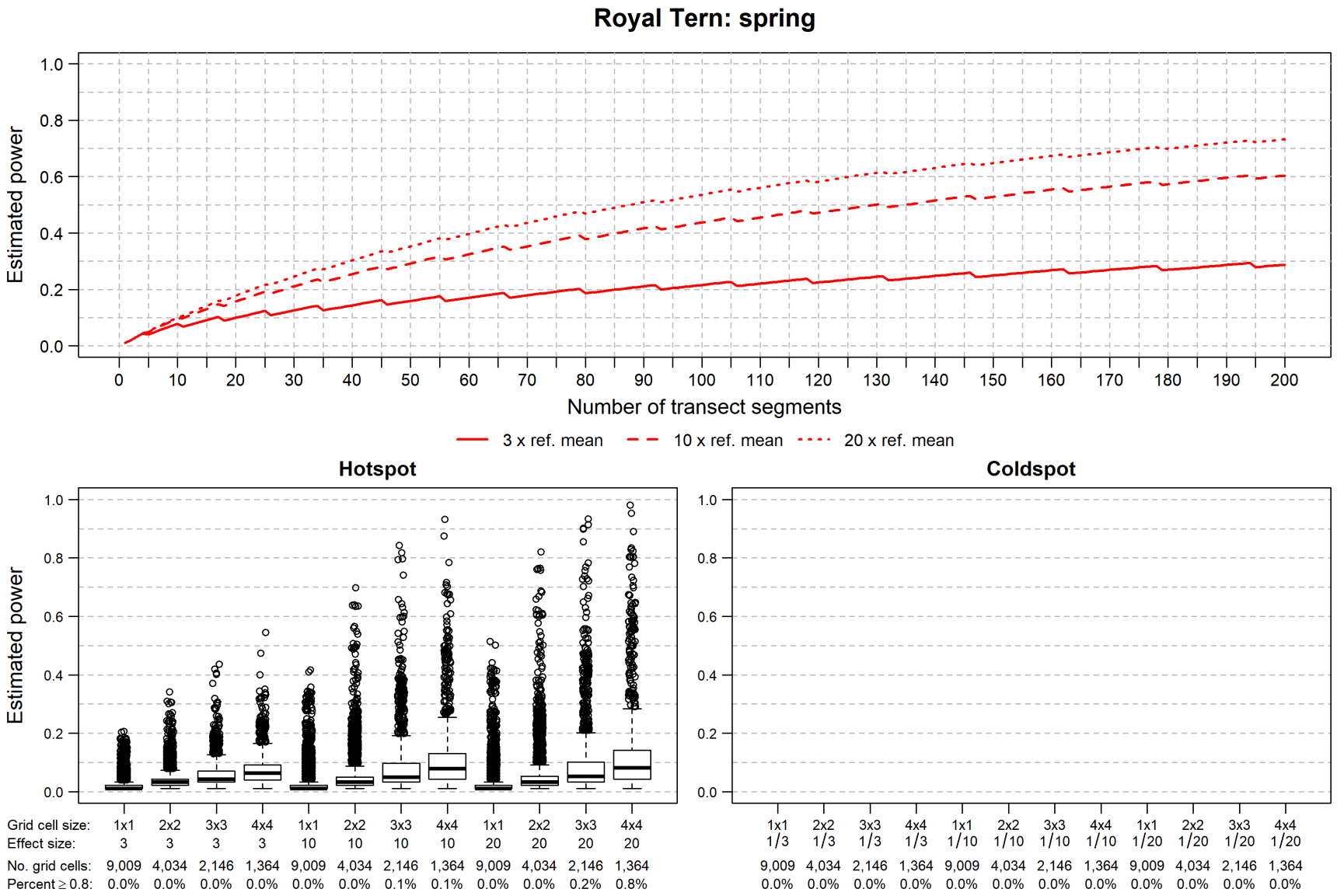


**Figure E38. Power analysis results for Royal Tern during spring based on the combined model (type I error rate = 0.05)**

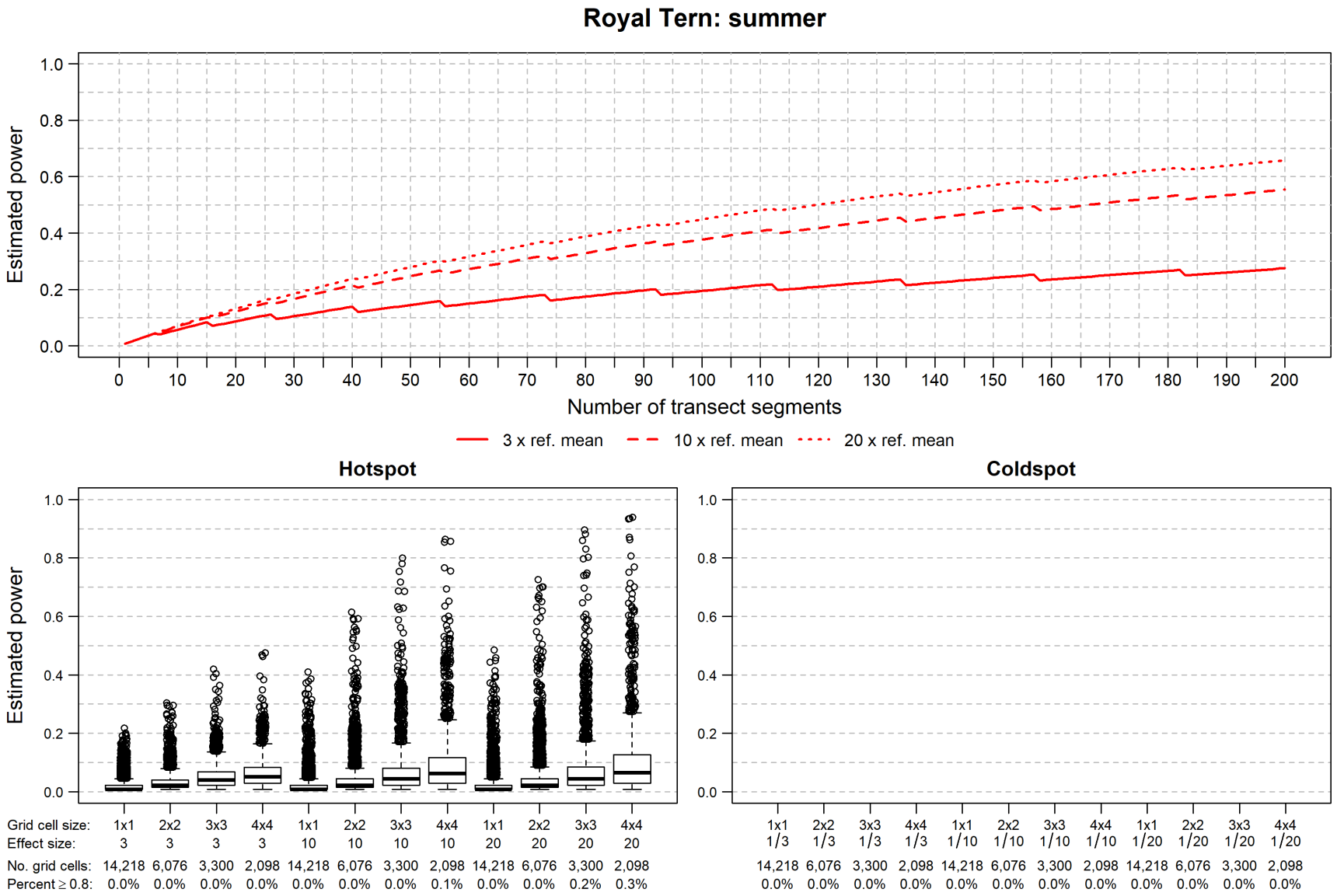


**Figure E39. Power analysis results for Royal Tern during summer based on the combined model (type I error rate = 0.05)**

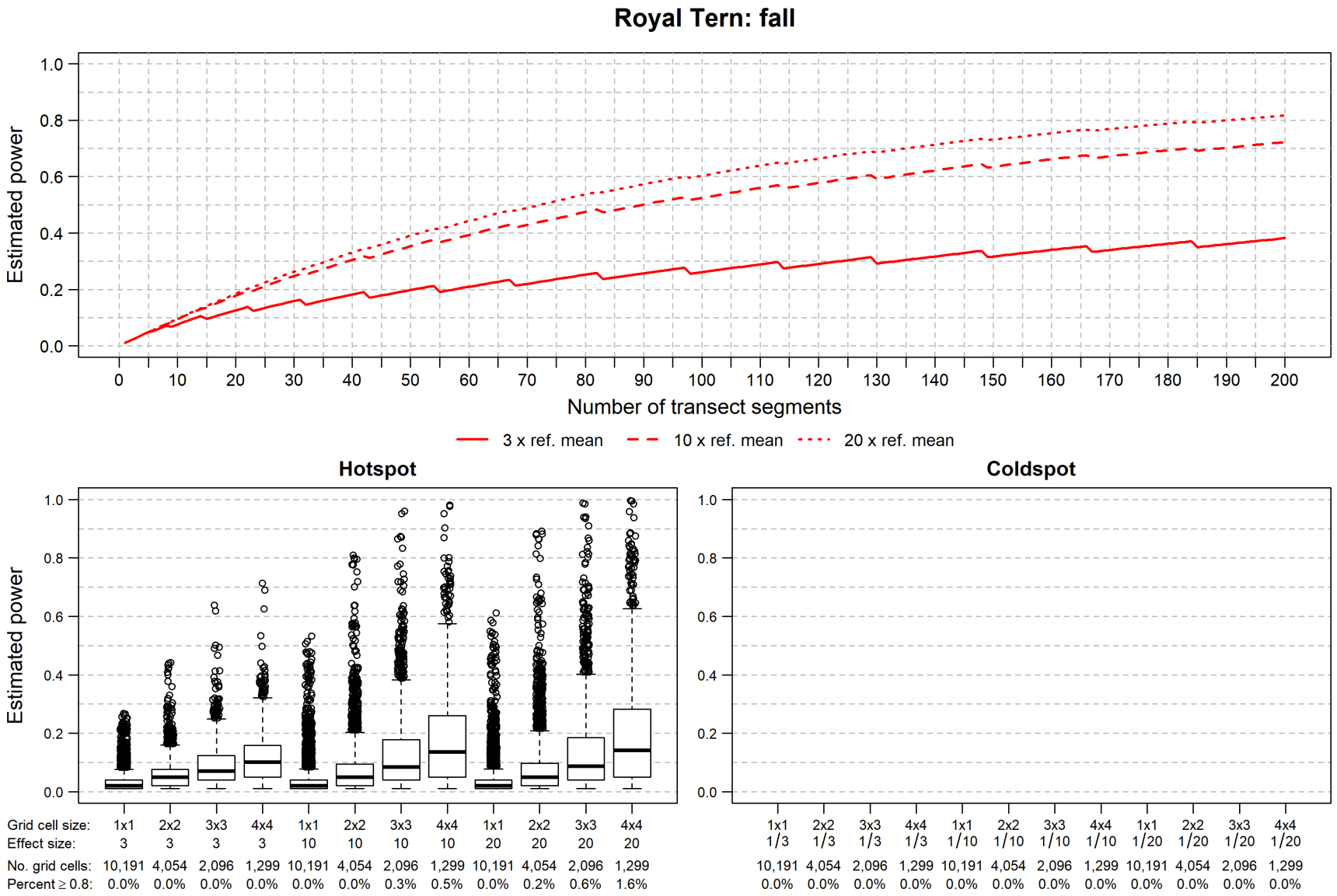


**Figure E40. Power analysis results for Royal Tern during fall based on the combined model (type I error rate = 0.05)**

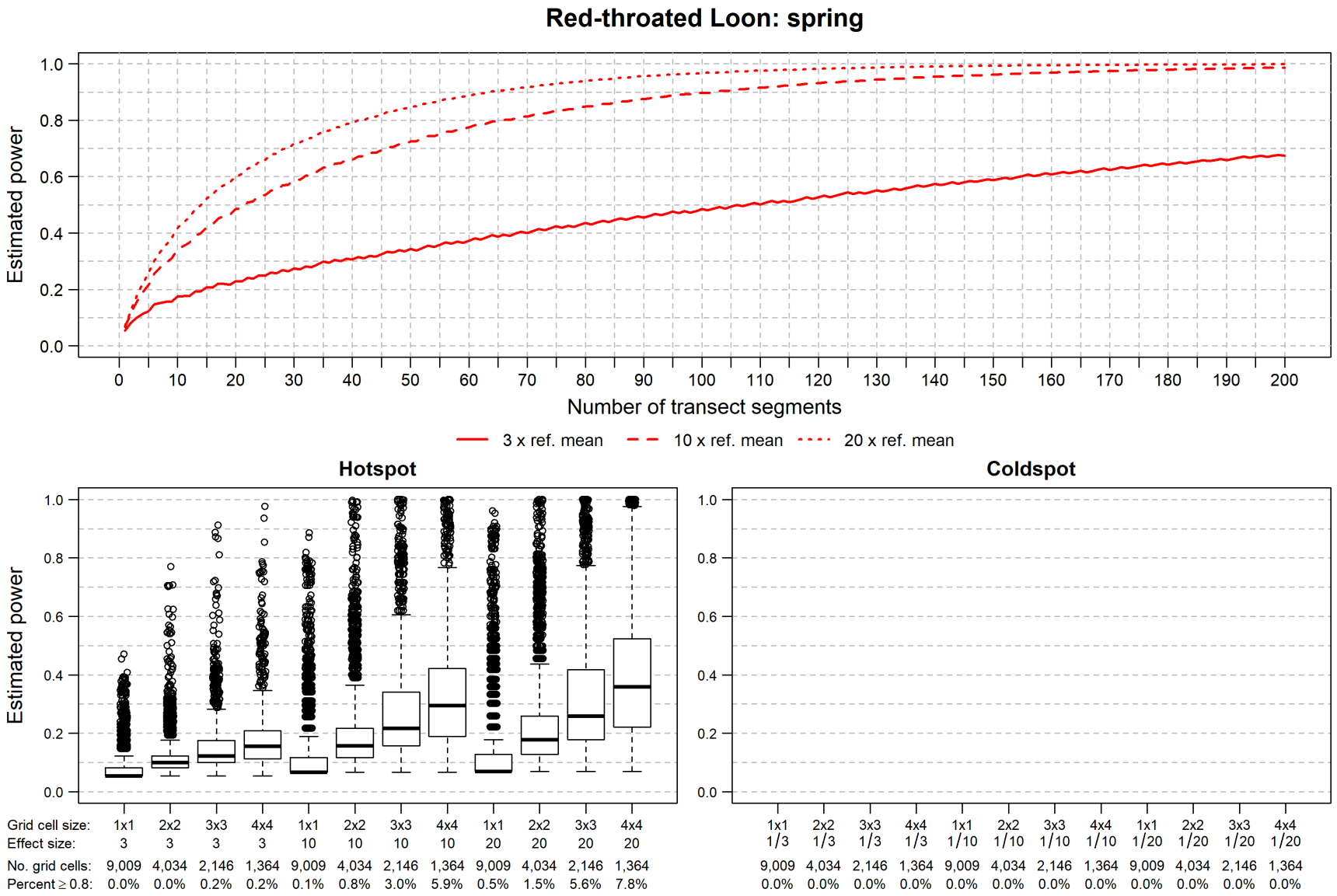


**Figure E41. Power analysis results for Red-throated Loon during spring based on the combined model (type I error rate = 0.05)**

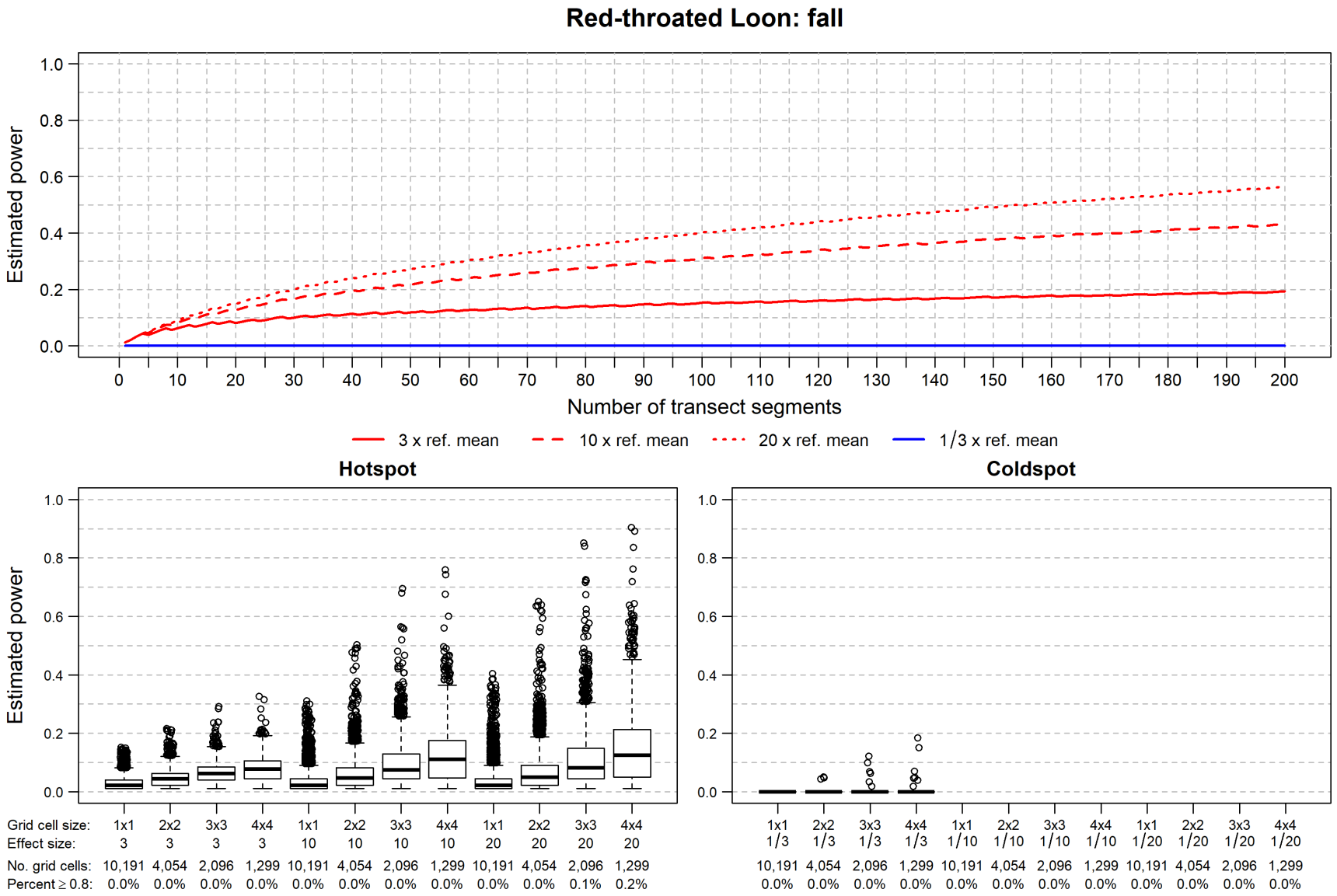


**Figure E42. Power analysis results for Red-throated Loon during fall based on the combined model (type I error rate = 0.05)**

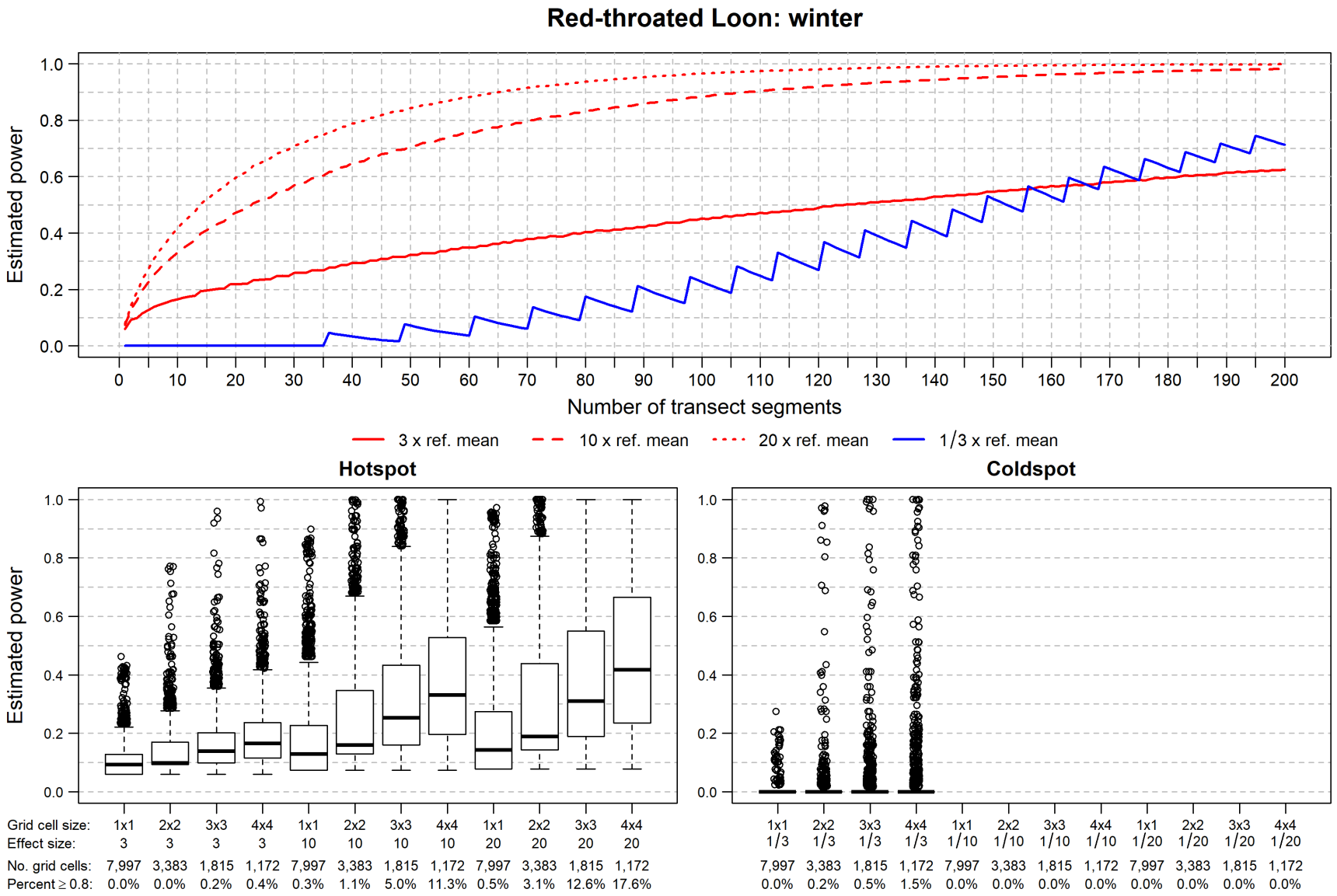


**Figure E43. Power analysis results for Red-throated Loon during winter based on the combined model (type I error rate = 0.05)**

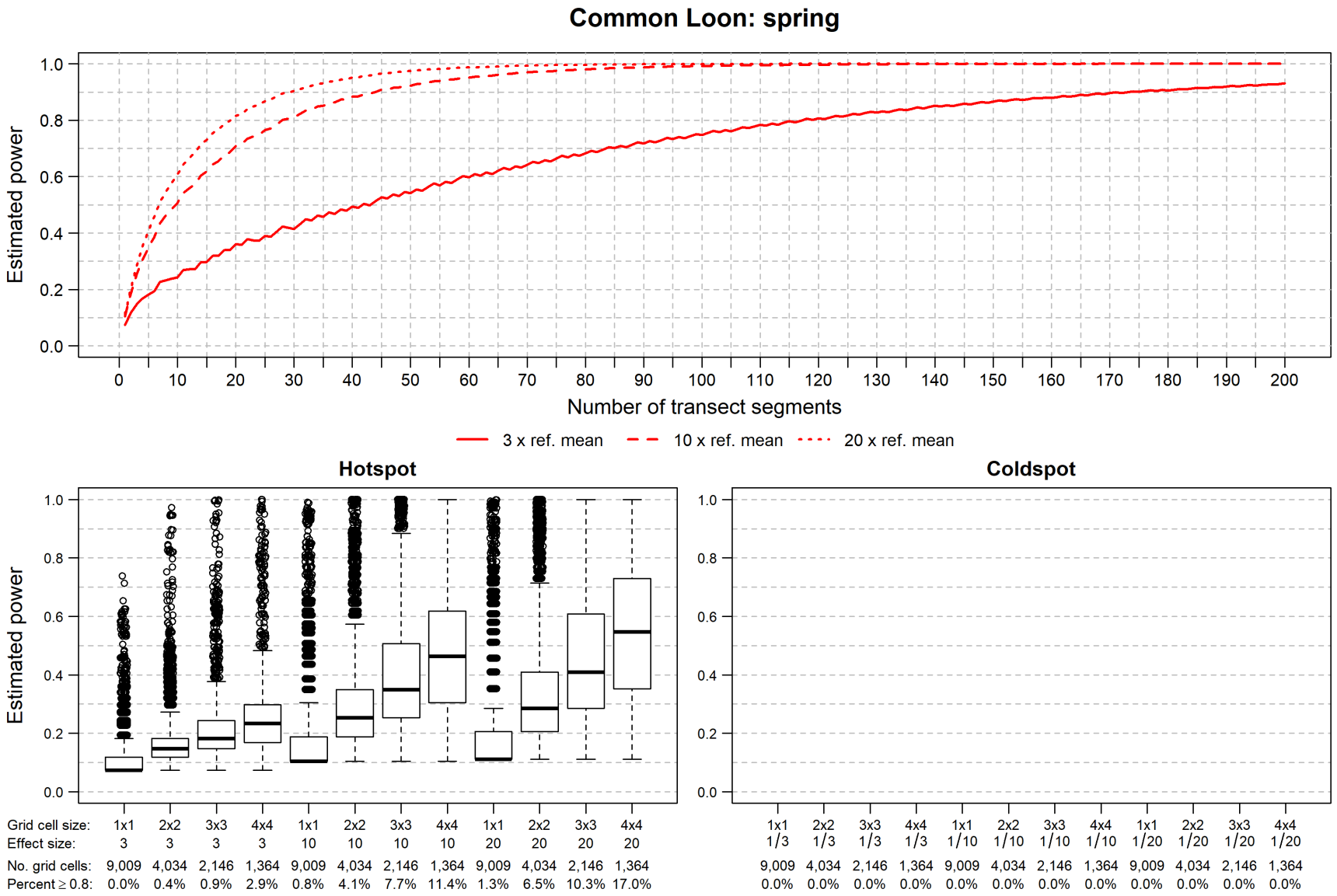


**Figure E44. Power analysis results for Common Loon during spring based on the combined model (type I error rate = 0.05)**

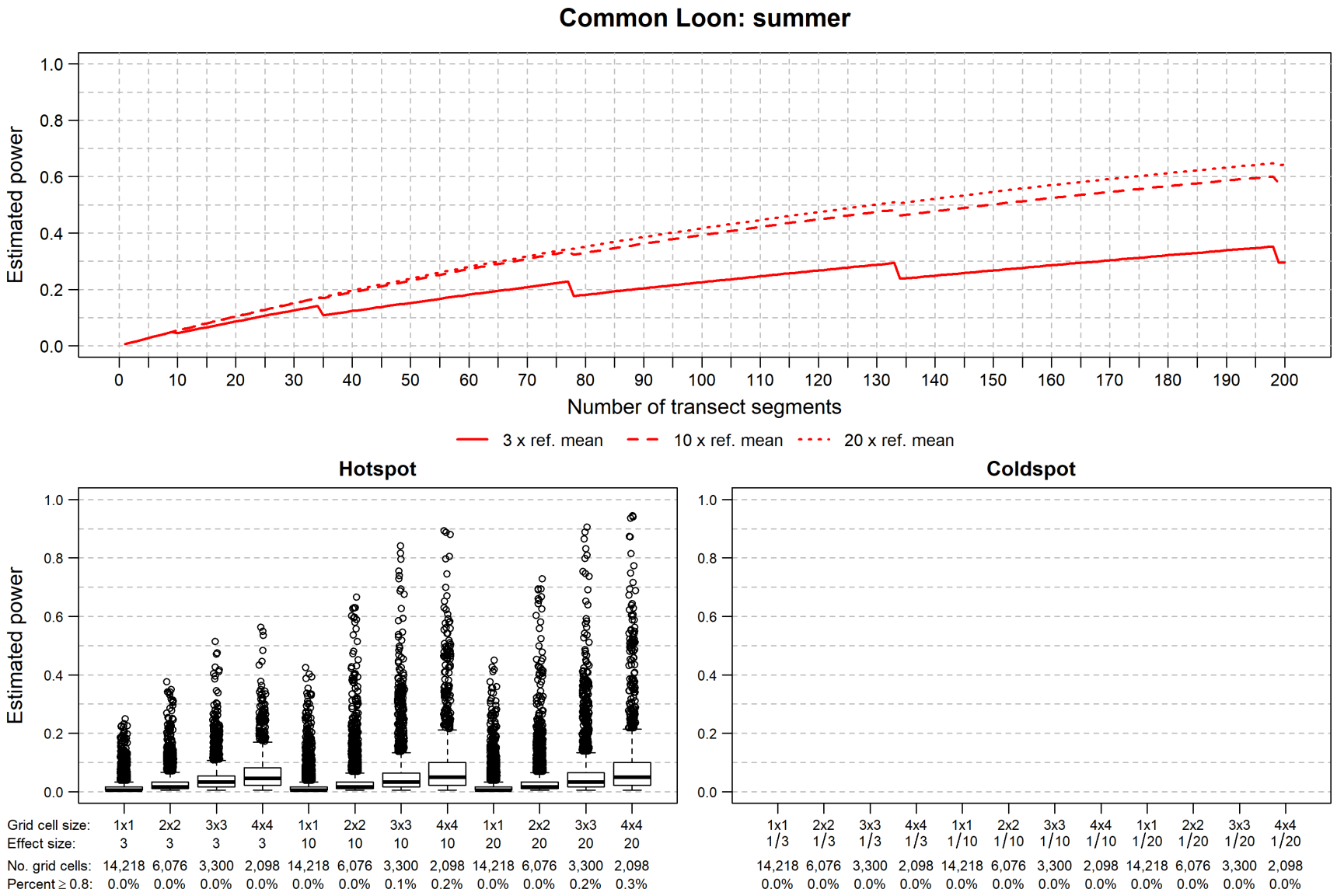


**Figure E45. Power analysis results for Common Loon during summer based on the combined model (type I error rate = 0.05)**

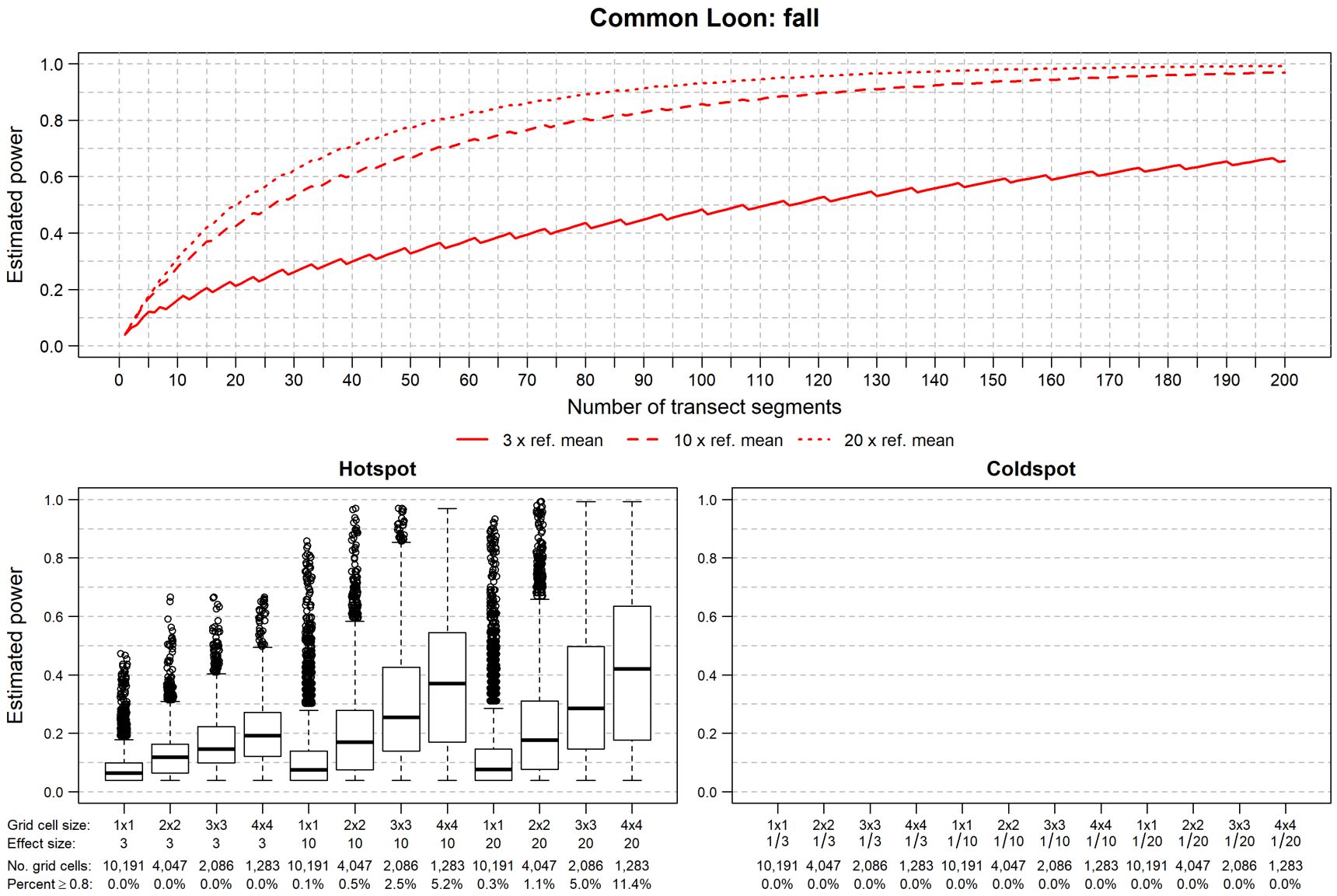


**Figure E46. Power analysis results for Common Loon during fall based on the combined model (type I error rate = 0.05)**

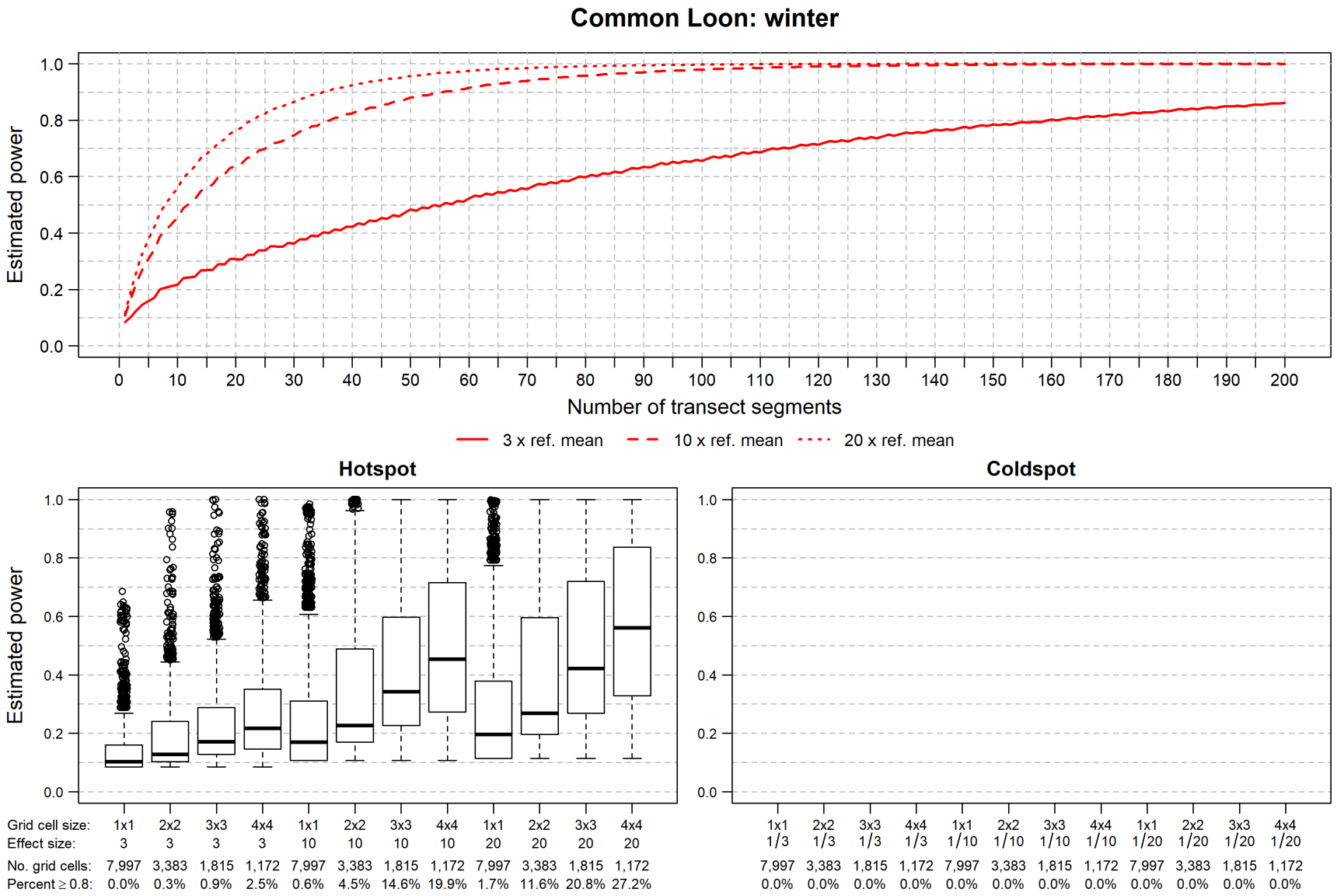


**Figure E47. Power analysis results for Common Loon during winter based on the combined model (type I error rate = 0.05)**

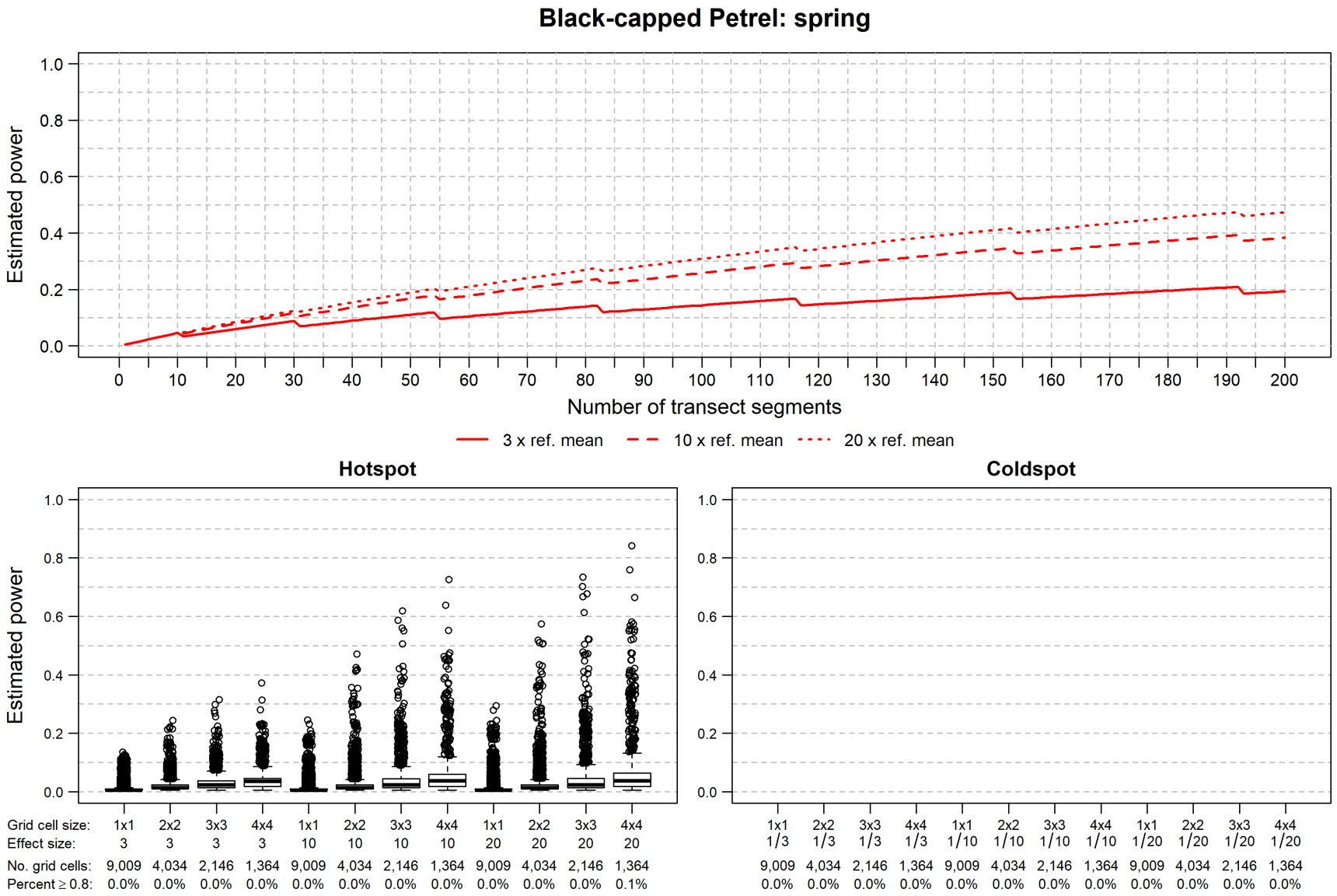


**Figure E48. Power analysis results for Black-capped Petrel during spring based on the combined model (type I error rate = 0.05)**

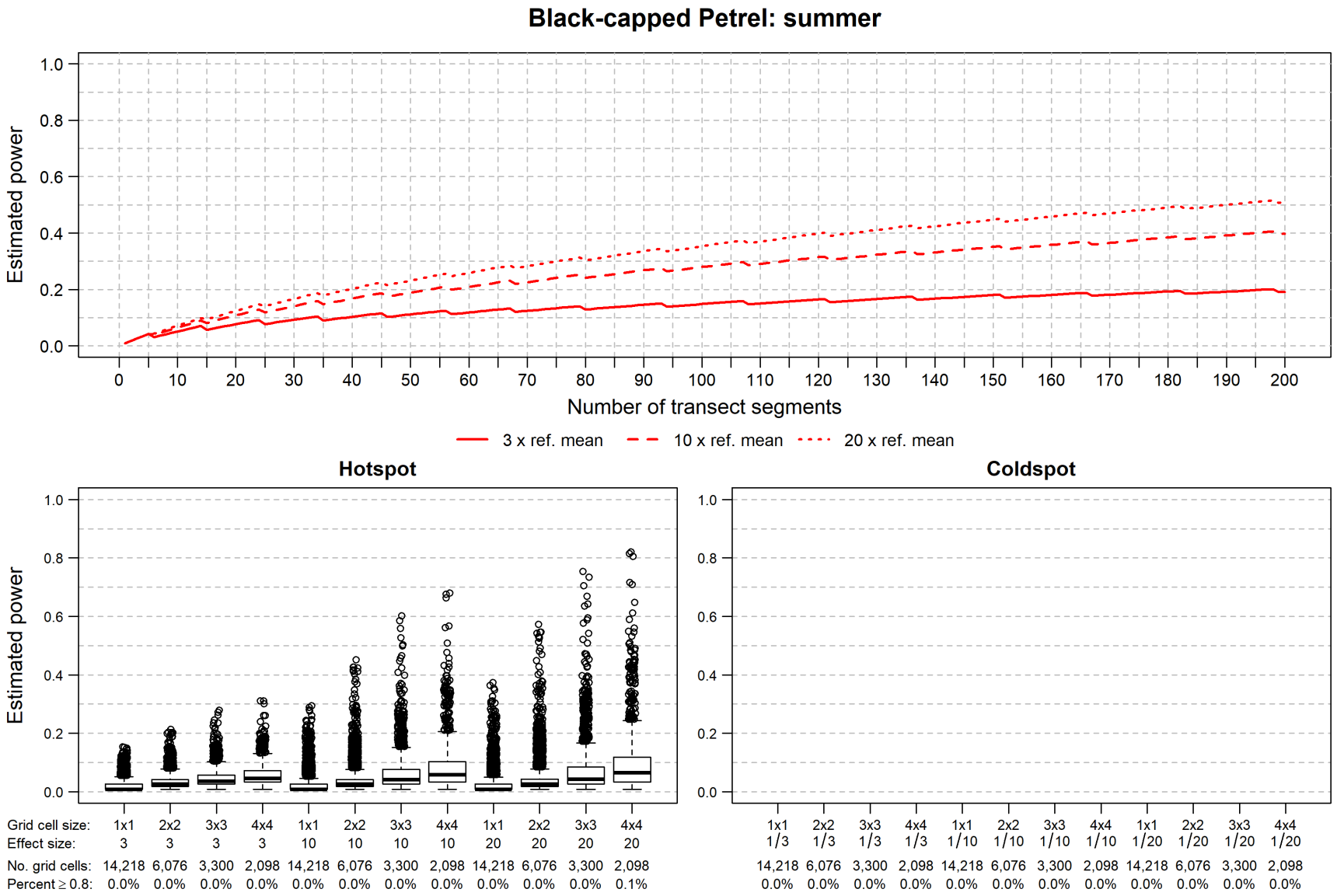


**Figure E49. Power analysis results for Black-capped Petrel during summer based on the combined model (type I error rate = 0.05)**

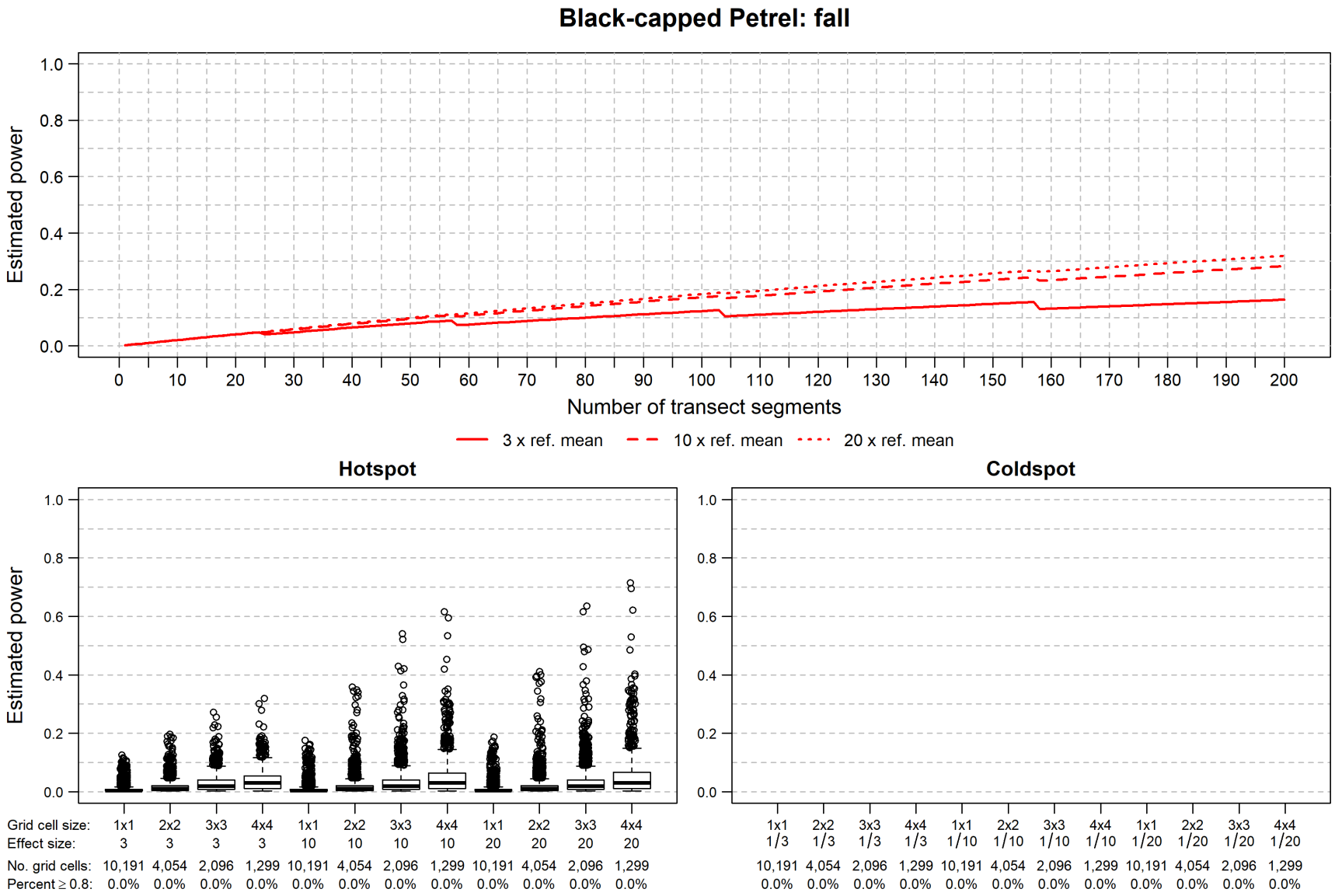


**Figure E50. Power analysis results for Black-capped Petrel during fall based on the combined model (type I error rate = 0.05)**

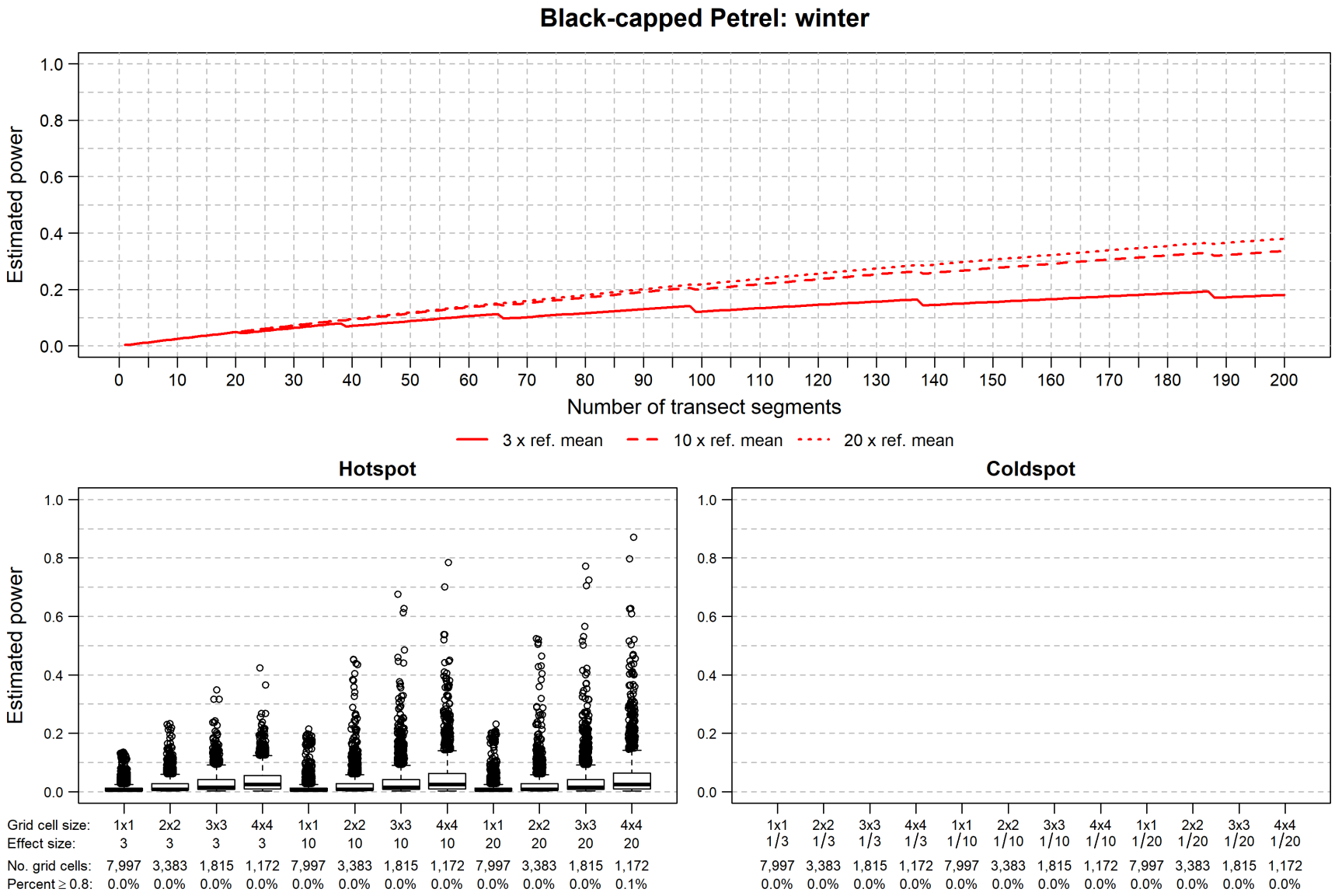


**Figure E51. Power analysis results for Black-capped Petrel during winter based on the combined model (type I error rate = 0.05)**

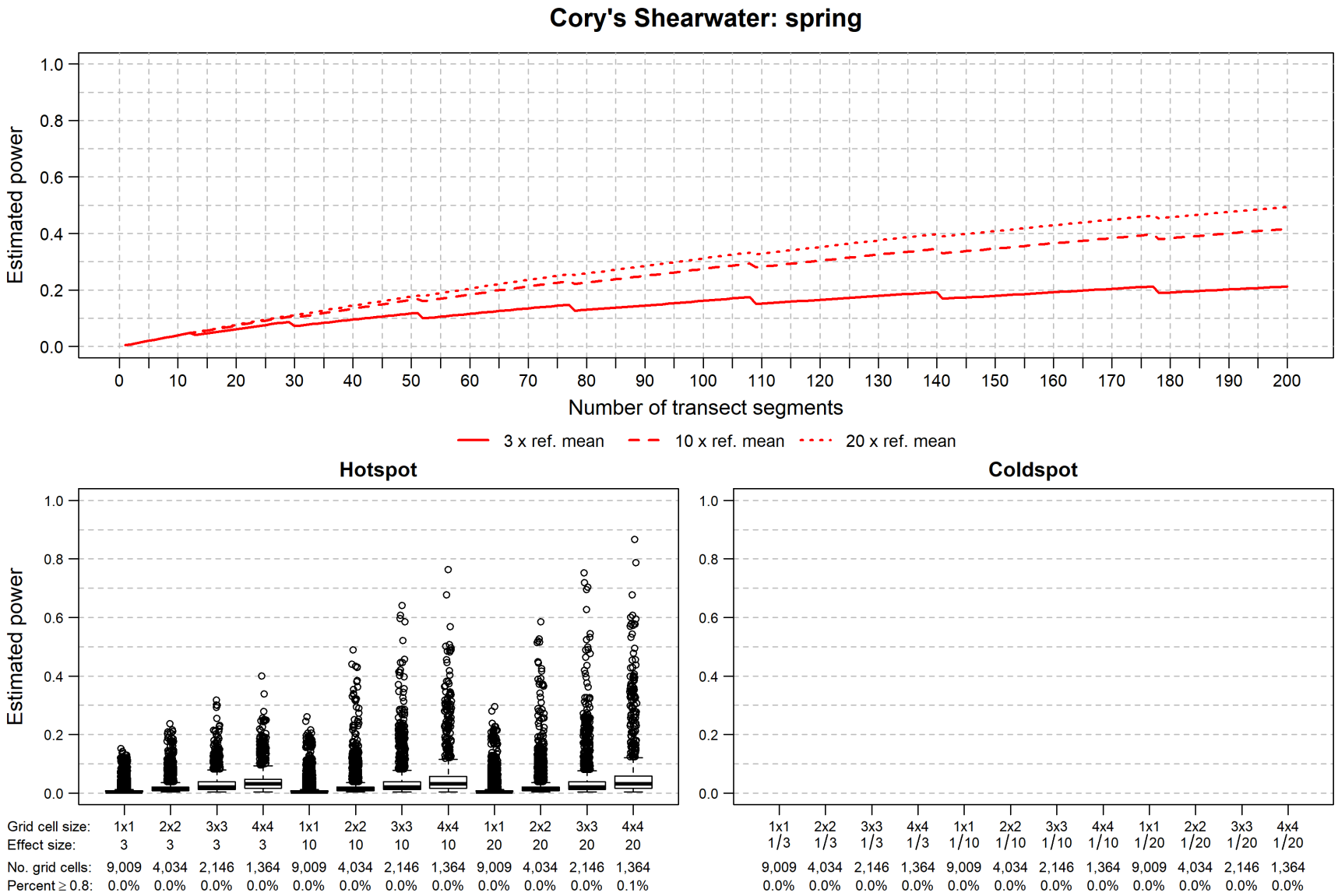


**Figure E52. Power analysis results for Cory's Shearwater during spring based on the combined model (type I error rate = 0.05)**

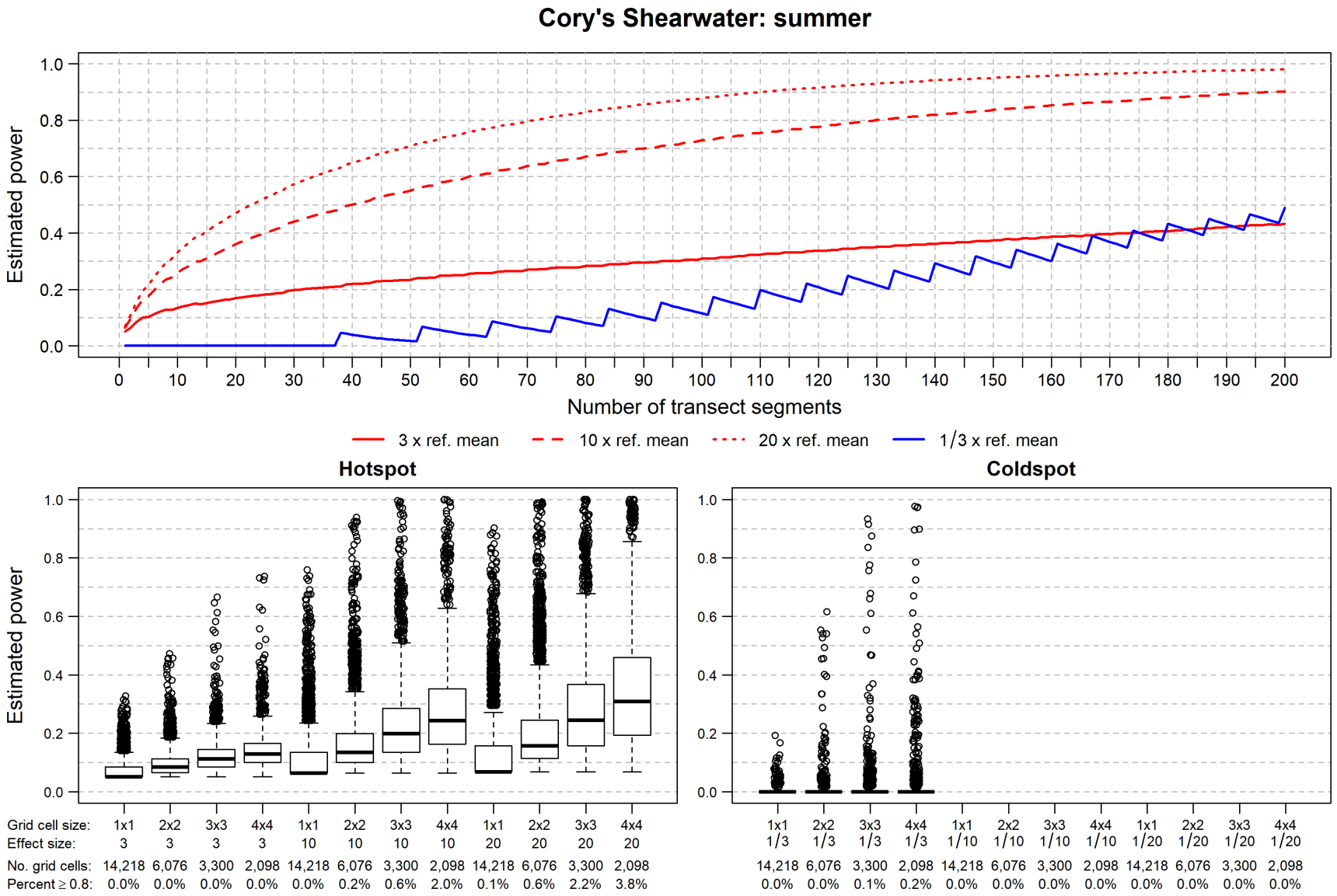


**Figure E53. Power analysis results for Cory's Shearwater during summer based on the combined model (type I error rate = 0.05)**

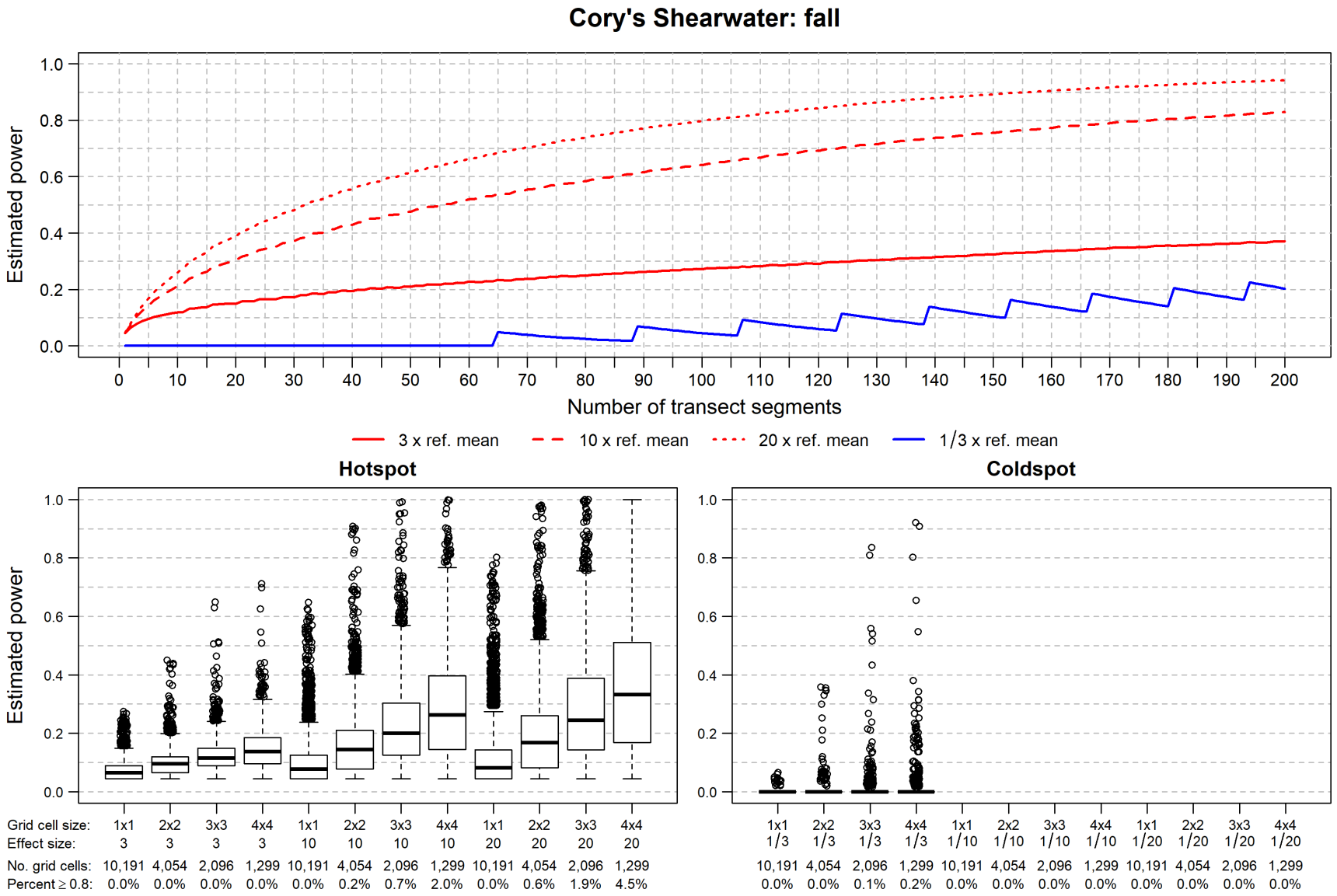


**Figure E54. Power analysis results for Cory's Shearwater during fall based on the combined model (type I error rate = 0.05)**

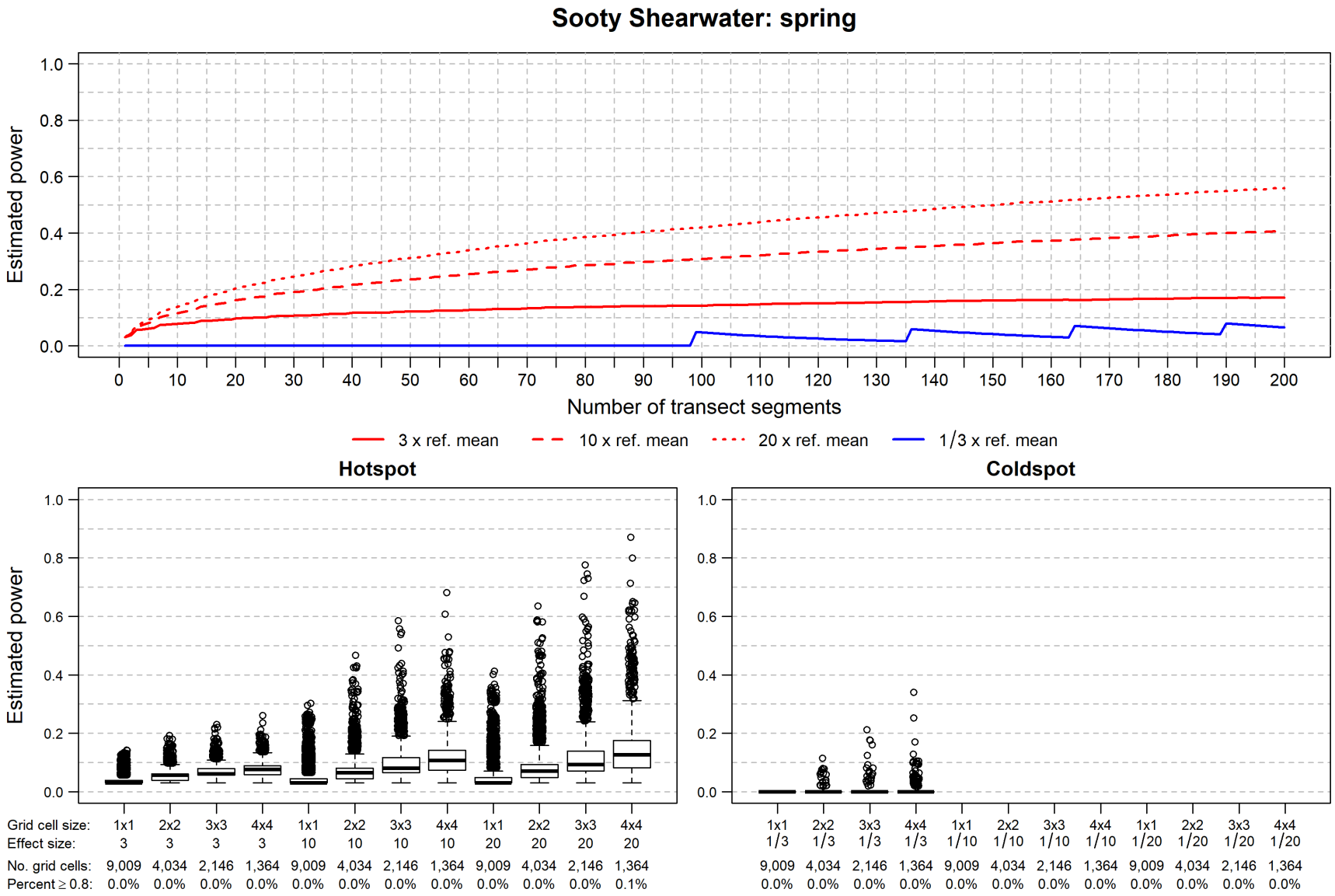


**Figure E55. Power analysis results for Sooty Shearwater during spring based on the combined model (type I error rate = 0.05)**

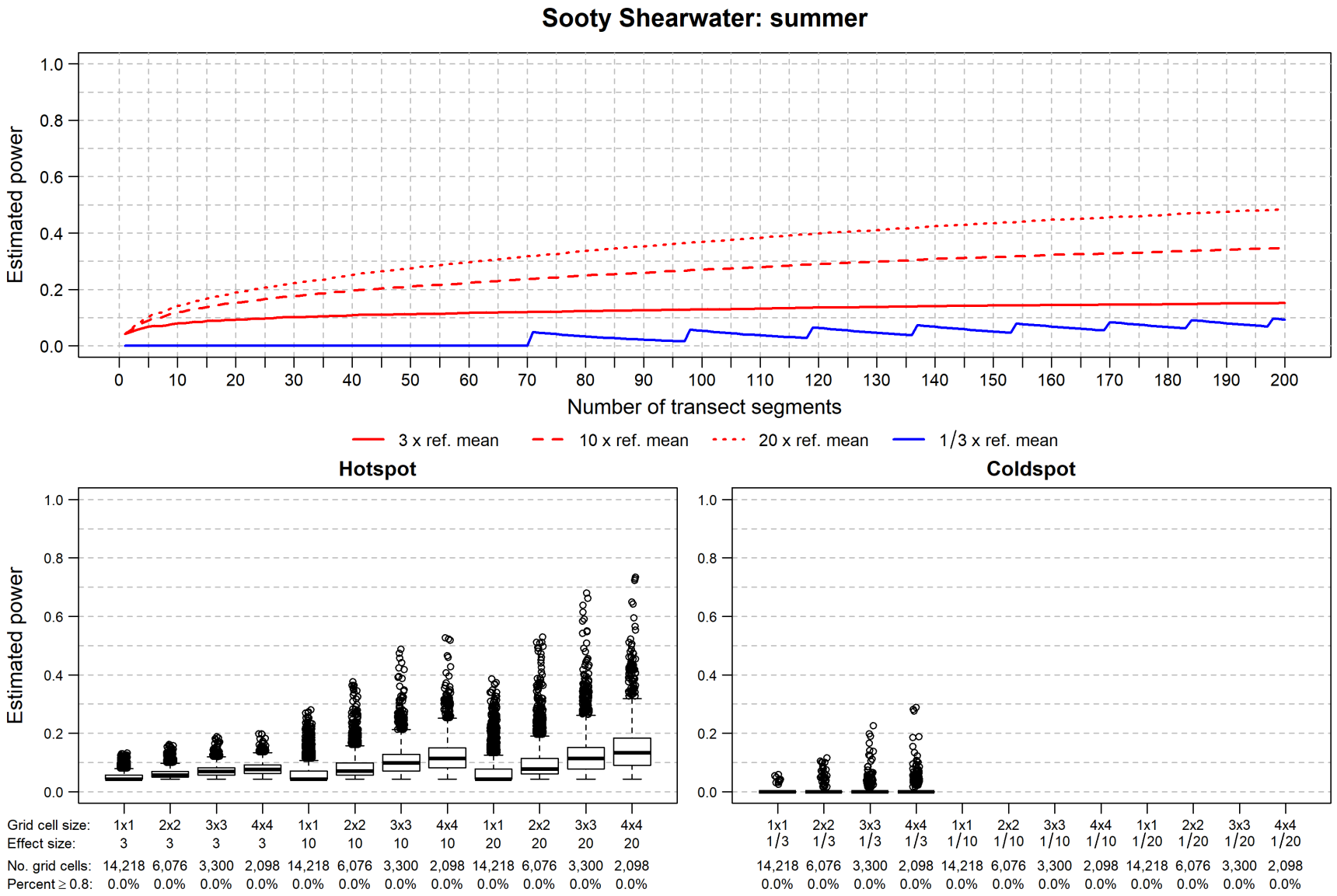


**Figure E56. Power analysis results for Sooty Shearwater during summer based on the combined model (type I error rate = 0.05)**

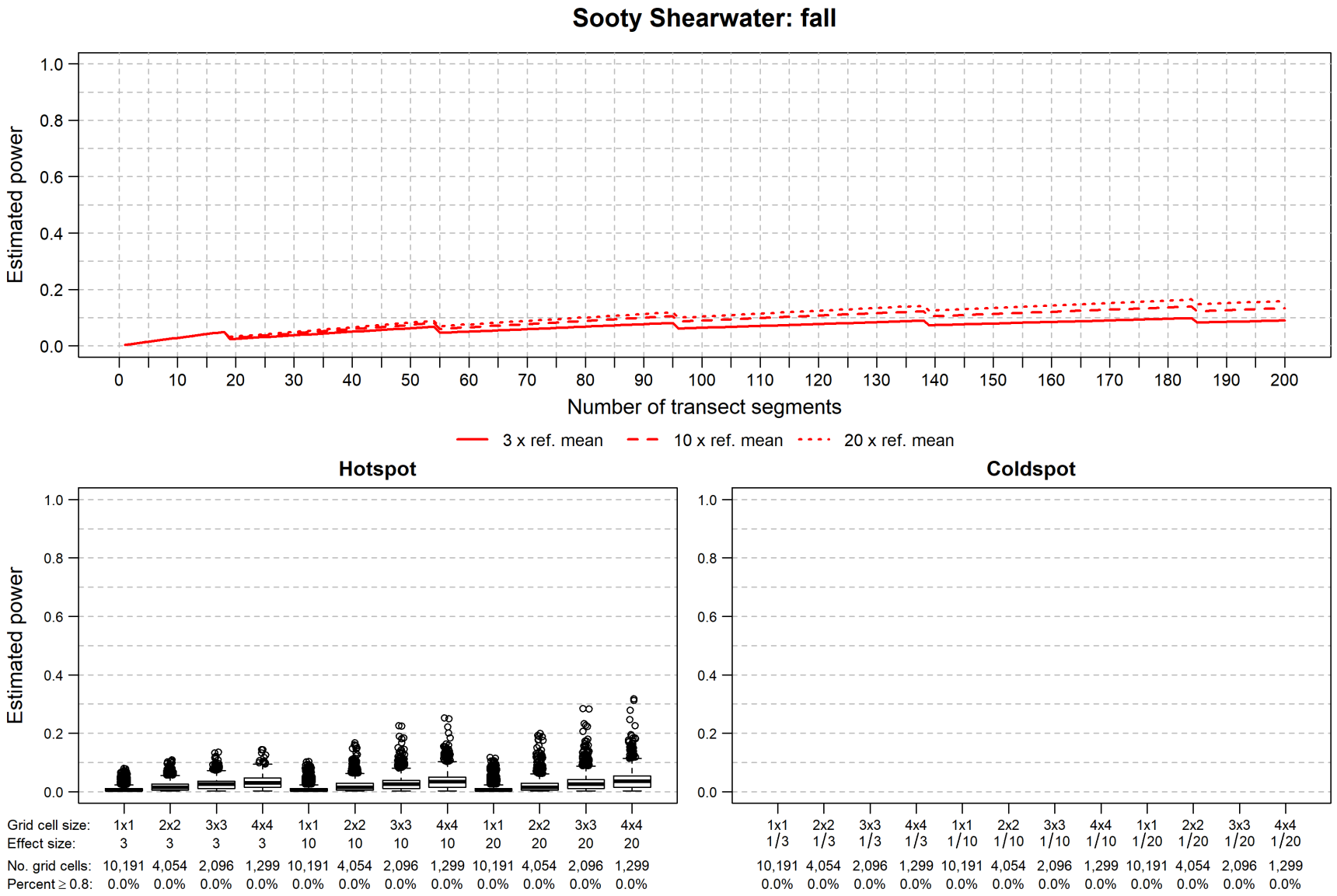


**Figure E57. Power analysis results for Sooty Shearwater during fall based on the combined model (type I error rate = 0.05)**

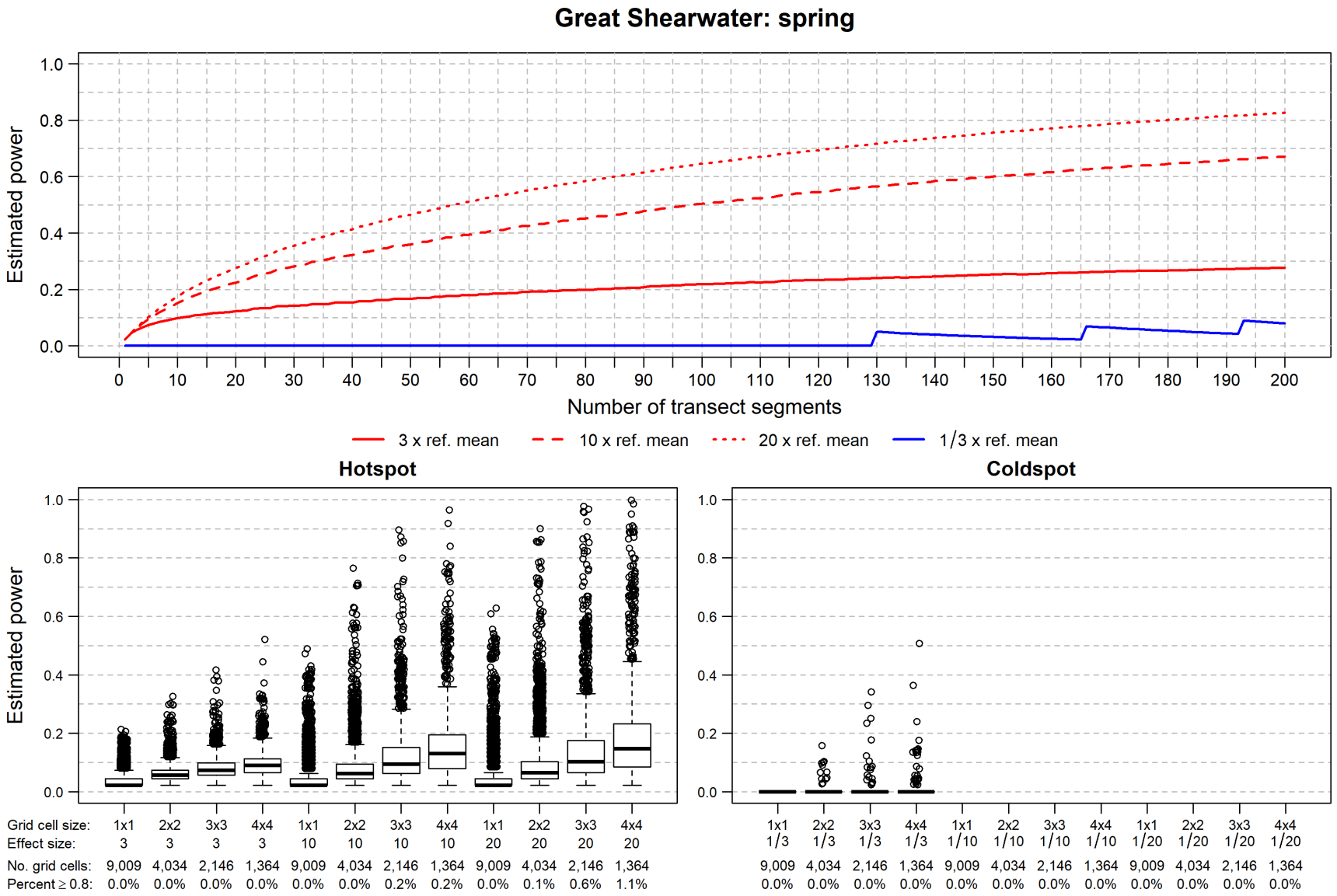


**Figure E58. Power analysis results for Great Shearwater during spring based on the combined model (type I error rate = 0.05)**

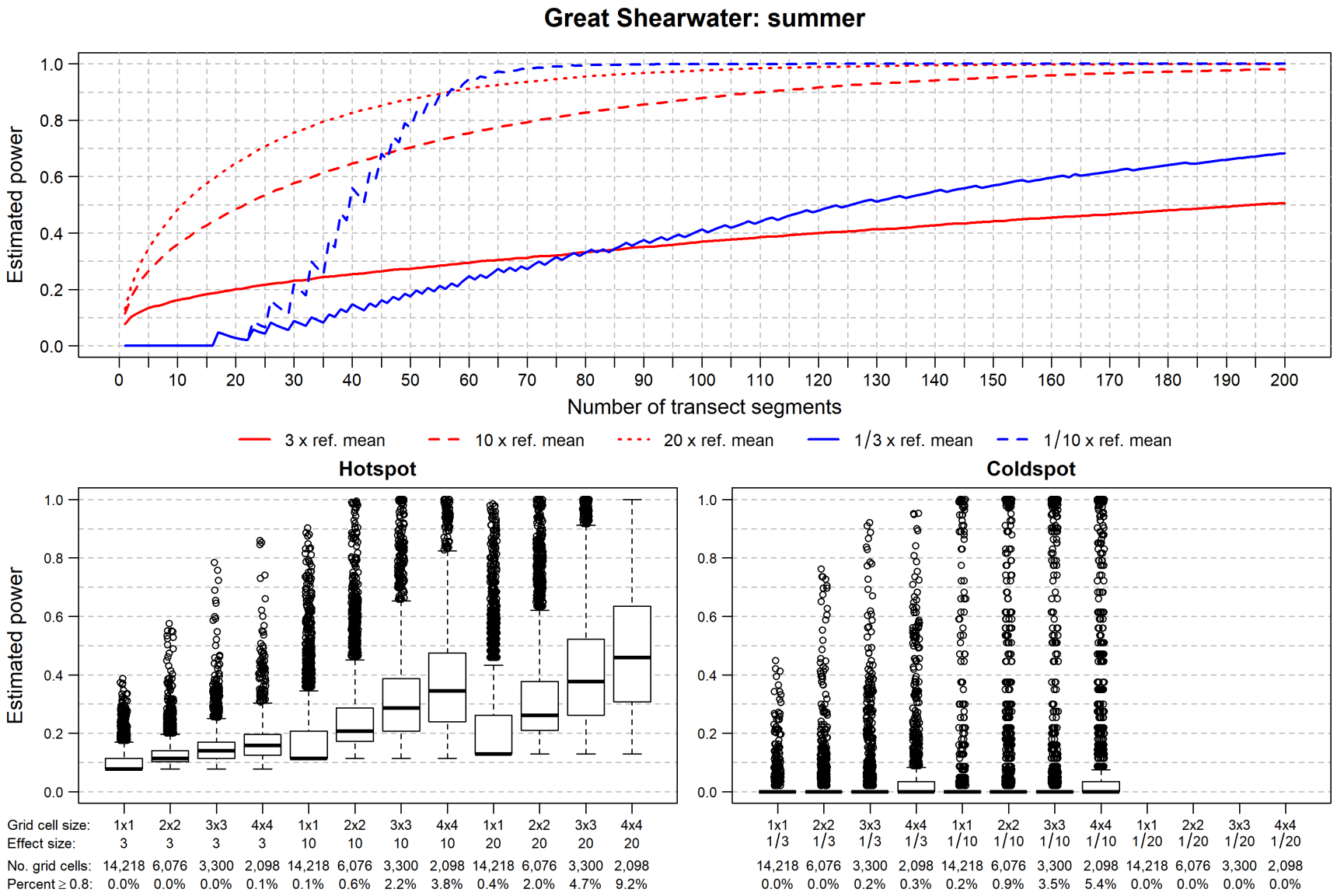


**Figure E59. Power analysis results for Great Shearwater during summer based on the combined model (type I error rate = 0.05)**

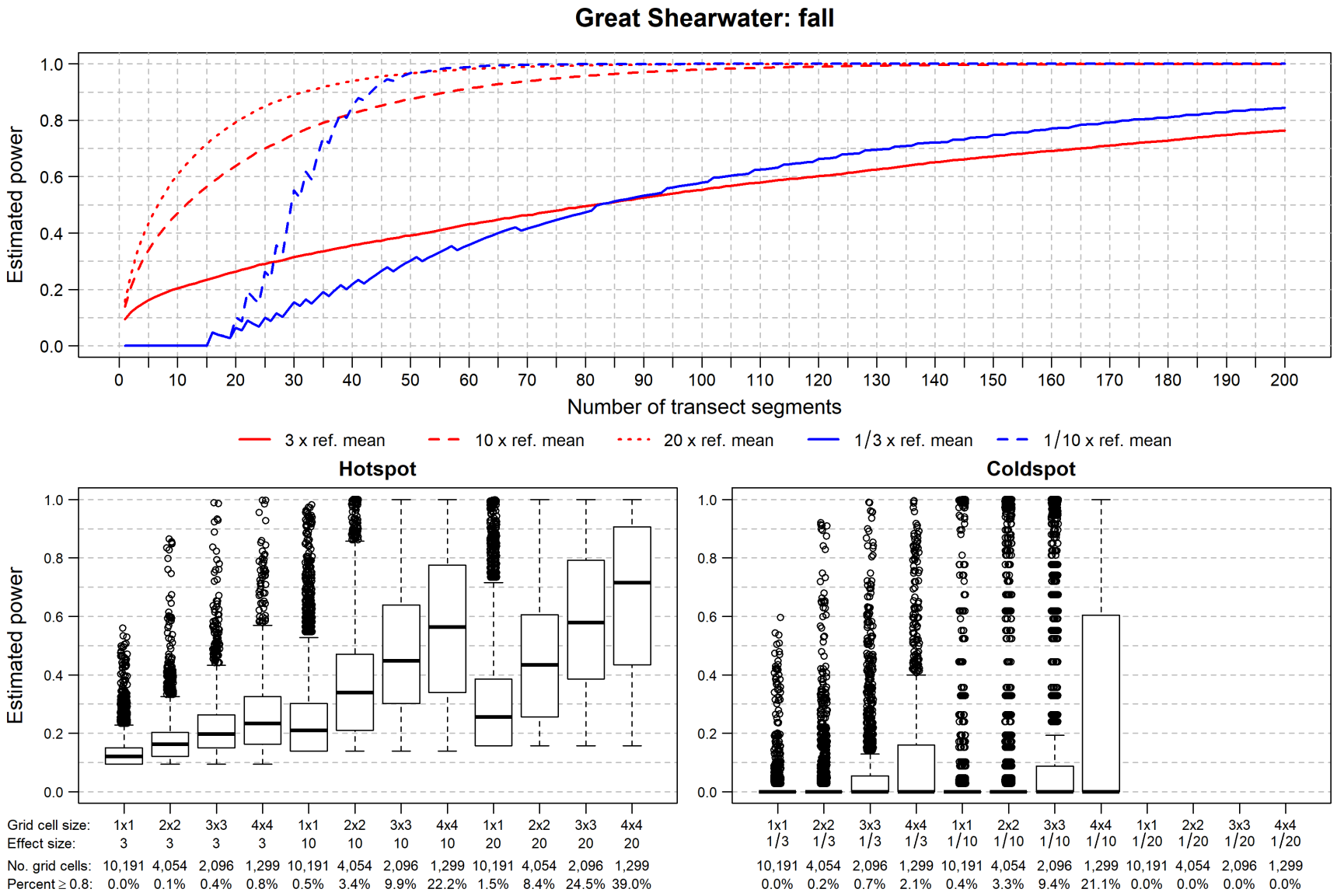


**Figure E60. Power analysis results for Great Shearwater during fall based on the combined model (type I error rate = 0.05)**

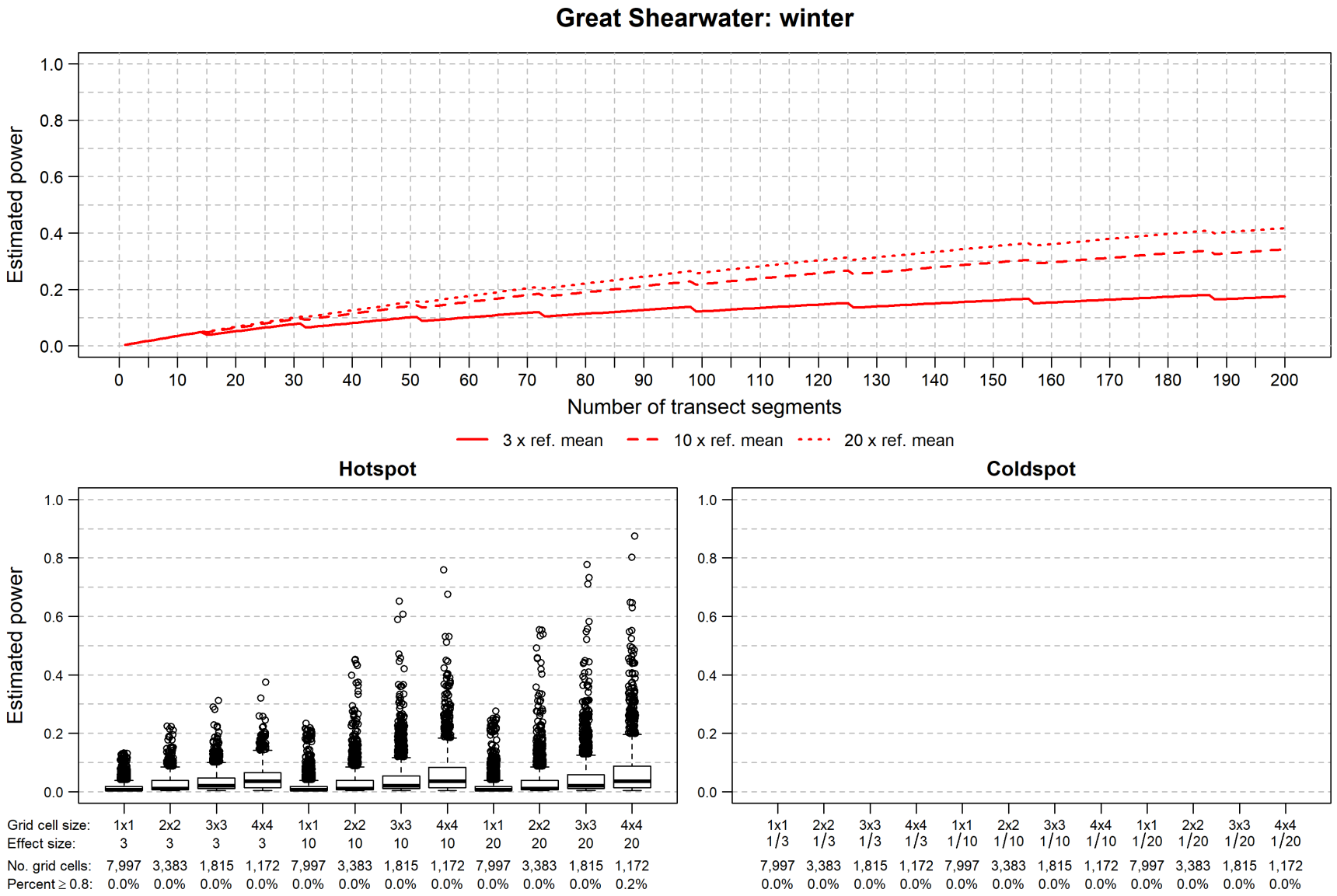


**Figure E61. Power analysis results for Great Shearwater during winter based on the combined model (type I error rate = 0.05)**

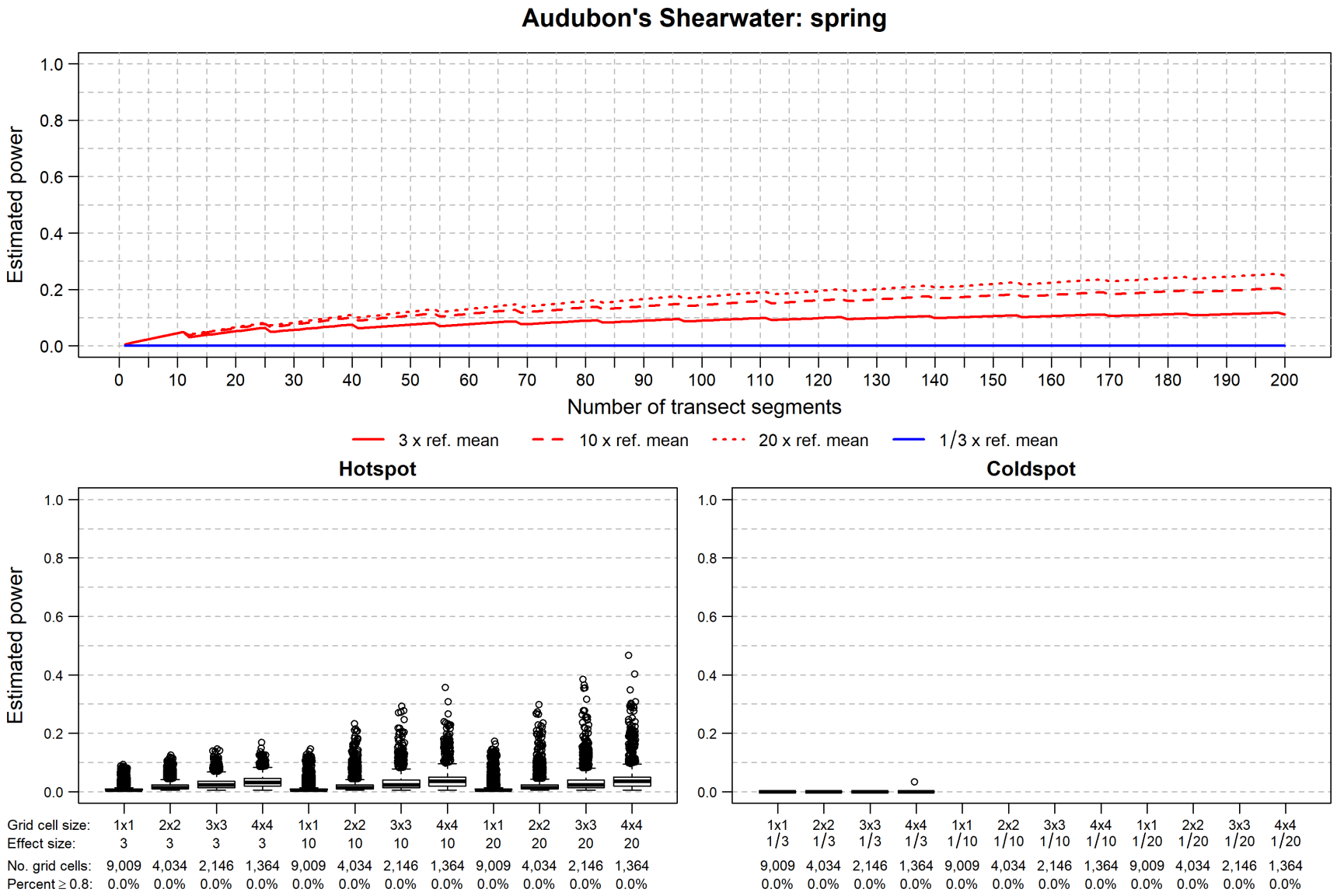


**Figure E62. Power analysis results for Audubon's Shearwater during spring based on the combined model (type I error rate = 0.05)**

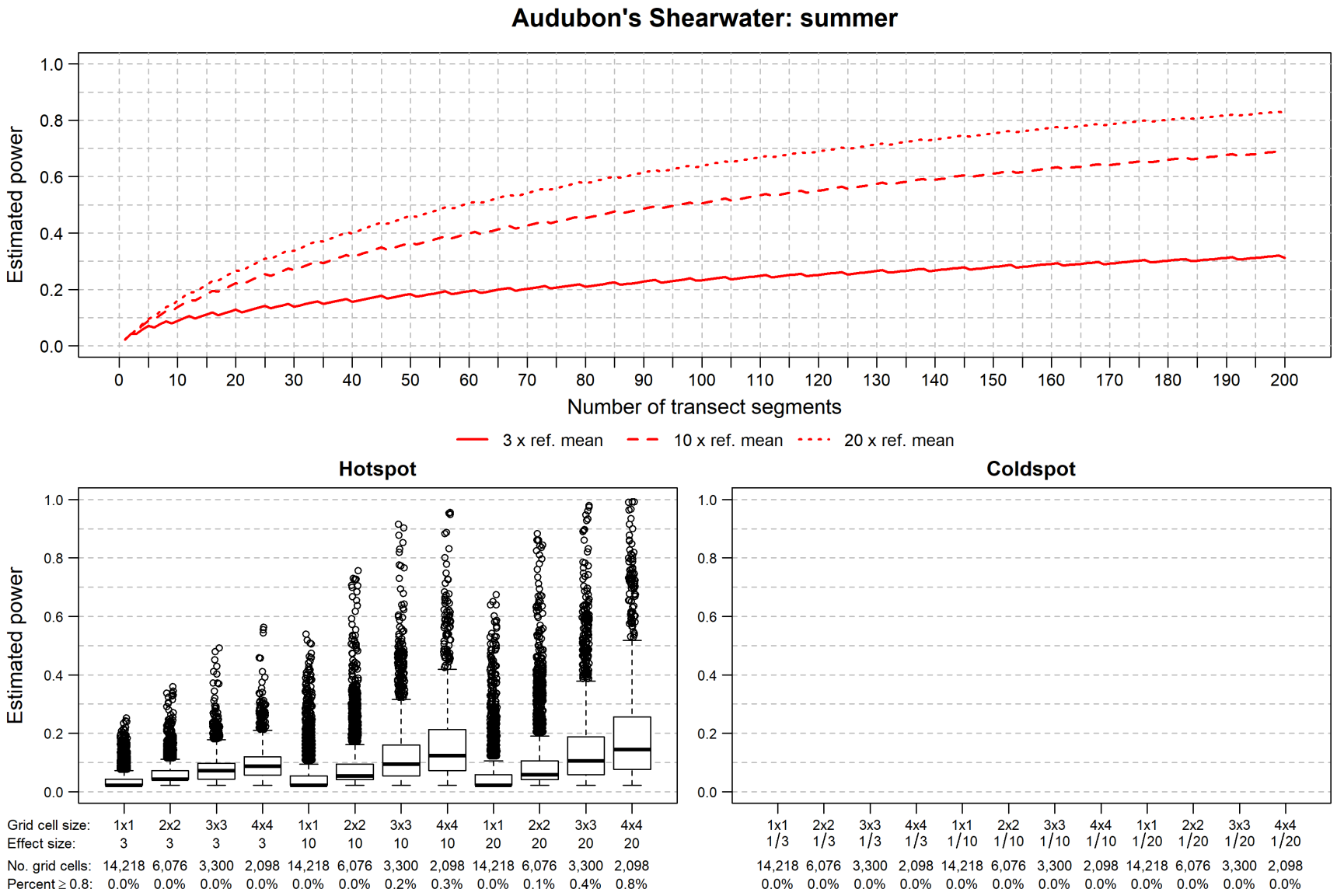


**Figure E63. Power analysis results for Audubon's Shearwater during summer based on the combined model (type I error rate = 0.05)**

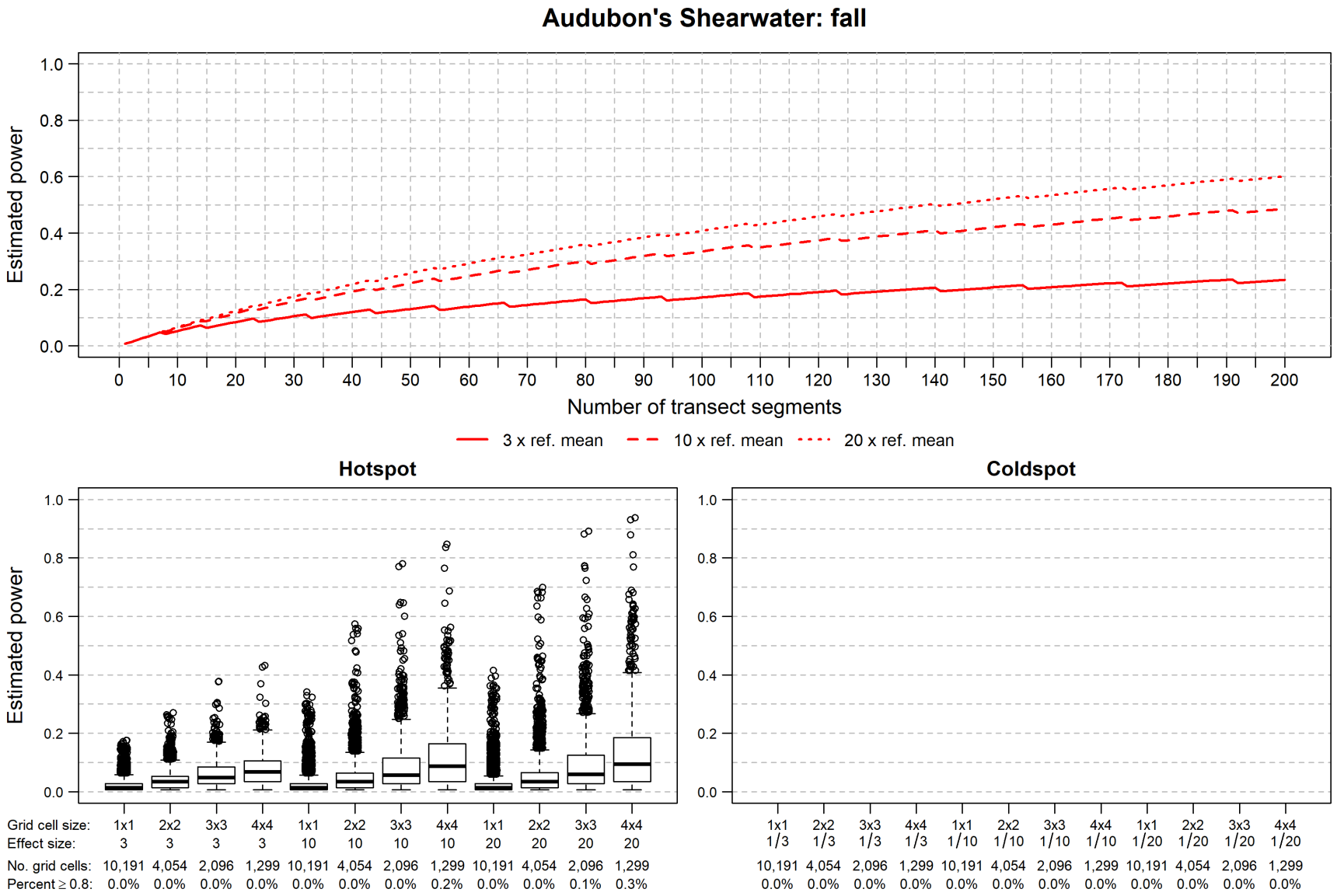


**Figure E64. Power analysis results for Audubon's Shearwater during fall based on the combined model (type I error rate = 0.05)**

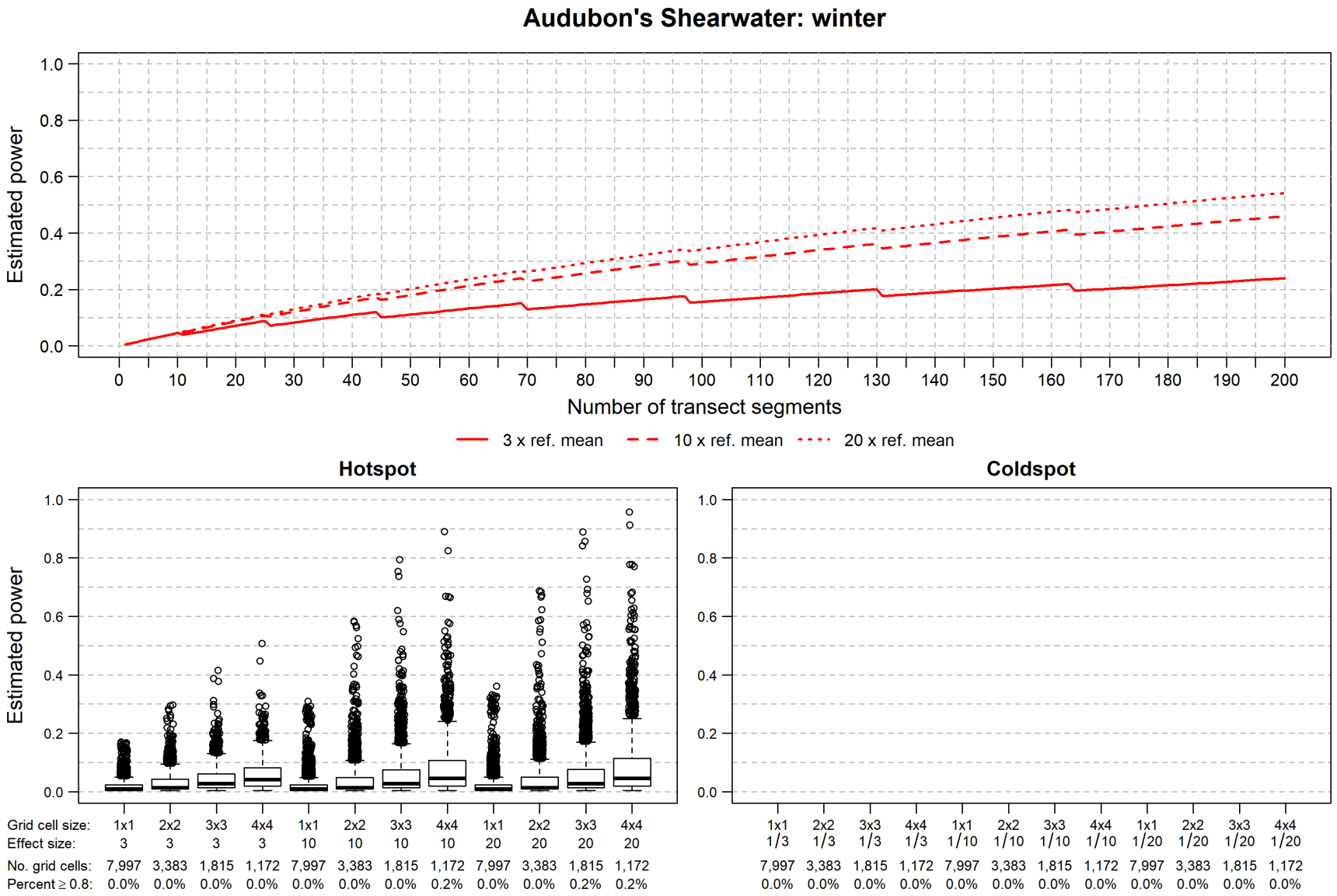


**Figure E65. Power analysis results for Audubon's Shearwater during winter based on the combined model (type I error rate = 0.05)**

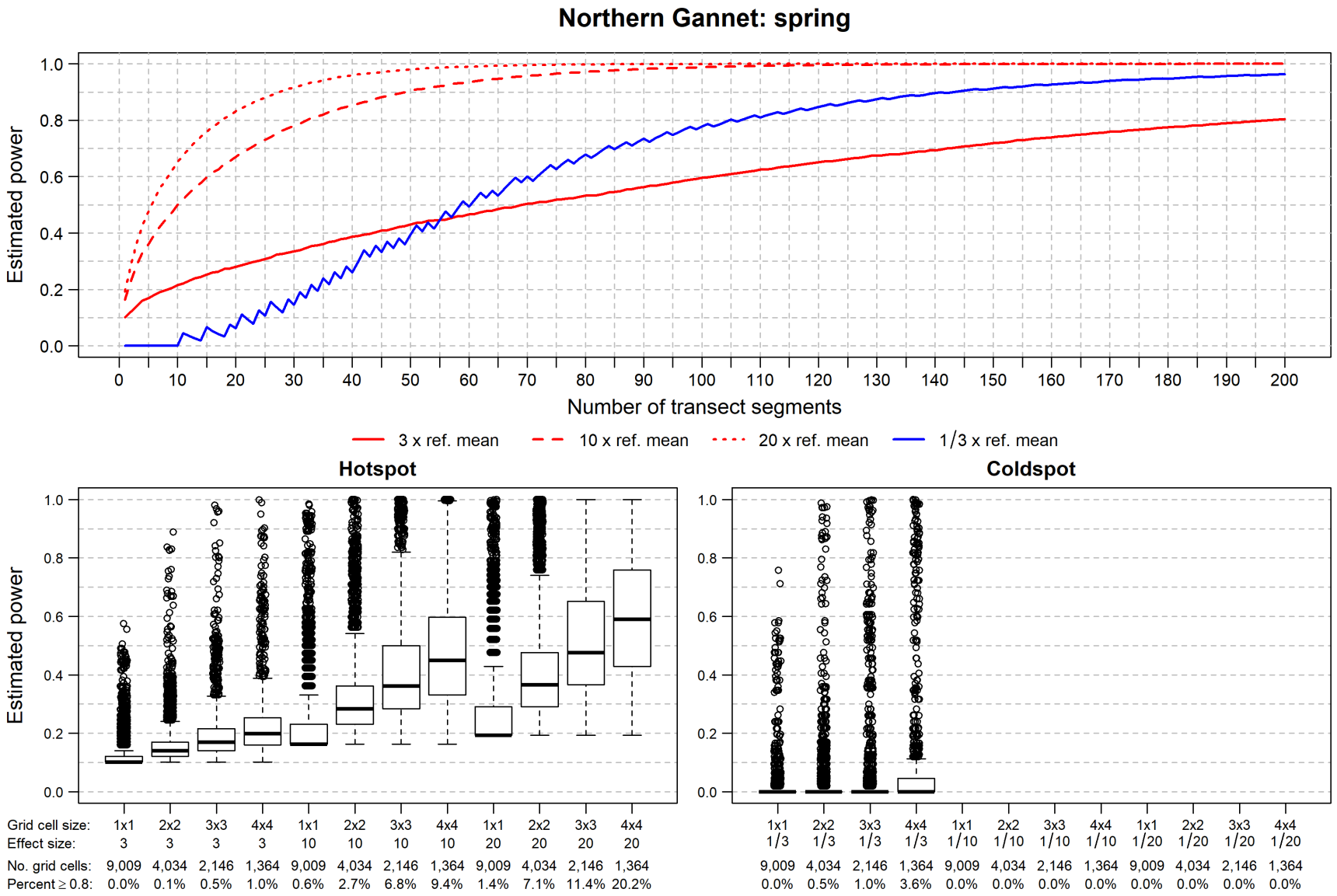


**Figure E66. Power analysis results for Northern Gannet during spring based on the combined model (type I error rate = 0.05)**

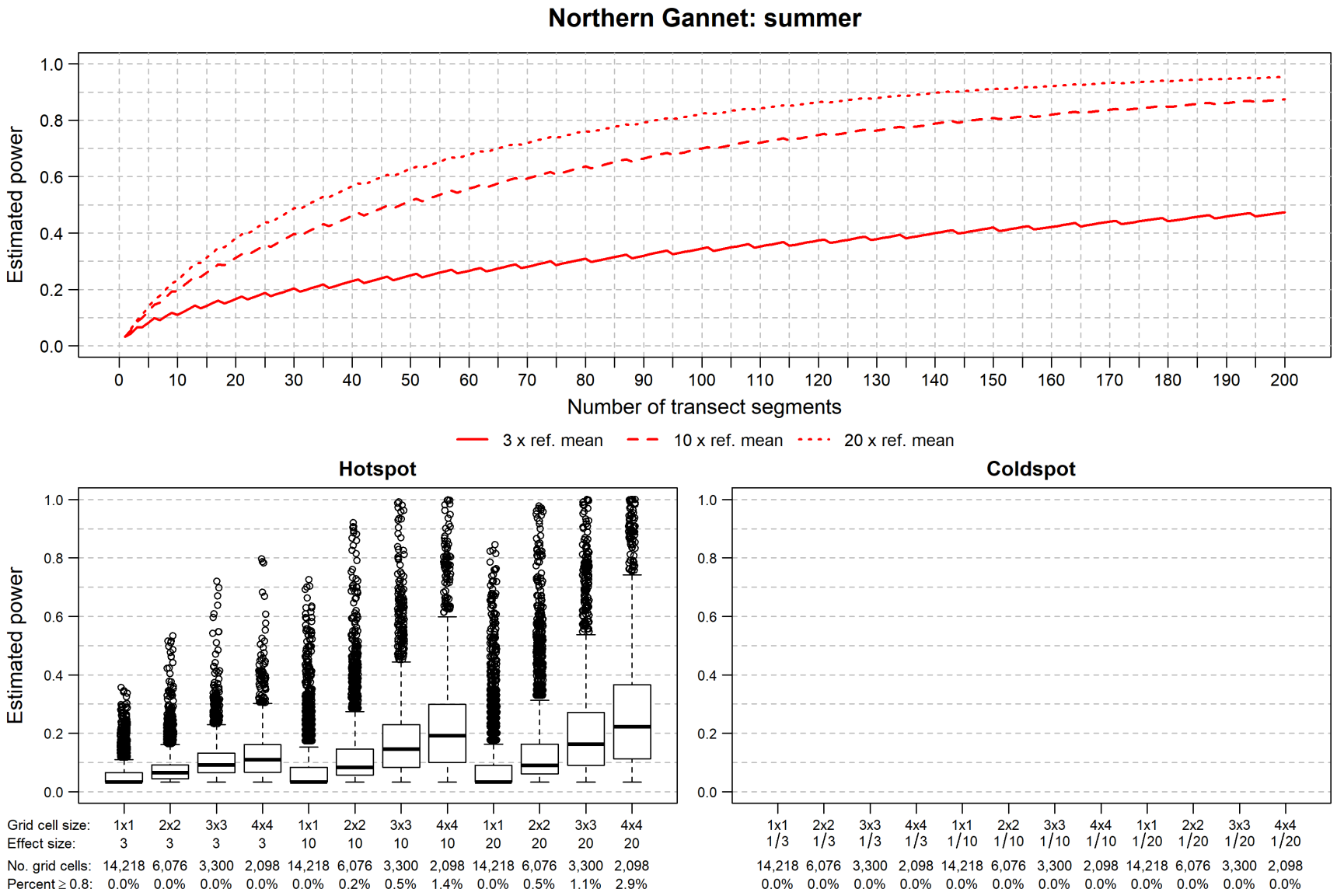


**Figure E67. Power analysis results for Northern Gannet during summer based on the combined model (type I error rate = 0.05)**

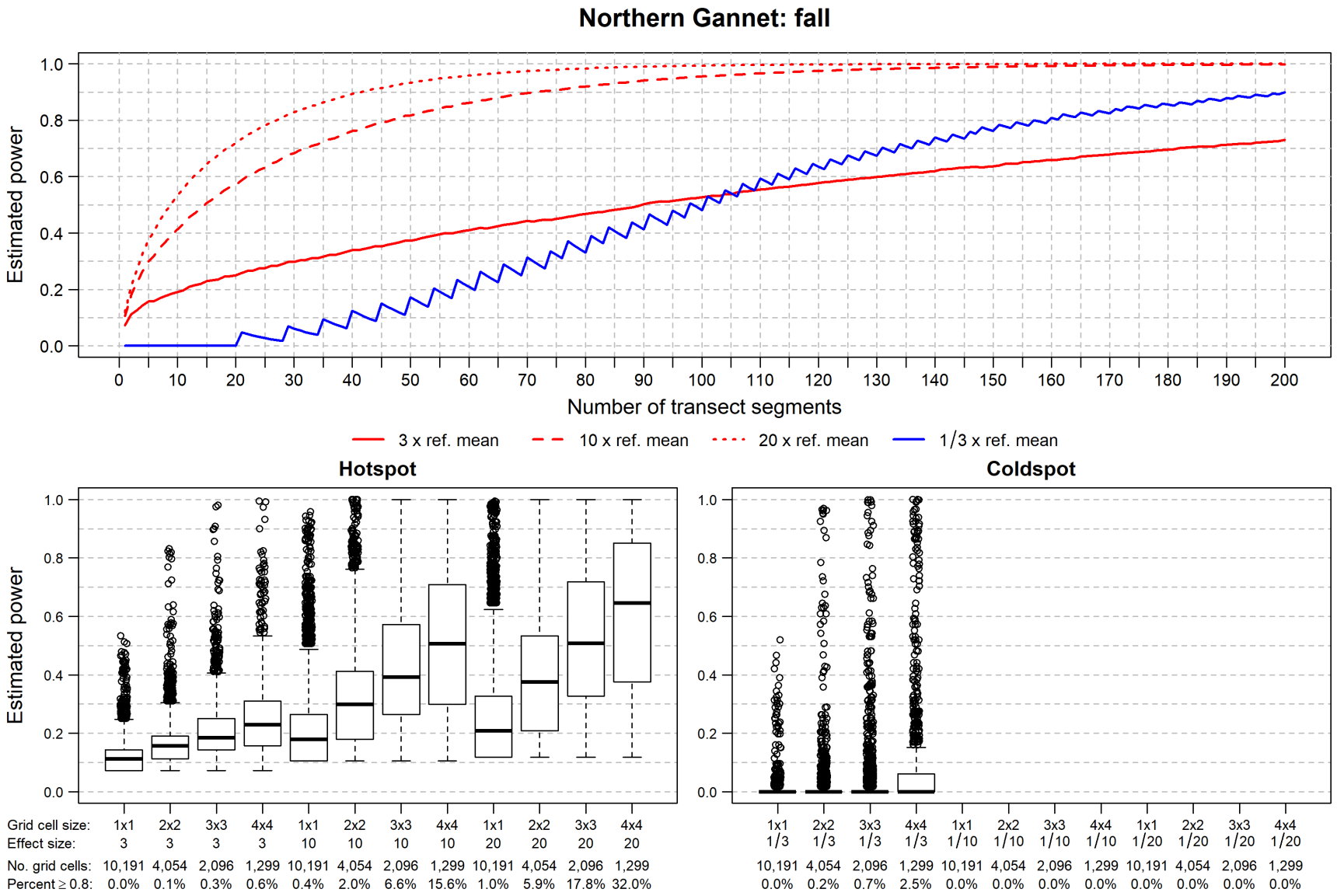


**Figure E68. Power analysis results for Northern Gannet during fall based on the combined model (type I error rate = 0.05)**

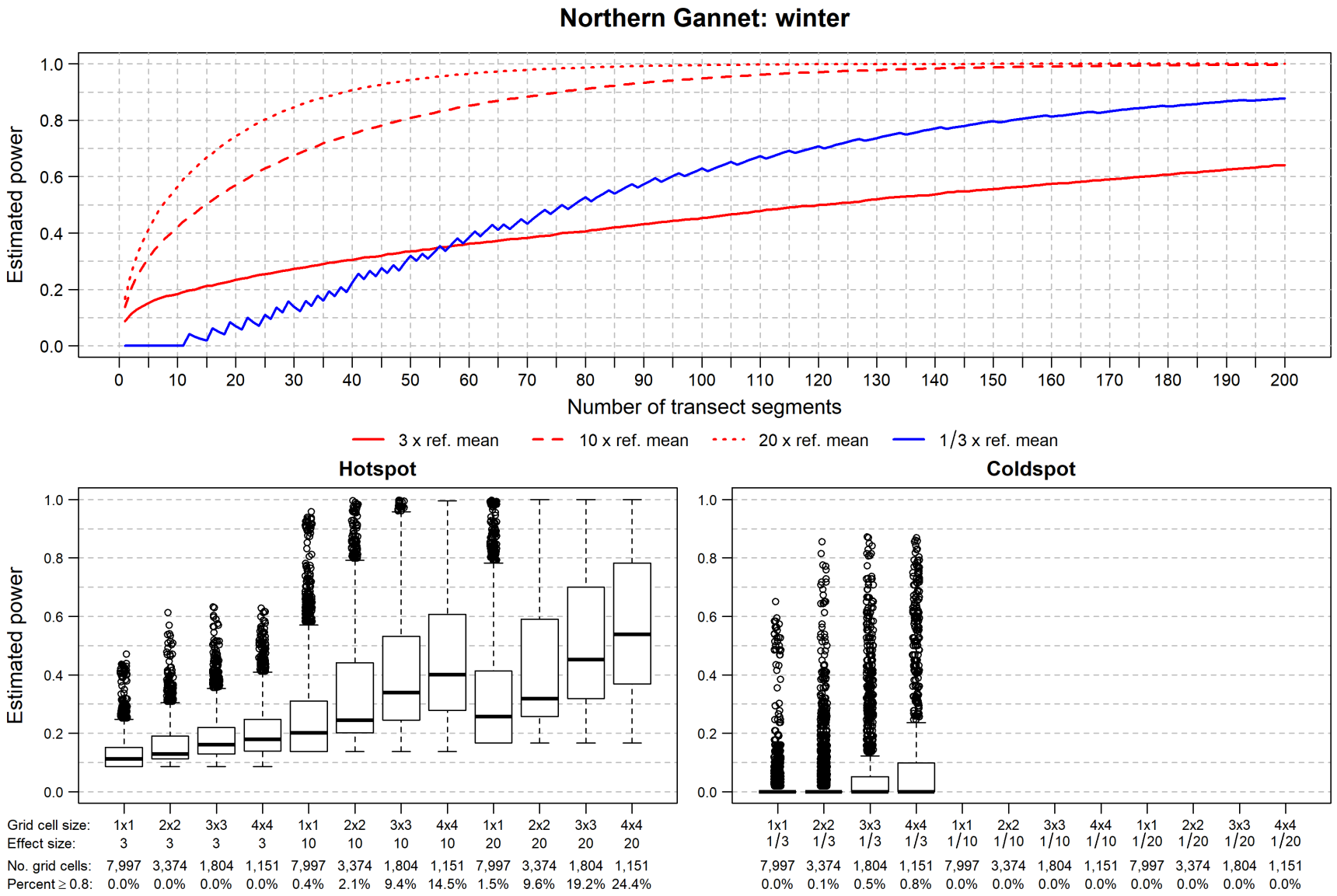


**Figure E69. Power analysis results for Northern Gannet during winter based on the combined model (type I error rate = 0.05)**